

# РІЗАННЯ ТА ІНСТРУМЕНТИ

В ТЕХНОЛОГІЧНИХ СИСТЕМАХ

101 '2024



МІНІСТЕРСТВО ОСВІТИ ТА НАУКИ УКРАЇНИ  
НАЦІОНАЛЬНИЙ ТЕХНІЧНИЙ УНІВЕРСИТЕТ  
«ХАРКІВСЬКИЙ ПОЛІТЕХНІЧНИЙ ІНСТИТУТ»

Ministry of Education & Science of Ukraine  
National Technical University  
«Kharkiv Polytechnic Institute»

**РІЗАННЯ  
ТА  
ІНСТРУМЕНТИ  
В ТЕХНОЛОГІЧНИХ СИСТЕМАХ**

---

**CUTTING & TOOLS  
IN TECHNOLOGICAL SYSTEM**

**Збірник наукових праць  
Collection of scientific papers**

*Заснований у 1966 р. М. Ф. Семко  
Found by M. F. Semko in 1966*

**ВИПУСК № 101  
Edition № 101**

Харків НТУ «ХПІ» – 2024 – Kharkiv NTU «KhPI»

ISSN (print) 2078-7405  
УДК 621.91

Ідентифікатор медіа R30-02559, згідно з рішенням Національної ради України з питань телебачення і радіомовлення від 27.07.2023 р. №598  
Друкується за рішенням Вченої ради НТУ «ХПІ»,  
протокол № 10 від 27 грудня 2024 р.

#### Редакційна колегія:

*Головний редактор* Федорович В.О., *заступники головного редактора* Беліков С.Б., Ковальов В.Д., Залога В.О., Триш Р.М., *відповідальний редактор* Островерх Є.В., *члени редакційної колегії, рецензенти:* Антонюк В.С., Басова Є.В., Волкогон В.М., Добротворський С.С., Іванов В.О., Іванова М.С., Кальченко В.В., Криворучко Д.В., Лавріненко В.І., Павленко І.В., Пермяков О.А., Піжов І.М., Пупань Л.І., Ступницький В.В., Тонконогий В.М., Усов А.В., Хавін Г.Л. (Україна), Міко Балаш, Кундрак Янош, Тамаш Петер, Віктор Молнар, Фельо Чаба, (Угорщина), Хатала Міхал, Каганова Дагмар, Манкова Ільдико, Хорнакова Наталія (Словаччина), Маркопулос Ангелос, Мамаліс Атанасіос (Греція), Гуйда Доменіко (Італія), Дашич Предраг (Сербія), Мір'янич Драголюб (Боснія і Герцоговина), Марусіч Влатко (Хорватія), Цішак Олаф, Трояновска Юстіна (Польща), Еммер Томас (Німеччина), Едл Мілан (Чехія), Турманідзе Рауль (Грузія).

У збірнику представлені наукові статті, в яких розглядаються актуальні питання в області механічної обробки різних сучасних матеріалів із застосуванням високопродуктивних технологій, нових методик, вимірювальних приладів для контролю якості оброблених поверхонь і високоефективних різальних інструментів. Розглядаються аспекти оптимізації та математичного моделювання на різних етапах технологічного процесу.

Для інженерів і наукових співробітників, що працюють в області технології машинобудування, різання матеріалів, проектування різальних інструментів в технологічних системах.

*Збірник наукових праць «Різання та інструменти в технологічних системах» включений в Перелік фахових видань України категорії «Б», наказ МОН України від 17.03.2020 р., № 409*

**Різання та інструменти в технологічних системах/Cutting and Tools in Technological Systems: Збірник наукових праць.** – Харків: НТУ «ХПІ», 2024. – Вип. 101. – 126 с.

**Адреса редакційної колегії:** вул. Кирпичова, 2, Харків, 61002, Національний технічний університет «Харківський політехнічний інститут», кафедра «Інтегровані технології машинобудування» ім. М.Ф. Семка, тел. +38 (057) 706-41-43.

**УДК 621.91**

Матеріали відтворені з авторських оригіналів  
НТУ «ХПІ», 2024

## **A REVIEW OF ADDITIVE MANUFACTURING TECHNOLOGIES AND THEIR APPLICATIONS IN THE MEDICAL FIELD**

Andra Gabriela **Tirnov**ean<sup>1</sup>, Nicolas Daniel **Csoregi**<sup>1</sup>, Cristina **Borzan**<sup>1</sup> [\[0000-0001-9545-0829\]](#), Gyula **Varga**<sup>2</sup> [\[0009-0001-8698-1043\]](#)

<sup>1</sup>Technical University of Cluj-Napoca, Romania,

<sup>2</sup>University of Miskolc, 3515 Miskolc-Egyetemváros, Hungary  
[gyulavarga@uni-miskolc.hu](mailto:gyulavarga@uni-miskolc.hu)

**Received: 29 October 2024 / Revised: 12 November 2024 / Accepted: 27 November 2024 /  
Published: 15 December 2024**

**Abstract.** *This review paper contains a literature survey about some additive manufacturing technologies and their medical use. Additive Manufacturing is a generic term referring to several technologies used to create physical models or prototype parts based on 3D drawings. Additive Manufacturing models can be used for various testing methods. The paper summarizes the application of Additive Manufacturing Technologies in medicine. It describes the main steps for how to create 3D models for medical applications. Some details can be found on the topics: Data acquisition using medical scanners; Data transformation; Creation of virtual 3D models; Surgical planning and simulation on the virtual 3D model; and Creation of Physical 3D Models for Additive Manufacturing Technologies. 3D physical models can be extremely useful in planning complex surgical interventions, which can be simulated on these models before the actual procedure.*

**Keywords:** *Additive Manufacturing; medical imaging; Selective Laser Sintering.*

### **1. Introduction**

In the scientific literature, there are several classifications of the manufacturing technologies known and used until the early 1990s. One of these classifications [1] considers two main groups:

1. Material removal processing technologies. These technologies start with a large quantity of raw material, and by using conventional methods (turning, milling, grinding, etc.) or non-conventional methods (electroerosion, laser processing, ultrasound, etc.), the excess material is removed, resulting in the final piece.

2. Material redistribution processing technologies. These technologies start with the correct amount of raw material, which is redistributed into the required shape through deformation in the solid state (forging, stamping, drawing, extrusion, etc.) or redistribution in the liquid or semi-liquid phase (casting, injection molding, etc.).

In the 1990s, a third group of technologies emerged, Rapid Prototyping (RP) technologies (also known as Additive Manufacturing). This new technology is

©A. G. Tirnov

different from the existing ones because it uses a different principle for materializing parts, where material is added only where and as much as is needed. Due to the manufacturers' efforts to reduce the time from conception to market release and lower the costs of assimilating and producing new products, Rapid Prototyping technologies began to grow in importance [1].

Starting from a CAD description without the need for machine tools or specific devices, these systems can produce complex three-dimensional models.

Regardless of the chosen Additive Manufacturing technology, the part production algorithm remains the same [2]:

1. Modeling the part using a CAD software package.
2. Conversion to a\*. STL format (Standard Triangulation Language), a format adopted as the industry standard for rapid prototyping production [3]. This format represents the 3D surface as a collection of flat triangles. The file contains the coordinates of the vertices and the outer normal direction of each triangle.
3. Slicing the \*.STL file: A pre-processing program prepares the \*.STL file for building. Various programs are available, and most allow the user to adjust layer size, placement, and orientation of the model. Depending on the construction technique, the pre-processing software slices the \*.STL model into layers ranging from 0.01mm to 0.7mm [3]. The program can also generate a supporting structure for the model during the construction process. Each RP machine manufacturer provides its own pre-processing software.
4. Constructing the model "layer by layer." The material used for model construction varies depending on the chosen Rapid Prototyping technology (polymers, metal powder, paper).
5. Cleaning and finishing the model is the final step in the part-building algorithm (post-processing). This involves removing the prototype from the machine and detaching any supporting structures. After cleaning the model, a surface treatment can be applied to improve appearance and durability [4].

The most significant successes of RP system users are found in processes and technologies that justify their investment in these systems. They see RP systems as the basis for new technologies that allow them to function more efficiently and perform better compared to past methods [1].

In Figure 1, the upper curve refers to traditional manufacturing technologies, while the two lower curves refer to computer-aided manufacturing technologies. Computer-aided manufacturing is more flexible and efficient, regardless of the geometric complexity of the parts, involving significantly fewer tools [5].

Current rapid prototyping systems have become available to users, even though they were still in the experimental phase in the early 1990s. Initially, these systems required highly skilled personnel who understood and adjusted numerous parameters that characterized the operation of these systems and technologies. Today, adjusting

these parameters has been simplified through standardization, making system operation easier and requiring less skilled personnel. From a mechanical point of

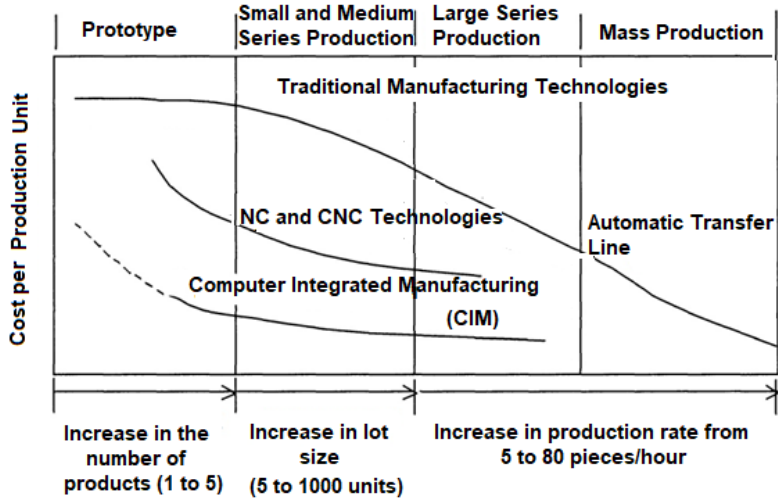


Figure 1. The impact of technology on the cost of production units, adapted from [5]

view, rapid prototyping systems are much more robust, reliable, and easy to maintain. Dimensional accuracy, surface quality, and deposition speed have all improved and continue to improve [1].

Since product development is a creative process, an algorithm must exist for the process. An example of an algorithm is presented in Figure 2. As with any design and development concept, this must be evaluated, preferably with the help of a prototype, thus allowing opportunities for product improvement to be identified. This cycle must be repeated until the final design and functionality are satisfactory. The main advantage of prototypes is that they offer various stakeholders (engineering, sales and marketing, manufacturing, suppliers and subcontractors, logistics) a visual representation of the future product and the possibility of modifying the product's characteristics according to stakeholder requirements [5].

Additive Manufacturing models can be successfully used for the physical visualization of the product. This can be done from the design phase of a new product or for the modernization of an existing one. By using this technology, communication between the manufacturer and the customer is improved. Thus, the product is developed in close collaboration with the customer.

Due to AM technology, manufacturers can sell products long before their actual production. By presenting AM models to customers, they can learn the characteristics

of a new product. After such consultation and product acceptance, the manufacturer can begin production preparation [5].

Additive Manufacturing is a generic term referring to several technologies used to create physical models or prototype parts based on 3D drawings (files). Proposals for new products are studied and analyzed after being drawn up, but a physical model made of a certain material is much more convincing, especially if it is used in the environment in which it will function. Thus, AM models are used in the creation of mockups. The entire mockup is built piece by piece and then used to study shape, design, assembly, the space required, and even function. These mockups are often used in architecture or in the automotive industry [6].

These technologies rely on layered manufacturing, allowing the creation of a physical model at a low cost and in a short time.

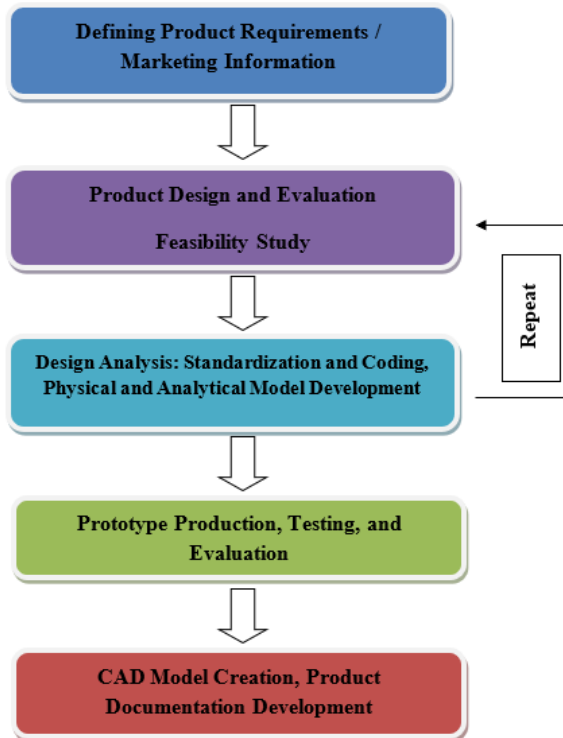


Figure 2. Product development algorithm, adapted from [5]

Additive Manufacturing models can be used for various testing methods. There are three factors that influence the testing of a product [1]:

1. Material: The material must be chosen according to the purpose of the test.
2. Model size: The size is conditioned by the capabilities of RP systems; the part should not have wall thicknesses smaller than 0.2mm (the average diameter of the laser beam); for sufficient rigidity during processing and testing, wall thicknesses of 1.5mm - 3mm are recommended.
3. Model design: This is critical for the solidification process or construction, along with the model's orientation during manufacturing. This factor can determine the appearance of shrinkage and deformations during or after construction.

These tests are used to verify the visual acceptance of the product, to understand its construction and functionality, as well as to finalize the final elements.

The most used tests are functional tests, simulation tests, manufacturing control, fixing and assembly, and packaging.

One of the advantages of these technologies is the reduction of time required to assimilate new products and the costs of creating new tools (devices and verification gauges) [6].

Rapid Tooling (RT) describes a process that combines Rapid Prototyping techniques with conventional processing practices to quickly produce a mold or parts of a functional model based on the CAD (Computer Aided Design) model in the shortest possible time and at the lowest possible cost compared to traditional methods.

There are two categories of Rapid Tooling: indirect and direct [7].

- In Indirect Rapid Tooling methods, parts created through AM processes are used as models for making molds, where the primary goal is not to obtain final parts. "Master" models made of wood, plastic, aluminum, steel, or cast iron are used to create a mold into which the material for the final model is cast. AM models can be indirectly used in several manufacturing processes. The most used indirect Rapid Tooling methods are vacuum casting, sand casting, investment casting, and injection molding [2].
- Direct Rapid Tooling involves directly obtaining the model by adding material layer by layer, often followed by post-processing operations to improve surface quality [5].

Rapid Prototyping technologies have and will continue to have a significant impact in many sectors, from industrial production to medicine, giving this technology strategic importance in companies that use RP [1].

## **2. Application of additive manufacturing technologies in medicine**

In medical imaging, the introduction of X-ray computed tomography (CT), and magnetic resonance imaging (MRI) has broadened the general applicability of

paraclinical investigation techniques, providing essential diagnostic justification for determining therapeutic interventions. These techniques are an important component of evidence-based medicine. Although the cost of these examinations remains high and access to the offered investigations is restricted due to economic factors, the benefits for actual interventions are significant for both the patient and the healthcare system. These non-invasive diagnostic techniques offer decision-makers the ability to plan appropriate and timely surgical interventions, including the surgical technique itself [8].

Additive Manufacturing Technologies assist designers in constructing physical replicas of virtual models created in CAD systems, providing a physical model that offers more information about the same object and is easier to understand. In medicine, medical imaging provides high-resolution images of internal structures of the human body. Based on this information, a physical model useful for preparing complex surgical interventions can be created [9].

These 3D models have three main uses [6]:

1. Surgical planning: 3D physical models can be extremely useful for planning very complex surgical interventions, which can be simulated on these models before the actual surgery. For example, in maxillofacial surgery, the greatest advantage of simulations is the ability to make decisions about bone fixation and to measure all intra- and post-operative bone movements.
2. Diagnostics: The 3D solid model can serve as a physical copy of a dataset and can form a solid basis for diagnosis, choosing the appropriate therapy, and teaching purposes. The model simplifies communication between members of surgical teams, between the radiologist and the surgeon, and between the doctor and the patient. This is important because the two-dimensional images provided by radiologists must be transformed into realistic 3D images that are extremely useful to the surgeon, allowing them to measure and simulate intraoperative situations.
3. Prosthetics: Creating a prosthesis is much easier with the existence of an accurate physical model of an existing structure. The model can be used as a negative or as a master model for making the implant. To reconstruct damaged parts in order to achieve symmetry, mirror images of healthy areas can be used. One forward-looking solution is to create these physical models directly on rapid prototyping systems using biocompatible materials with the human body.

These models produced by AM Technologies replace older models made using other technologies to understand various internal structures of the human body.

### **3. Steps to create 3D models for medical applications**

Creating three-dimensional images involves the following steps [10]:

1. Data acquisition using medical scanners (CT, MRI, etc.).
2. Transferring data into DICOM format (Digital Imaging and

Communication in Medicine).

3. Creating virtual three-dimensional models.
4. Planning and simulation on virtual models (optional).
5. Creating physical three-dimensional (3D) models using Additive Manufacturing technologies.

These steps are visually summarized in Figure 3.

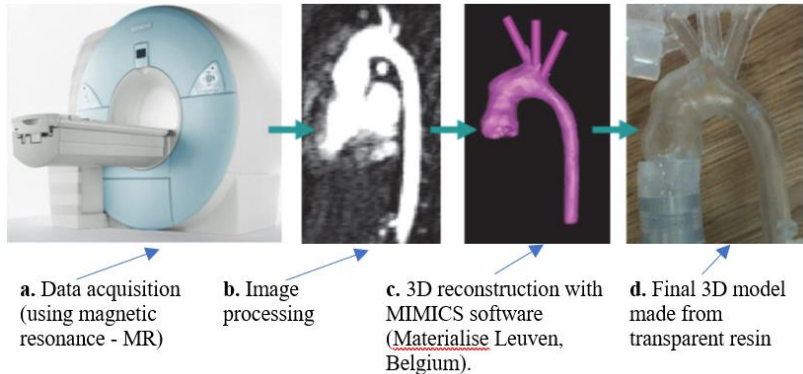


Figure 3. Visual synthesis of the stages of creating a patient's aortic arch [11].

### 3.1. Steps to create 3D models for medical applications

To obtain images, sensors are required to convert radiation energy into electrical signals. There is a wide range of sensors that detect radiation, from gamma rays, X-rays, ultraviolet rays, visible radiation (light), infrared radiation, microwaves, and radio waves.

Images can be captured sequentially using "linear" scanners, by scanning the object in one direction, or using cameras that directly produce a two-dimensional image. To obtain 3D information, which is increasingly in demand, scanners, or camera systems are arranged to capture spatial information. Most medical applications are based on images directly captured from the patient [12].

The informational content of medical images varies significantly depending on the image acquisition system used. Therefore, the first step in medical imaging is selecting the acquisition system appropriate for the intended purpose.

The informational support for creating 3D virtual models can be obtained through various types of medical scanning such as computed tomography (CT), magnetic resonance imaging (MRI), ultrasound, etc. The most used methods for acquiring data for 3D models are computed tomography (CT), which provides accurate information about bone structures, and magnetic resonance imaging (MRI),

which provides details about soft tissues. These two methods can be combined when 3D models are needed that include both the skeleton and soft tissues [10].

### 3.2. Transferring data into dicom format

Image processing has multiple applications in medicine, aimed at optimizing analysis and interpretation by the human observer of the information received from the external environment.

The human body includes an image analyzer for the external environment, represented by the human eye, responsible for capturing, transmitting, and converting light impulses into visual images.

In the technical field, the development of new image acquisition, storage, and transmission technologies finds application in diversifying equipment with medical applications.

Based on the visual sense, computer-assisted image processing attempts to create equipment capable of integrating visual facilities as simply as possible into electronic devices.

A digital image represents the numerical replication of an optical image. It can be stored in files with various formats, each adapted for specific uses (capture, processing, archiving, printing).

Images can be divided into two categories [13]:

1. Vector images (coordinate files).
2. Matrix images (composed of pixels).

Among matrix images, formats such as BMP, JPEG, GIF, and DICOM are common. In medical imaging, the most frequently used formats are DICOM and ANALYZE, which aim to store information related to slice thickness, voxels, the patient, the device used, and the medical facility where the images were obtained.

DICOM format (Digital Imaging and Communications in Medicine) is a standard created by the National Electrical Manufacturers Association (NEMA) to regulate the distribution and visualization of medical images obtained through CT, MRI, and ultrasound. Data in this format is included in a single file (\*.dcm) that contains two parts: a header, intended for auxiliary information, and the other part for graphic data [14].

### 3.3. Creating virtual 3D models

Special programs are required for visualizing and performing additional operations (3D visualization, image modification, measurement, or exporting images in other formats).

In addition to proprietary programs for each medical scanner, there are many programs that can perform the operations (MIMICS, AGNOSCO, DICOM VIEWER, SANTE DICOM VIEWER, RADIANT DICOM VIEWER, WEASIS DICOM VIEWER, MITO MEDICAL IMAGING TOOLKIT, etc.). An example of Graphic user interface of the MIMICS application is shown in Figure 4.

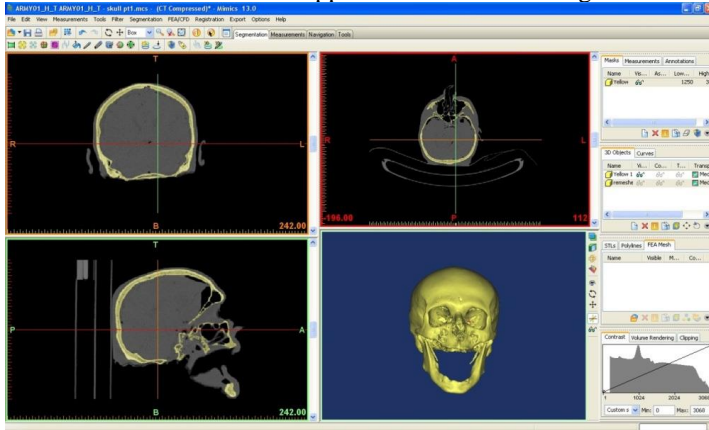


Figure 4. Graphic user interface of the MIMICS application [15].

Certain measurement techniques require pre-processing to obtain 3D coordinates of the scanned surface points. In the case of computed tomography, sections are obtained containing images with transverse densities and known distances between adjacent sections [5].

For the three-dimensional modeling of an anatomical system, three major steps are necessary:

1. Reading and processing input data.
2. Segmenting the input data to automatically identify objects in the images (useful when the goal is to detect and highlight areas of interest).
3. Three-dimensional reconstruction of anatomical models [16].

Processing images acquired through tomography is an essential step in obtaining valid \*.STL models and then producing accurate physical models. For this purpose, the Belgian company Materialise created a specialized software package that simplifies the methodology of obtaining models within certain limits [1].

The MIMICS software includes several modules. Figure 5 shows the links between the main program and its various modules [17].

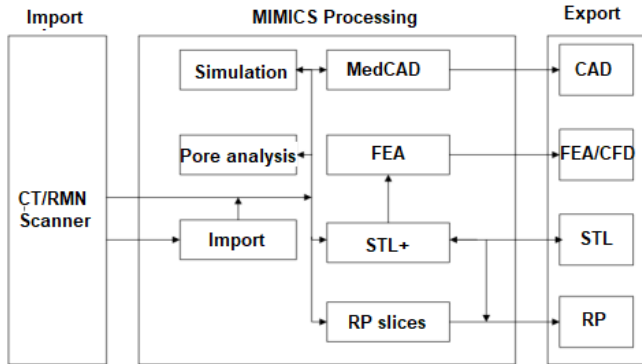


Figure 5. Modules of the MIMICS program, adapted from [17].

The MIMICS program displays image data in multiple ways, each providing unique information. MIMICS divides the screen into three or four windows, each offering a specific view or image:

1. The axial view of the image.
2. The processed coronal image.
3. The processed sagittal image.
4. A three-dimensional reconstruction view (Figures 6).

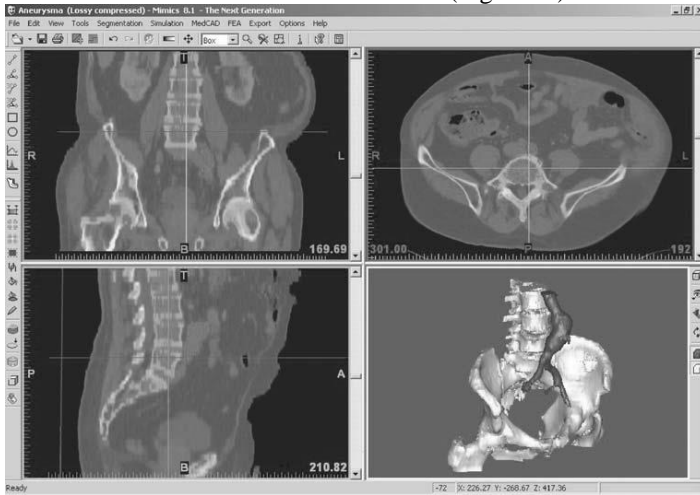


Figure 6. Results in the MIMICS program [18].

### 3.4. Surgical planning and simulation on the virtual 3D model

Three-dimensional visualization of the patient's internal anatomy before the surgical phase represented a significant leap in diagnosing and treating various conditions. Once the 3D model is created, it faithfully represents both the anatomy and pathology of the patient. It can be used for diagnostic purposes as well as for planning and simulating surgical interventions.

Software packages allow the surgeon to rotate the virtual model in all desired directions and to section it into different planes. This way, the diagnosis is precise, and the planning of the surgery can be done in detail [10].

### 3.5. Creation of physical 3D models for additive manufacturing Technologies

Using AM technologies, real models are transformed into physical models. The new techniques are based on CAD/CAM (Computer-Aided Design/Computer-Aided Manufacturing) processes and utilize special machines controlled by computers to generate physical 3D models using specific technologies. This technique is widespread globally, so much so that it can be said that most people use, in their daily activities, at least one product made by AM.

The main processes of AM are [1]:

- Stereolithography (STL)
- Fused Deposition Modeling (FDM)
- Laminated Object Manufacturing (LOM)
- Selective Laser Sintering (SLS)
- 3D Printing
- Wax Object Manufacturing (WOM)
- Model Maker Manufacturing System
- Stratoconception Manufacturing System

### 3.6. Selective laser sintering (SLS)

Selective laser sintering (SLS) is a very popular AM technique. Selective Laser Sintering (SLS) is a freeform fabrication process of components through the sintering of powders. This process is one of the most used for creating prototypes from various metallic and non-metallic powders [20].

SLS uses a laser beam directed by a computer over the surface of the powder bed to rapidly produce solid copies of virtual models. It is one of the few RP processes capable of producing durable and functional parts from a wide range of materials [5].

This process is based on materializing a CAD product by adding successive layers. The laser used in this process is typically a CO<sub>2</sub> laser. The laser covers the entire surface of the section (point by point), sintering the fine layer of material deposited on the work platform [1].

Through this process, three-dimensional parts can be obtained by heating and bonding powders at temperatures below their melting points.

The laser system generates laser radiation, which is focused by a lens and directed through a system of mirrors to the surface of the work platform (Figure 7). At the beginning of the work process, the platform is in the upper position. A feed system deposits a thin layer of powder of controlled thickness on the surface of the platform. The laser beam scans the platform's surface according to the geometry of the first section of the workpiece. As a result of the scanning process, the laser radiation locally sinters the powder layer.

After the laser has scanned the entire surface of the first layer, the work platform lowers by a distance equal to the thickness of one layer. The feed system deposits a new powder layer over the previous one. Once again, the laser beam scans the current powder layer according to the geometry of the next section through the solid model of the workpiece.

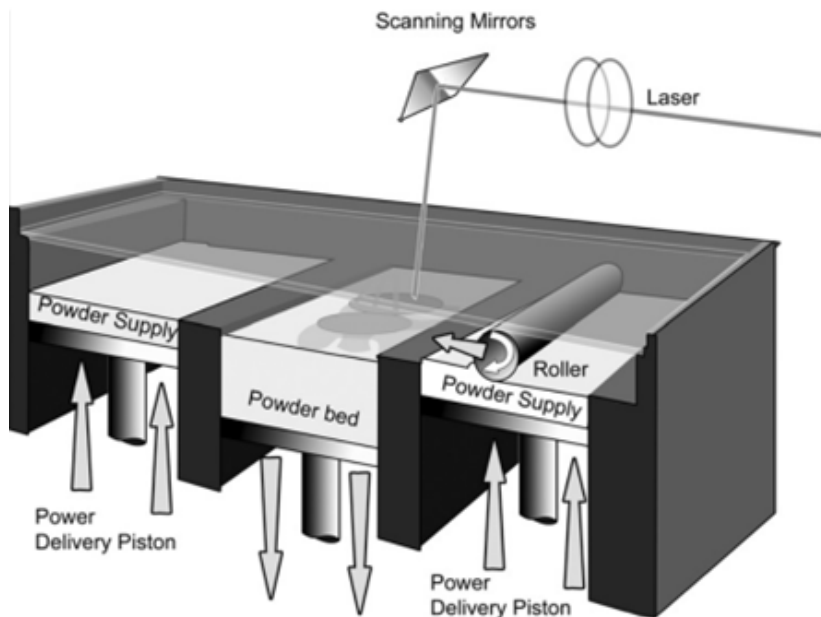


Figure 7. Schematic diagram of the Selective Laser Sintering process [21].

During the process, there is constant control over the thickness of the powder layer deposited on the platform, the distance between the sections created by the computer program through the model, and the distance moved by the work platform after each processed layer [1].

SLS systems are primarily produced by DTM Products Inc. in the USA and in Europe by Electro Optical Systems GmbH from Germany.

The materials used in the SLS process are very diverse, including a wide array of thermoplastics, such as polyamides, ABS, polycarbonates, and nylons, but also metal powders, quartz-based powders, or zirconium-based powders [22].

Selective Laser Sintering (SLS) offers multiple advantages such as high mechanical strength of the manufactured parts, recyclability of unused powders, and the ability to print large batches without support structures [23].

#### **4. Conclusions**

The main advantage of physical prototypes is that they provide various stakeholders (engineering, sales and marketing, manufacturing, suppliers and subcontractors, logistics) with a visual representation of the future product and the opportunity to modify the product characteristics according to needs.

AM models can be successfully used for physical visualization of the product, starting from the design phase of a new product or when modernizing an existing one.

Additive Manufacturing technologies allow the creation of physical models using layer-by-layer manufacturing, at a low cost and in a short timeframe.

3D physical models can be extremely useful in planning complex surgical interventions, which can be simulated on these models before the actual procedure.

Radiological images presented in two dimensions must be transformed into realistic 3D images that are extremely useful to the surgeon, as the models allow for measuring and simulating intraoperative conditions.

Creating a prosthesis is made much easier by having an accurate physical model of a structure. The model can be used as a negative or as a master model for creating the implant.

The physical model can be used both for diagnosis and for planning and simulating surgical interventions.

#### **Acknowledgements**

The research was funded by the cooperation within CEEPUS project CIII-RO-0013-20-2425 - Teaching and Research of Environment-oriented Technologies in Manufacturing, which coordinator is Professor Ph.D. Marian Borzan.

**References:** **1.** Berce P., Bâlc N., Ancău M., ș.a.: Fabricarea Rapidă a Prototipurilor, Ed. Tehnică, București, (2000). **2.** Boboulos Miltiadis A.: CAD-CAM & Rapid Prototyping Applications Evaluation. Ventus Publishing ApS, (2010), ISBN 978-87-7681-676-6. **3.** Bibb Richard, Winder John A review of the issues surrounding three-dimensional computed tomography for medical modelling using rapid prototyping techniques. Radiography, Volume 16, Issue 1, February (2010), pp. 78–83. **4.** Yan Y., Shengjie L., Renji Z., Feng L., Rendong W., Qingping L., Zhuo X., Wang X.: Rapid Prototyping and Manufacturing Technology: Principle, Representative Technics, Applications, and Development Trends, Tsinghua Science & Technology, Volume 14, Supplement 1, June (2009), pp. 1–12. **5.** Venunod P. K. and Weiyin M.: Rapid Prototyping, Laser-based and Other Technologies. Kluwer Academic Publishers, 2004, ISBN 978-1-4419-5388-9. **6.** Borzan C.: Theoretical and experimental research regarding manufacturing by selective laser sintering of custom implants from biocompatible materials, PhD Thesis, Technical University of Cluj-Napoca (2014). **7.** Louh R.F., Ku Yiwen, Tsai Irene: Rapid Prototyping: Fast Track to Product Realization. Society of Mechanical Engineers, 1994, Rapid prototyping technique for ceramic minidevices containing internal channels with asymmetrical contour. Journal of the European Ceramic Society, Volume 30, Issue 14, October (2010), pp.: 2841–2847. **8.** Popat A.H.: Rapid prototyping and medical modeling, Phidias Newsletter, Denmark, 1998;1, pp.: 10–12. **9.** Radu. C.: Contributions to the protection elements of studies through rapid prototyping, PhD Thesis, Transilvania University, Brasov (2009) **10.** Rotaru H.: Reconstrucții și modele Tridimensionale Medicale. Ed. Casa Cărții de Știință, Cluj-Napoca, (2001). **11.** Hoque E.M.: Advanced applications of Rapid Prototyping technology in modern Engineering, (2011), InTech, Rijeka, Croatia, ISBN 978-953-307-698-0. **12.** Barrett H.H., Swindell W.: Radiological Imaging, The Theory of Image Formation, Detection and Processing, Vol. I, Academic Press, New York, USA, (1981), pp.: 438–439. **13.** Tărăță Mihai.: Informatică medicală, SITECH, Craiova ISBN 978-606-530-816-9, vol. I and II, p.: 568, Cap. Analiza și prelucrarea imaginilor medicale, (2010). **14.** Costache A.: DICOM in medical imaging, (2024) <https://www.medicalai.ro/dicom-in-imagistica-medicala>. **15.** Patel A. and Goswami T.: Chapter 6. Comparison of Intracranial Pressure by Lateral and Frontal Impacts – Validation of Computational Model, Book: Injury and Skeletal Biomechanics, ISBN 978-953-51-0690-6, (2012). **16.** Radu C.: 3D Modeling and Static Finite Element Analysis of Human Tibia, 99 Advanced Engineering 2, ISSN 1846-5900, (2008). **17.** MIMICS. Reference Guide Version 10.0, Belgia: Materialise, (2006). **18.** Dhoore E.: Software for Medical Data Transfer, Rapid Digital Manufacture in Complex Medical Treatments, John Wiley & Sons, Ltd., Hong-Kong, (2005), ISBN 0-470-01688-4. **19.** Christensen A. M., Humphries S. M.: Role of Rapid Digital Manufacture in Planning and Implementation of Complex Medical Treatments, Rapid Digital Manufacture in Complex Medical Treatments, John Wiley & Sons, Ltd., Hong-Kong, (2005), ISBN 0-470-01688-4. **20.** Palm G., Shafie, A.M.: Product Model Driven Laser Sintering, Proceeding of the 5th European Conference on Rapid Prototyping and Manufacturing, Helsinki, Finland, 4th – 6th June (1996). **21.** R.D. Goodridge, C.J. Tuck, R.J.M. Hague: Laser sintering of polyamides and other polymers, Progress in Materials Science 57 (2012) pp.: 229–267. **22.** H. Yehia, A. Hamada, T. A. Sebaey, W. Abd-Elaziem: Selective Laser Sintering of Polymers: Process Parameters, Machine Learning Approaches, and Future Directions, J. Manuf. Mater. Process. (2024) 8, 197. **23.** M. U. Azam, I. Belyamani, A. Schiffer, S. Kumar, K. Askar.: Progress in selective laser sintering of multifunctional polymer composites for strain- and self-sensing applications, Journal of Materials Research and Technology, Volume 30, (2024), pp.: 9625–9646, ISSN 2238-7854.

Андрa Габрієла Тірновеан, Ніколас Данієль Чорегі, Крістіна Стефана Борзан,  
Клуж-Напока, Румунія, Дьюла Варга, Мішкольц, Угорщина

## ОГЛЯД ТЕХНОЛОГІЙ АДИТИВНОГО ВИРОБНИЦТВА ТА ЇХ ЗАСТОСУВАННЯ В МЕДИЧНІЙ СФЕРІ

**Анотація.** Дана стаття містить огляд літератури щодо деяких технологій адитивного виробництва та їх медичного застосування. Адитивне виробництво — це загальний термін, що стосується кількох технологій, які використовуються для створення фізичних моделей або прототипів деталей на основі 3D-креслень. Моделі адитивного виробництва можуть використовуватися для різних методів тестування. У статті узагальнено застосування технологій адитивного виробництва в медицині. У ньому описані основні етапи створення 3D-моделей для медичних застосувань. Основна перевага фізичних прототипів полягає в тому, що вони надають різним зацікавленим сторонам (інженерія, продажі і маркетинг, виробництво, постачальники і субпідрядники, логістика) візуальне представлення майбутнього продукту і можливість модифікувати характеристики продукту відповідно до потреб. Моделі адитивного моделювання можуть успішно використовуватися для фізичної візуалізації продукту, починаючи з етапу проектування нового продукту або при модернізації вже існуючого. Технології адитивного виробництва дозволяють створювати фізичні моделі з використанням пошарового виробництва, з невеликими витратами і в стислі терміни. 3D фізичні моделі можуть бути надзвичайно корисними при плануванні складних хірургічних втручань, які можна змоделювати на цих моделях перед фактичною процедурою. Рентгенологічні зображення, представлені у двох вимірах, повинні бути перетворені на реалістичні 3D-зображення, які є надзвичайно корисними для хірурга, оскільки моделі дозволяють вимірювати та моделювати інтраопераційні умови. Створення протеза значно спрощується завдяки наявності точної фізичної моделі конструкції. Модель може використовуватися як майстер-модель для створення імплантату. Фізична модель може використовуватися як для діагностики, так і для планування та моделювання хірургічних втручань. Деякі подробиці можна знайти на теми: збір даних за допомогою медичних сканерів; трансформація даних; створення віртуальних 3D моделей; хірургічне планування та симуляція на віртуальній 3D моделі; створення фізичних 3D-моделей для технологій адитивного виробництва. 3D фізичні моделі можуть бути надзвичайно корисними при плануванні складних хірургічних втручань, які можна змоделювати на цих моделях перед фактичною процедурою.

**Ключові слова:** адитивне виробництво; медична візуалізація; селективне лазерне спікання.

## THE INFLUENCE OF DIFFERENT HARDNESS OF THE TOOL MATERIAL ON THE WEAR OF SHM GRINDING WHEELS AND THE SPECIFIC ENERGY INTENSITY OF GRINDING

Valerii Lavrinenko<sup>1</sup>[\[0000-0003-2098-7992\]](#), Volodymyr Solod<sup>2</sup>[\[0000-0002-7516-9535\]](#),  
Volodymyr Tyshchenko<sup>2</sup>[\[0009-0001-6473-5909\]](#), Yevgeniy Ostroverkh<sup>3</sup>[\[0000-0002-8926-1324\]](#)

<sup>1</sup>V. Bakul Institute for Superhard Materials NAS Ukraine, Kyiv, Ukraine

<sup>2</sup>Dniprovsk State Technical University, Kamianske, Ukraine

<sup>4</sup>National Technical University «Kharkiv Polytechnic Institute», Kharkiv, Ukraine

[lavrinenko@ism.kiev.ua](mailto:lavrinenko@ism.kiev.ua)

Received: 29 October 2024 / Revised: 12 November 2024 / Accepted: 27 November 2024 /  
Published: 15 December 2024

**Abstract.** *It was established that conditionally viscous-brittle tool materials (high-speed steels and hard alloys) behave in the same way with an increase in hardness: wheel wear and the specific energy consumption of their grinding decrease. As the hardness of brittle tool oxide-carbide ceramics increases, both wheel wear and the specific energy consumption of grinding, on the contrary, increase. That is, an increase in the hardness of viscous-brittle materials facilitates the separation of elementary chips, less energy is needed for this, and accordingly the wear of the wheel and the specific energy consumption of their grinding are reduced. On brittle ceramics, with increasing hardness, there is no change in chip removal, but harder sludge becomes more abrasive and, as a result, the wear of the wheel and the specific energy consumption of their grinding increase. The conclusion from the literature that hard and less plastic materials require relatively less specific energy for grinding is confirmed by us when comparing materials of approximately the same hardness - hard alloys and ceramics. In ceramics, the energy consumption of grinding is actually four times lower than that of hard alloys.*

**Keywords:** *hardness; high-speed steels; hard alloys; ceramics; wear of SHM grinding wheels; specific energy intensity of processing.*

### 1. Introduction

The hardness of materials is related to a complex of mechanical properties, such as elasticity, plasticity, strength and yield limits, as well as micro- and nanohardness with such thermodynamic characteristics of substances – the energy of the crystal lattice, the energy of breaking crystal bonds, surface energy, melting

point [1]. The hardness indicator characterizes a state of stress close to non-equilibrium compression, and thus determines the resistance to contact stresses arising in the working part of the cutting tool [2]. Therefore, for a cutting tool, the hardness of the tool material has a determining role. At the same time, it affects their processability, although there are certain features noted in publications [2–4]. Thus, the hardness of ceramics based on silicon nitride and silicon carbide has a smaller effect on their machinability than their density [3], and in [4] it is indicated that when grinding hardened steels, the cutting force does not depend on their hardness. The hardness of heat-resistant tool steels is determined by the dispersion and amount of carbides released during tempering, and residual austenite as a soft component [2]. Up to the hardness index of tool steels of 65 HRC, with increasing hardness, their strength also increases. However, their high hardness corresponds to a sharp decrease in viscosity [2]. That is why studies of the influence of the hardness index on the machinability of the tool material, when the hardness changes on one material, may be of some interest.

## **2. Modern studies on the influence of hardness on the operational characteristics of the material**

Let us point out that modern researchers pay due attention to the hardness indicator, even in areas related to abrasive processing. Let us point out that modern researchers pay due attention to the hardness indicator. A vivid example is the polygonization of a railway wheel, which is a type of uneven wear of the material that worsens the directional stability of trains. On the railway, wheels and rails of different hardness are used, respectively HW and HR. An important factor affecting wear is wheel-rail hardness matching (ie HW/HR hardness ratio), which can affect the formation of a polygonal wheel. The results show that when fitting a softer rail, the wheel is less likely to become polygonal as HW/HR increases. When paired with a stiffer rail, the wheel showed early polygon initiation. The highest HW/HR ratio of 1.263 represented the best anti-polygonal condition for the wheel material [5].

Attention was also paid to hardness in the study [6], where the mechanism of plasticity with a deformation gradient was applied to study the size effect in the behavior of single-crystal copper during scratching. It is shown that the scratch hardness, which takes into account both the size effect and the dependence on the crystallographic direction, is a suitable property of the material for the evaluation of wear. Laser exposure and the use of a diamond tool with a negative front angle are promising methods of processing hard and brittle materials.

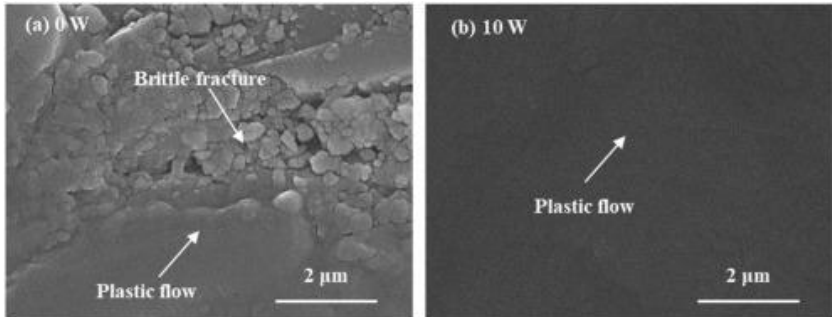


Fig.1. View of the surface, after processing with a diamond tool with grains with a front angle of  $-65^\circ$  and without laser exposure (a) with exposure (b) with a power of 10 W [7].

In article [7], the mechanism of plastic removal of fused quartz is investigated. And here the effect on hardness is important. The results showed that ductile removal was improved with the laser due to hardness reduction and brittle fracture was reduced due to high hydrostatic compressive stress when using a diamond tool with negative rake grains (Fig. 1). Let's pay attention to the fact that we can observe this type of surface (see Fig. 1, a) under the conditions of diamond grinding of tool ceramics, when both plastic flow and brittle fracture zones are observed on the processed surface, which we described in more detail in the article [8].

In work [9], this was already considered for ultra-thin Ti-Al-Diamond wheels with variable abrasive sizes, concentration and shape, i.e. not due to a directed decrease in the hardness of the processed brittle material, but due to a change in the characteristics of the diamond layer of the wheel. Experimental results indicate that diamond abrasives significantly affect chip formation and material removal of SiC workpieces by changing the thickness of undeformed chips (Fig. 2). A theoretical analysis based on the classical brittle-plastic transition model shows that a hard but brittle SiC single crystal can be removed in the plastic regime using a relatively large abrasive size and low concentration in the work layer as long as the undeformed chip thickness is sufficiently smaller than the calculated critical cutting depth [9].

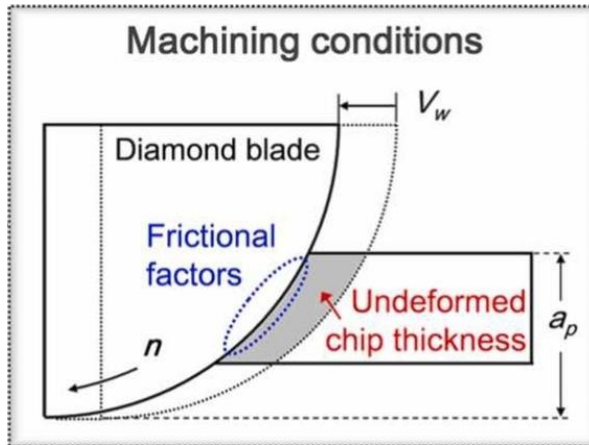


Fig. 2. Machining conditions: diamond blade – frictional factors – undeformed chip thickness

It was confirmed [10] that the specific energy during material removal has an asymptotic behavior with the speed of material removal, and as this speed increases, the specific energy consumption decreases. It is shown that in plastic materials, the viscosity of the material due to the release of heat and a higher fracture toughness compared to brittle materials increase the complexity of processing and, accordingly, require more specific energy during grinding. When grinding hard and less plastic materials, the growth rate of cracks when cutting with abrasive grains is higher, which reduces energy costs for material deformation. For this reason, hard and less plastic materials require relatively less specific energy for grinding [10].

Finally, let's pay attention to how the change in hardness of the studied material affects its operational characteristics, especially since it is relevant for modern conditions in Ukraine. The main role of the armor plate is to increase the safety of the combatants. Armor plates are made by welding high-hardness armor steel (HHA), but a reduction in hardness may occur. Taking into account the direct correlation between the hardness of armor steel and its ballistic characteristics, avoiding softening becomes important. For this, welding was performed using a flux consisting of nanoparticles of tungsten carbide (WC), titanium carbide (TiC), silicon carbide (SiC) and ethanol. As an example, hardness values of 654.0 HV and 590.4 HV were observed with 8% WC and 8% SiC, respectively, i.e. increases by 16.6% and 5.28% compared to no nanoparticle flow [11]. That is, the use of flux with

nanoparticles increases the hardness in the welding zone and the ballistic characteristics of armor steel.

Let's summarize the above.

First, hardness is an important indicator, and in order to improve the operational characteristics of products, one should strive to increase it [5, 11];

secondly, a decrease in hardness improves plasticity, i.e., the transition to the plasticity mode when processing brittle materials is associated with a decrease in their hardness [7];

thirdly, during diamond-abrasive processing, for such transfer to the plasticity mode, it is necessary to increase the grain size of the abrasive and reduce the concentration of abrasive grains in the working layer [9];

fourth, hard and less plastic materials require relatively less specific energy for grinding [10].

### **3. Formulation of the purpose of the research**

That is, the hardness of the processed material is an important factor that affects its machinability and specific energy intensity during grinding. At the same time, in the literature there are no studies of the performance indicators of the diamond abrasive tool during the processing of different tool materials, but with a study of the effect of changing their hardness in a certain range on the same material, which was the goal of this work.

### **4. Presenting main material**

At the same time, an exclusively brittle material (oxide-carbide ceramic VOK60, range of hardness change 82–94 HRA) and conditionally viscous-brittle materials (hard alloy TT21K9, range of hardness change 90.5–92.0 HRA and high-speed steels P18 and P6M5, hardness change range 60–64 HRC). The hardness ranges specified above were determined by the possibilities of selecting a significant batch of samples of one tool material and the presence of a noticeable range of hardness at the same time. It should be noted that it was not possible to achieve this only for hard alloy, but taking into account the large number of hard alloy plates, it was possible to divide them into three sub-ranges according to the hardness of HRA: 90.5–90.9, 91.0–91.5 and 91.6–92.0. At the first stage, deep grinding of high-speed steels with a productivity of 1920 mm<sup>3</sup>/min was considered. with a cubonite wheel 12A2-45° 150x10x3x32 – KPS 100/80 M1-10 100. Samples 100x20x8 mm in size with a hardness of 60±0.5 and 64±0.5 HRC were pre-selected.

The wear resistance of the grinding tool was studied based on the relative consumption of KNB grains in the wheel during grinding ( $q$ , mg/g), and the effective grinding power ( $N_{ef}$ , kW) and the specific energy intensity of grinding ( $E_{pyt}$ , kJ/kg) were determined. The specific energy capacity of grinding was calculated according to the new method described in the article [12]. The test results are shown in Table. 1.

In our opinion, as the hardness of steels increases, they become less viscous, chips are removed more easily, and therefore both wheel wear and the specific energy consumption of grinding are reduced. Indirect confirmation of this is the fact that in P18 steel, where tungsten is almost 3 times more than in P6M5 steel, fragility is also greater and, therefore, similarly, wheel wear and specific energy capacity are lower than in P6M5 steel (see Table 1).

Table 1 – Grinding indicators of high-speed steels at a productivity of 1920 mm<sup>3</sup>/min.

Steel brand	Hardness, HRC	$N_{ef}$ , kW	$q$ , mg/g	$E_{pyt}$ , kJ/kg
P6M5	60	1.8	1.61	106.5
	64	1.8	1.30	86.0
P18	60	1.6	1.01	59.4
	64	1.6	0.86	50.6

At the second stage, grinding of TT21K9 hard alloy was considered at a productivity of 480 mm<sup>3</sup>/min with a diamond wheel 12A2-45° 150x10x3x32 – AC4MA 63/50 B1-11П-2 125. Hard alloy samples measuring 16x16x6 mm were, as indicated above, previously divided into 3 groups by hardness. Let's pay attention to the fact that TT21K9 is one of the most difficult-to-machine hard alloys containing (% by volume): TiC – 8.7 and TaC – 12.5. Its standard hardness should be 91 HRA, so even small deviations in the smaller or larger direction, in our opinion, should definitely cause a change in the diamond grinding performance. We investigated the wear resistance of the grinding tool based on the indicator of the relative consumption of diamonds in the circle during grinding ( $q$ , mg/g) and determined the effective grinding power ( $N_{ef}$ , kW) and the specific energy intensity of grinding ( $E_{pyt}$ , kJ/kg). The test results are shown in table. 2.

Table 2 – Grinding indicators of hard alloy TT21K9 at a productivity of 480 mm<sup>3</sup>/min.

Range of hardness, HRA	$N_{ef}$ , kW	$q$ , mg/g	$E_{pyt}$ , kJ/kg
90.5 – 90.9	0.95	2.8	304
91.0 – 91.5	1.00	2.4	274
91.6 – 92.0	1.20	1.5	206

From the table 2, it can be seen that a slight decrease in hardness (to 90.5 HRA), relative to the standard 91.0 HRA, slightly increases the wear of the wheel and the energy intensity of processing, while with an increase in hardness to 92.0 HRA, the wear of the wheel and the energy intensity of grinding are significantly reduced. That is, these two conditionally viscous-brittle materials (high-speed steels and hard alloys) react in the same way to an increase in their hardness: wheel wear and specific energy capacity decrease.

At the third stage, we considered the grinding of already extremely fragile oxide-carbide ceramics VOK60 with a productivity of 1750 mm<sup>3</sup>/min with a diamond wheel 12A2-45° 150x10x3x32 – AC4 100/80 B1-13 100. Samples of alloy ceramics measuring 12x12x4 mm were previously divided into 4 groups by hardness. We would like to point out that the standard hardness of VOK60 ceramics should be 93 HRA, but in the process of manufacturing these ceramics, we selected samples with an abnormally lower hardness, which made it possible to obtain an additional, quite noticeable hardness range of 82–91 HRA. The wear resistance of the grinding tool was investigated by the indicator of the relative consumption of diamonds in the circle during grinding ( $q$ , mg/g) and the effective power of grinding ( $N_{ef}$ , kW) and the specific energy intensity of grinding ( $E_{pyt}$ , kJ/kg) were determined. The test results are shown in Table. 3.

From the Table 3, it can be seen that with the increase in the hardness of such conditionally exceptionally brittle oxide-carbide ceramics VOK60, both the wear of the wheel and the specific energy intensity of grinding do not decrease, as in the conditionally viscous-brittle materials described above (high-speed steels and hard alloys), but on the contrary, they increase. That is, here, in our opinion, with an increase in the hardness of ceramics, there is no transition to increased fragility and easier material removal, which is indicated not by a decrease, but, on the contrary, by an increase in the specific energy intensity of grinding. At the same time, an increase in the hardness of sludge particles improves their abrasive properties, which is reflected in an increase in the wear of the diamond wheel (see Table 3).

Table 3 – Grinding indicators of oxide-carbide ceramics VOK60 at a productivity of 1750 mm<sup>3</sup>/min.

Range of hardness, HRA	$N_{ef}$ , kW	$q$ , mg/g	$E_{pyb}$ , kJ/kg
82 – 83	0.95	1.23	45.8
85 – 88	1.07	1.41	59.1
90 – 91	1.17	1.75	80.2
93 – 94	1.28	1.93	96.8

## 5. Conclusions

Thus, it is possible to draw the following conclusions from the above.

1. Both conditionally viscous-brittle materials (high-speed steels and hard alloys) react equally to an increase in hardness: wheel wear and the specific energy consumption of their grinding decrease.

2. With an increase in the hardness of such conditionally exceptionally brittle oxide-carbide ceramics VOK60, both wheel wear and specific grinding energy do not decrease, as in conditionally viscous-brittle materials (high-speed steels and hard alloys), but, on the contrary, increase.

3. That is, it is likely that an increase in the hardness of conditionally viscous-brittle materials improves the separation of elementary chips, less energy is needed for their separation and, accordingly, the wear of the wheel and the specific energy consumption of their grinding are reduced. On exceptionally fragile materials (ceramics), with increasing hardness, there is no change in chip removal, but the slurry becomes harder and, accordingly, more abrasive, and, as a result, wheel wear and the specific energy consumption of their grinding increase.

4. The conclusion from the literature that hard and less plastic materials require relatively less specific energy for grinding is confirmed by us when comparing materials of approximately the same hardness (in HRA units), hard alloys and ceramics. In ceramics, the specific energy intensity of grinding is actually four times lower than that of hard alloys.

**References:** 1. Synthetic superhard materials: V 3 т. Т. 1: Synthesis of Superhard Materials/ V.G. Aljoshin, V.D. Andreev, H.P. Bogatyryjova, S.A. Boszko; (Ed.) N.V. Novikov. (in Russian) Kyiv: Nauk. dumka, 1986. – 280 p. 2. Pozdnyak L.A. Instrumental Steels. (in Russian) Kyiv: Naukova dumka, 1996. – 487 p. 3. Schleifen von nichoxidischen keramischen Werkstoffen. Industrie Anzeiger. 1985. 107, N 53 (3). pp. 43–44. 4. Buttery T.C., Hamed M.S. Some factors affecting the efficiency of individual grits in simulated experiments. Wear. 1977. 44, N 2. pp. 231–245. 5. Initiation and evolution of wheel polygonal wear: Influence of wheel-rail hardness ratios / Wenjian Wang, Jinwei Huang, Haohao Ding, Zefeng Wen, Xiaolu Cui, Roger Lewis, Qiyue Liu. Wear. Volumes 540–541, 15 March 2024, 205255 <https://doi.org/10.1016/j.wear.2024.205255> 6. Jinxuan Zhu, Ramin Aghababaei. On the size effect in scratch and wear response of single crystalline copper. Tribology International. Volume 186, August 2023, 108573 <https://doi.org/10.1016/j.triboint.2023.108573>. 7. Experimental and theoretical investigation on the ductile removal mechanism in in-situ laser assisted diamond cutting of fused silica / Chuangting Lin, Wenbin He, Xiao Chen, Zhengding Zheng, Kai Huang, Weiqi Huang, Jianguo Zhang, Jianfeng Xu. Journal of Materials Research and Technology. Volume 24, May–June 2023, pp. 7704–7719 <https://doi.org/10.1016/j.jmrt.2023.05.033>. 8. Lavrinenko V.I., Solod V.Yu. Determining the conditions for achieving the plastic regime of diamond grinding of ceramics from the standpoint of estimating energy costs of processing. Journal of Superhard Materials, 2023, Vol. 45, No. 1, pp. 65–71 <https://doi.org/10.3103/S1063457623010070>. 9. Influence of diamond abrasives on material removal of single crystal SiC in mechanical dicing / Mian Li, Dekui Mu, Yueqin Wu, Guoqing Huang, Hui Meng, Xipeng Xu, Han Huang. Journal of Materials Processing Technology. Volume 327, June 2024, 118390 <https://doi.org/10.1016/j.jmatprotec.2024.118390>. 10. Specific energy modeling of abrasive cut off operation based on sliding, plowing, and cutting / Muhammad Rizwan Awan, Hernán A. González Rojas, José I. Perat Benavides. Saqib Hameed, Abrar Hussai, Antonio J. Sánchez Egea. Journal of Materials Research and Technology. Volume 18, May–June 2022, pp. 3302–3310 <https://doi.org/10.1016/j.jmrt.2022.03.185>. 11. Revolutionizing hardness via nanoparticle flux in welding of high-hardness armor steel / Chang Jong Kim, Young Cheol Jeong, Hwi Jun Son, Bo Wook Seo, Seok Kim, Sung-Ki Lyu, Xiangying Hou, Young Tae Cho. Materials & Design. Volume 242, June 2024, 113001 <https://doi.org/10.1016/j.matdes.2024.113001>. 12. Lavrinenko V.I. To the analysis of the estimate of energy expenditures in the diamond abrasive treatment by wheels from superhard materials. Journal of Superhard Materials, 2022, Vol. 44, No. 4, pp. 285–291 <https://doi.org/10.3103/S1063457622040050>.

Валерій Лавріненко, Київ, Україна, Володимир Солод, Володимир Тищенко,  
Кам'янське, Україна, Євгеній Острочерх, Харків, Україна

## **ВПЛИВ РІЗНОЇ ТВЕРДОСТІ ІНСТРУМЕНТАЛЬНОГО МАТЕРІАЛУ НА ЗНОС ШЛІФУВАЛЬНИХ КРУГІВ З НТМ ТА ПИТОМУ ЕНЕРГОЄМНІСТЬ ШЛІФУВАННЯ**

**Анотація.** Для різального інструменту визначальну роль відіграє твердість матеріалу інструменту. Водночас це впливає на їх технологічність, хоча є певні особливості. Так, твердість кераміки на основі нітриду кремнію і карбїду кремнію має менший вплив на їх обробованість, ніж щільність, а при шліфуванні загартованих сталей сила різання не залежить від їх твердості. Твердість жароміцних інструментальних сталей визначається дисперсністю і кількістю карбїдів, що виділяються при відпусканні, і залишкового аустенїту в якості м'якого компонента. Аж до показника твердості інструментальних сталей 65 HRC, зі збільшенням твердості

зростає і їх міцність. Однак їх висока твердість відповідає різкому зниженню в'язкості. Саме тому певний інтерес можуть представляти дослідження впливу показника твердості на оброблюваність матеріалу інструменту, коли змінюється твердість на одному матеріалі.

Встановлено, що умовно в'язко-крихкі інструментальні матеріали (швидкорізальні сталі та тверді сплави) однаково поводять себе із підвищенням твердості: знос круга і питома енергоємність їх шліфування зменшуються. Зі збільшенням твердості крихкої інструментальної оксидно-карбідної кераміки, як знос круга, так і питома енергоємність шліфування навпаки, підвищуються. Тобто, підвищення твердості в'язко-крихких матеріалів полегшує відділення елементної стружки, енергії для цього треба менше і відповідно знос круга і питома енергоємність їх шліфування зменшуються. На крихкій кераміці зі збільшенням твердості якоїсь зміни у видаленні стружки не відбувається, але більш твердий шлам стає і більш абразивним і, як наслідок, знос круга і питома енергоємність їх шліфування збільшуються. Висновок з літератури про, те, що тверді і м'які пластичні матеріали потребують порівняно менше питомої енергії на шліфування підтверджується нами при порівнянні матеріалів приблизно однакової твердості – твердих сплавів та керамік. У керамік енергоємність шліфування фактично у чотири рази є меншою, аніж у твердих сплавах.

**Ключові слова:** твердість; швидкорізальні сталі; тверді сплави; кераміка; знос шліфувальних кругів з НТМ; питома енергоємність обробки.

UDC 621.9.048

doi: 10.20998/2078-7405.2024.101.03

## **INFLUENCE OF DIAMOND BURNISHING ON CORE HEIGHT AN TEN-POINT HEIGHT**

Viktoria Ferencsik [\[0000-0002-8673-1095\]](https://orcid.org/0000-0002-8673-1095)

University of Miskolc, 3515 Miskolc-Egyetemváros, Hungary  
[ferencsik.viktoria@uni-miskolc.hu](mailto:ferencsik.viktoria@uni-miskolc.hu)

**Received: 27 October 2024 / Revised: 10 November 2024 / Accepted: 26 November 2024 /  
Published: 15 December 2024**

**Abstract.** *Diamond burnishing is a cold plastic forming process, which used as surface improvement finishing treatment after conventional chip removal procedures. This paper presents the experimental study of the impact of different burnishing parameters on 3D surface roughness on cylindrical low alloyed aluminium workpieces. To carry out comparative analysis, measurement of surface roughness was implemented before and after burnishing with an Altisurf 520 measuring device. The results enable a more accurate understanding of the processes that take place during the procedure and, for industrial applications, can help reduce machining time and costs by better defining the set-up parameters.*

**Keywords:** *3D roughness parameters; diamond burnishing; surface integrity; polycrystalline diamond tool.*

### **1. Introduction**

Surface quality always plays a very important role in the proper design of machine parts with properties that can positively influence, for example, lifetime, wear and corrosion resistance, contact stiffness, vibration, etc. For traditional machining processes, many researchers have shown that the required surface quality can be achieved by setting the right parameter combinations [1–4]. For this reason, in this research work I study a non-cutting finishing method, the sliding burnishing which reduces the roughness parameters of the component and contributes to better corrosion resistance. This is due to the fact that, compressive residual stresses are formed in the near-surface layer, thereby increasing the microhardness of it. The process also results in increased fatigue strength, greater resistance to frictional fatigue, and reduced wear.

Several researchers have worked on analysing burnished surface roughness, in addition more and more scientists became convinced that the third dimension

© V. Ferencsik, 2024

should be added to the surface analysis [1]. Korzynski et al. [5] investigated the influence of tool tip radius, burnishing force and feed on 28 different 3D surface roughness parameters in the case of machining austenitic stainless steel 317Ti. To plan and execute experiments they used the so-called Hartley plan, and the most important finding of their work is that with the applied setting parameters, all but one of the obtained equations is non-linear. The only linear equation concerns the  $S_{tr}$  roughness parameter, which is a measure of uniformity of the surface texture. Swirad also used Hartley plan in his study [6], but the input parameters considered in it include speed, force and line-to-line pitch. According to results, he observed that burnishing force exerts the greatest influence on the values of the indicators of the geometric structure. Kebede and Felho [7] used orthogonal L9 array Taguchi design to examine the impact of burnishing force, feed rate and number of passes on 3D surface roughness of medium carbon steel after CNC milling process. One of their important observations is the similarity of the responses between pairs of surface roughness parameters:  $S_q$  and  $S_a$ , as well as  $S_v$  and  $S_z$ , showed similar trends with the change of the burnishing parameters.

In this paper, I examine the effect of burnishing force ( $F$ ), feed ( $f$ ), speed ( $v$ ), and number passes ( $i$ ) on 2 kinds of 3D roughness parameters ( $S_k$ ,  $S_{10z}$ ) investigating the correlation between these setting parameters on low alloyed aluminium workpieces

## **2. Execution of diamond burnishing**

During burnishing of cylindrical surfaces, a deforming tool moves under burnishing force over the surface of the workpieces which rotates at a given speed, thus elastic-plastic deformation takes place on the near-surface layer [810] as shown in Figure 1.

Purpose of the application of this finishing process to improve surface roughness, increase lifetime by increasing compression residual stress and hardness of the near-surface layer [12, 13]. In this experiment the surface of the workpiece was pre-machined by finishing turning set at  $f_1 = 0.2$  than  $f_2 = 0.15$  mm/rev, then the burnishing operation was executed with the same machine (E400 universal lathe) applying 3.5 mm radius PCD (polycrystalline diamond) tool and manual dosing oil, which kinematic viscosity was  $\nu = 70$  mm<sup>2</sup>/s.

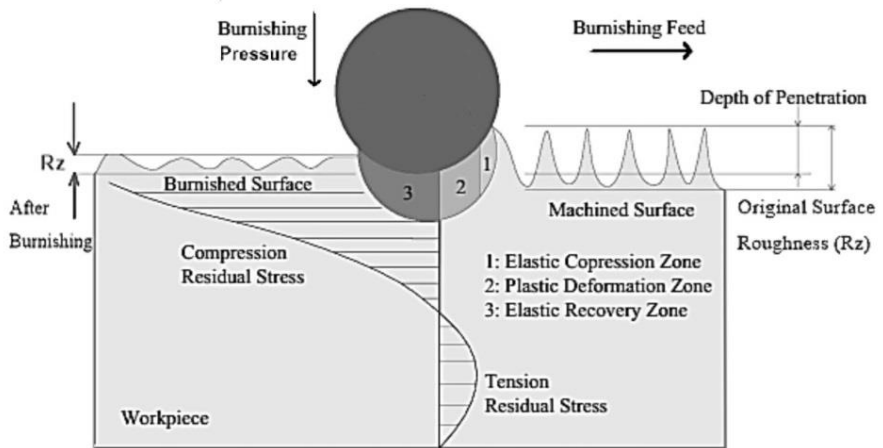


Figure 1. Schematic representation of burnishing treatment [11]

Table 1 contains the adjusted polishing parameters, which were determined based on the preliminary experimental work and taking account the mechanical properties of the burnished workpiece material.

Table 1, The numerical value of the examined burnishing parameters

No	F [N]	f [mm/rev]	v [m/min]	i [-]
1	15	0.05	50.54	2
2	25	0.05	50.54	2
3	35	0.05	50.54	2
4	25	0.01	50.54	2
5	25	0.1	50.54	2
6	25	0.05	35.71	2
7	25	0.05	71.43	2
8	25	0.05	50.54	1
9	25	0.05	50.54	3

### 3. Measurement of 3d surface roughness

3D roughness measurement of the turned and burnished surfaces on 3 areas of 2x2 mm – rotated by 120° - were conducted on Altisurf 520 surface profiler, equipped with a CL2 confocal chromatic sensor and MG140 magnifier. The results were evaluated with the Altimap Premium software, Figure 2 shows a state during the measurement process.

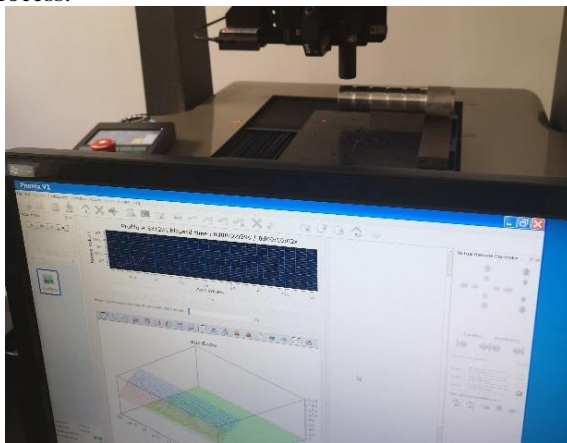


Figure 2. State during measurement

3D roughness parameters can be classified into 6 groups, from them a functional ( $S_k$ ) and a feature parameter ( $S_{10z}$ ) were examined. Core height ( $S_k$ ) means the difference between the upper and lower levels of the core and its values are calculated from the linear curve (equivalent linear curve) minimizing the sectional inclination corresponding to 40% of the material ratio curve, as it can be seen in Figure 3. This parameter is suitable for evaluating friction, abrasion and lubricity for engine cylinder surfaces.

Ten-point height of surface ( $S_{10z}$ ) is the average value of the heights of the five peaks (hill area) with the largest global peak height added to the average value of the heights of the five pits (dale area) with the largest global pit height.

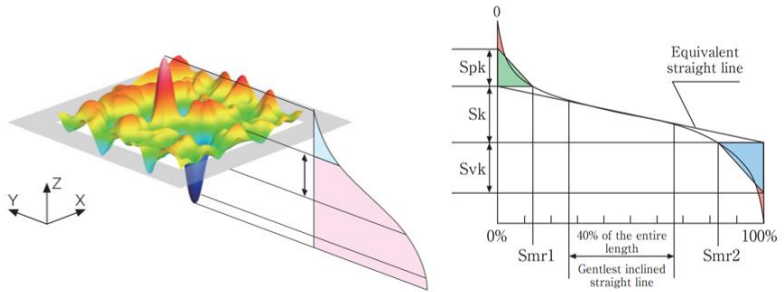


Figure 3. Identification of core height [15]

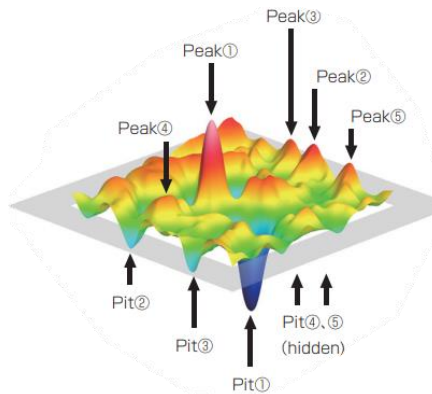


Figure 4. Identification of ten-point height [15]

#### 4. Results and discussion

Table 2 summarizes the averaged values of the measured roughness parameters and contains dimensionless ratios that were created to make more illustrative the changes.

The calculations were made according to El-Taweel and El-Axir [16]:

$$\Delta\rho_{S_x} \% = \left( \frac{S_{x\text{before}} - S_{x\text{after}}}{S_{x\text{before}}} \right) \cdot 100\%, \quad (1)$$

where:

- $S_x$  before                      Surface roughness parameter measured after turning,
- $S_x$  after                         Surface roughness parameter measured after burnishing,
- $\Delta\rho S_x\%$                         Percentage value of the calculated ratio.

Table 2, The results of  $S_k$  and  $S_{10z}$  with the calculated ratios of the experiment.

No.	$S_k$ [ $\mu\text{m}$ ]		$\Delta\rho S_k$ [%]	$S_{10z}$ [ $\mu\text{m}$ ]		$\Delta\rho S_{10z}$ [%]
	before	after		before	after	
1	3.2382	2.2516	30.4675	5.0187	3.4009	32.2354
2	2.9783	0.8761	70.5838	4.4061	2.6265	40.3894
3	0.8095	0.9067	-12.0074	3.4399	2.1603	37.1988
4	0.8347	0.9178	-9.9557	2.6209	2.3119	11.7898
5	0.8441	1.0632	-25.9576	2.8703	3.4611	-20.5832
6	3.2769	0.9292	71.6439	4.4580	2.6404	40.7716
7	3.0443	0.9465	68.9091	5.2193	2.7146	47.9892
8	3.4675	1.3365	61.4564	3.7883	2.7620	27.0913
9	3.6189	1.0423	71.1984	3.7851	3.7113	1.9497

The higher the value of the dimensionless ratios, the greater the improvement due to burnishing process. Table 2 clearly shows that the most advantageous parameter settings were in the cases of marked “6” and “7” surfaces, while the most unfavourable parameter setting belongs to the “5” surface. Figure 5-6 show the topography of marked “6” and “7” before and after burnishing.

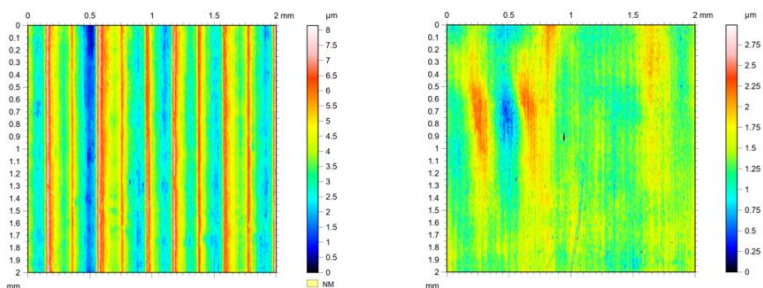


Figure 5. Surface topography of “6” surface before (left) and after (right) burnishing process

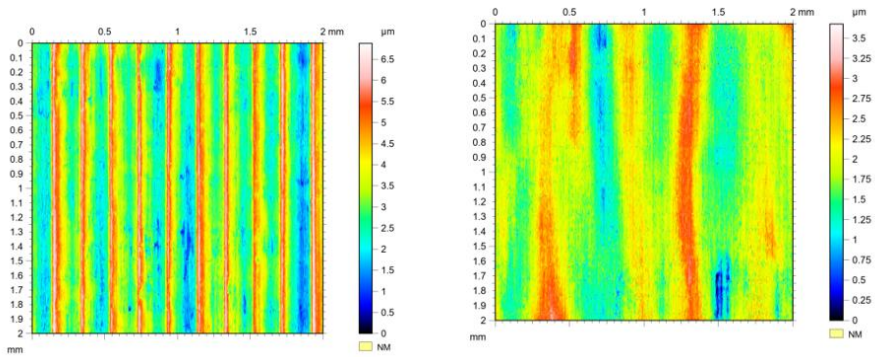


Figure 6. Surface topography of “7” surface before (left) and after (right) burnishing process

Effect of the examined burnishing parameters are presented in Diagram 1-4.

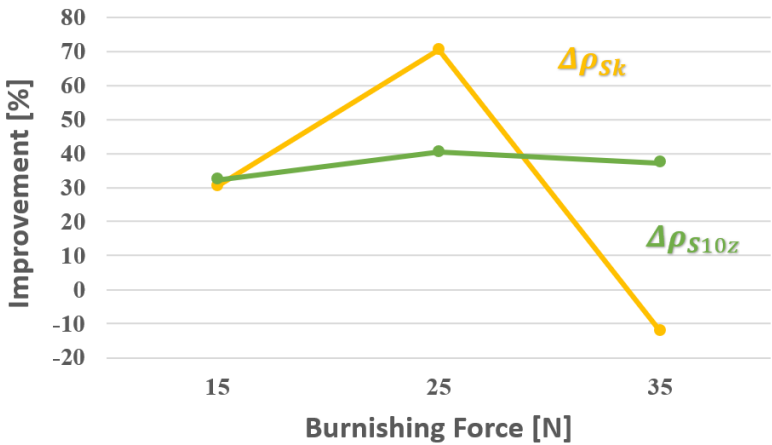


Diagram 1. Influence of burnishing force on the analysed parameters

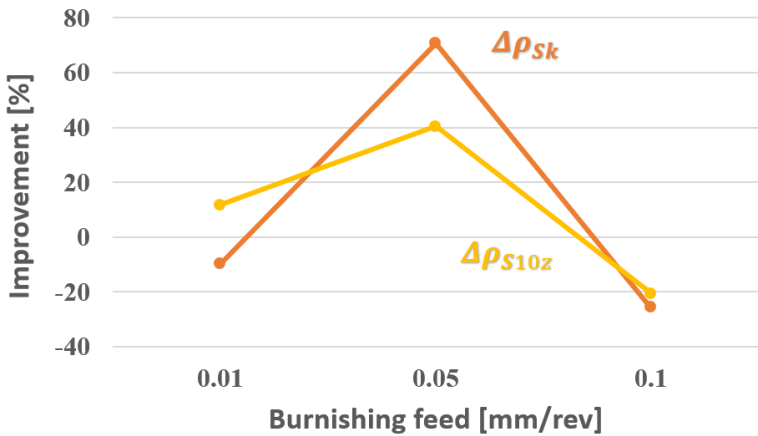


Diagram 2. Influence of feed rate on the analysed parameters

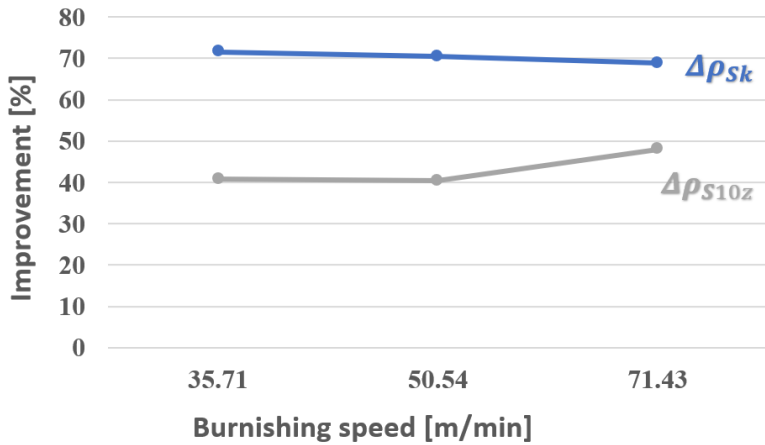


Diagram 3. Influence of burnishing speed on the analysed parameters

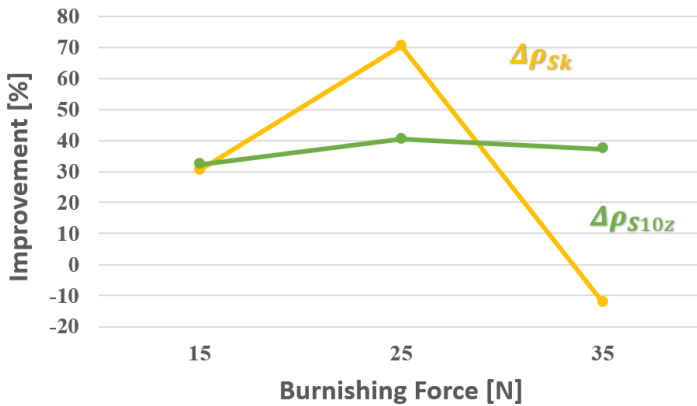


Diagram 4. Influence of number of passes on the analysed parameters

## 5. Summary

The paper presents the experimental investigation of burnishing process on cylindrical low alloyed aluminium workpieces, in which the analysed setting parameters were burnishing force, feed rate, speed and number of passes. The aim of the study was to examine the impact of these parameters on two different 3D surface roughness parameters: core height ( $S_k$ ) and ten-point height ( $S_{10z}$ ). Dimensionless ratios were designed to study the changes caused by burnishing and to make it even more obvious diagrams were created for each burnishing parameter. According to the measured, calculated and illustrated results, following statements can be made:

- As shown by the topography in Figures 6 and 7, the process corrected micro-threading caused by turning and reduced the distance between peaks and valleys.
- The most favourable changes in surface roughness were experienced in the cases of marked 6 and 7, when burnishing force was set to 15 N, feed rate was 0.05 mm/rev with 2 number of passes, while the speed was set to the higher values.

- Based on the diagrams, the middle values of the parameter ranges were the most advantageous and it can also be observed that changing the burnishing speed has only a small effect on the surface roughness

**References:** 1. V. Molnar: Minimization Method for 3D Surface Roughness Evaluation Area, *Machines* 192, pp. 1–16. 2021. 2. I. Sztankovics: Preliminary Study on the Function-Defining 3D Surface Roughness Parameters in Tangential Turning, *International Journal of Integrated Engineering* 15, pp. 1–10. 2023. 3. A. Nagy, J. Kundrak: Roughness of Face-Milled Surface Topography in Directions Relative to the Feed Movement, *Manufacturing Technology* 24, pp. 241–254. 2024. 4. A. Nagy: Influence of Measurement Settings on Areal Roughness with Confocal Chromatic Sensor on Face-Milled Surface, *Cutting & Tools in Technological System* 93, pp. 65–75. 2020. 5. M. Korzynski, K. Dudek, A. Palczak, B. Kruczek, P. Kocurek: Experimental Models and Correlations between Surface Parameters after Slide Diamond Burnishing, *Measurement Science Review* 18, pp. 123–129. 2018. 6. S. Swirad: Surface Texture Analysis after Hydrostatic Burnishing on X38CrMoV5-1 Steel, *Chinese Journal of Mechanical Engineering* 91, pp. 1–10. 2019. 7. F. T. Kebede, Cs. Felho: Examining the Impact of Slide Burnishing Parameters on the 3D Surface Features of Medium Carbon Steel, *Journal of Production Engineering* 27, pp. 30–35. 2024. 8. H. Luo, J. Liu, L. Wang, Q. Zhong: Investigation of the burnishing force during the burnishing process with a cylindrical surfaced tool, *Int. J. Advertising of Manufacture Technology* 25, pp. 454–459. 2005. 9. Y. Xinbo, W. Lijiang: Effect of Various Parameters on the Surface Roughness of an Aluminum Alloy Burnished with a Spherical Surfaced Polycrystalline Diamond Tool, *Int. J. of Machine Tools & Manufacture* 39, pp. 459–469. 1999. 10. A. Alexey Vereschaka: Improvement of working efficiency of cutting tools by modifying its surface properties by application of wear-resistant complexes, *Adv. Mat. Research*. 712-715, pp. 347–351. 2013. 11. H. Livatyali: A Novel Force Control Strategy for Improved Surface Integrity in Low Plasticity Burnishing, *Journal of Engineering Sciences* 10, pp. 18–26. 2024. 12. L. Luca, S. Neagu-Ventzel, I. Marinescu: Effects of working parameters on surface finish in ball-burnishing of hardened steels, *Precision Engineering* 29, pp. 253–256. 2005. 13. W. Grzeski, B. Kruszynski, A. Ruszaj: Surface integrity of machined surfaces, *Materials Science*, pp. 143–179. 2010. 14. ISO 22081:2021, Geometrical product specifications (GPS) — Geometrical tolerancing — General geometrical specifications and general size specifications, (2021), <https://www.iso.org/standard/72514.html> (Viewed: 14/09/24) 15. Olympus Introduction to Surface Roughness Measurement, *Roughness Measurement Guidebook*, pp. 34–36. 2017. 16. T.A. El-Taweel, M.H. El-Axir: Analysis and optimization of the ball burnishing process through the Taguchi technique, *International Journal of Advanced Manufacturing Technologies* 41, pp. 301–310. 2009.

Вікторія Ференчик, Мішкольц, Угорщина

## ВПЛИВ АЛМАЗНОГО ВИГЛАДЖУВАННЯ НА СЕРЕДНЄ ЗНАЧЕННЯ ВИСОТИ НЕРІВНОСТЕЙ ПОВЕРХНІ ( $R_z$ )

**Анотація.** Якість поверхні завжди відіграє дуже важливу роль у правильному проектуванні деталей машини з властивостями, які можуть позитивно вплинути, наприклад, на термін служби, зносостійкість та корозію, жорсткість контакту, вібрацію тощо. Для традиційних процесів обробки багато дослідників показали, що необхідної якості поверхні можна досягти

шляхом встановлення правильних комбінацій параметрів [1-4]. З цієї причини в даній дослідницькій роботі я вивчаю метод фінішної обробки, що не ріжеться, ковазюче вигладжування, яке знижує параметри шорсткості компонента і сприяє кращій корозійній стійкості. Це пов'язано з тим, що в приповерхневому шарі утворюються залишкові напруги стиснення, які тим самим підвищують його мікротвердість. Цей процес також призводить до підвищення втомної міцності, більшої стійкості до втоми від тертя та зменшення зносу. Алмазне вигладжування – це процес холодного пластичного формування, який використовується як фінішна обробка для покращення поверхні після звичайних процедур видалення стружки. Під час шліфування циліндричних поверхонь деформуючий інструмент переміщається під дією випалювальної сили по поверхні заготовок, яка обертається із заданою швидкістю, при цьому на приповерхневому шарі відбувається пружно-пластична деформація. У статті представлено експериментальне дослідження впливу різних параметрів вигладжування на шорсткість 3D поверхні на циліндричних заготовках з низьколегованого алюмінію. Для проведення порівняльного аналізу було реалізовано вимірювання шорсткості поверхні до і після шліфування вимірювальним приладом Altisurf 520. Результати дозволяють більш точно розуміти процеси, які відбуваються під час процедури, і для промислового застосування можуть допомогти скоротити час і витрати на обробку за рахунок кращого визначення параметрів налаштування.

**Ключові слова:** 3D параметри шорсткості; алмазне вигладжування; цілісність поверхні; полікристалічний алмазний інструмент.

## **CORRELATION ANALYSIS BETWEEN COMPONENTS OF FORCE AND VIBRATION IN TURNING OF 11SMN30 STEEL**

Tanuj **Namboodri** [0000-0002-6256-7075], Csaba **Felhő** [0000-0003-0997-666X]

University of Miskolc, 3515 Miskolc-Egyetemváros, Hungary  
[csaba.felho@uni-miskolc.hu](mailto:csaba.felho@uni-miskolc.hu)

**Received: 30 October 2024 / Revised: 15 November 2024 / Accepted: 27 November 2024 /  
Published: 15 December 2024**

**Abstract.** *Workability of material is defined as the ease of operating on it. 11SMn30 is widely used material in automobile manufacturing industries. Cutting forces have been shown to be the most effective measure for understanding metal machining processes. The forces which helps in performing machining operation also affects the cutting tool, in terms of deformation, bend, wear, which leads to the vibration in the machining system. This article aims to study the correlation between feed, components of cutting forces and components of vibration in turning of 11SMn30 steel grade using dynamometer and MPU6050 sensor.*

**Keywords:** *turning operation; cutting forces & vibrations; correlation; analysis of variance.*

### **1. Introduction**

Automation in manufacturing industries is rapidly growing, enhancing the efficiency, leading towards the reduced labour costs and with automation adoption of Artificial Intelligence is on the rise as industries recognises the benefits of in predictive maintenance and operational efficiency which helps industries in economic growth and provide low cost solutions in the market. In addition the companies are prioritizing the sustainable practices by focusing on use of material. Material selection one of the key variable in manufacturing industry, which frequently causes uncertainties regarding its workability. Workability of material is defined as the ease of operating on it. 11SMn30 is widely used material in automobile manufacturing industries. Joy. B. et al . [1], Varghese. L. et al. [2], quoted 11SMn30 is free cutting steel for bulk applications for joining elements in mechanical engineering and automotive components. Manganese and sulphide exist as globules in the microstructure which aid machining these act as discontinuities in the sites to form broken chips as a results there is need to investigate the workability of 11SMn30 steel grade. Sharma V. et al. [3] highlighted that to produce automotive parts like shafts, turning operation is more economical, turning is the most commonly used machining process in the manufacturing industries to produce shaft from hard material. For turning operation to be efficient selection of cutting

© T. Namboodri, C. Felhő, 2024

parameters is highly recommended by the researchers. Machining parameters like feed, cutting forces & vibrations induced from the interaction of workpiece and tool, because they directly influence the quality of product, production time, tool wear, which overall determines financial aspect of the manufacturing industries and has an impact on the environment. For successful implementation of turning study of cutting forces is critically important because cutting forces correlate strongly with cutting performance such as surface accuracy, tool wear, tool breakage, cutting temperature. The cutting force is one of the most significant characteristic variable to monitor the cutting operations, since its variation is directly proportional to the cutting conditions. Cutting forces have been shown to be the most effective measure for understanding metal machining processes. I.N. Tansel et al., Rashid Ali Laghari et al., Ulvi Şeker et al. [11, 12, 13] mentioned that a significant amount of this research has been focused on measuring and predicting cutting forces during milling. That is because understanding the cutting forces is critical because they have a direct impact on heat generation, tool wear, machined surface quality, and shape precision. They are also used to design machine tools, cutting tools, and fixtures. The forces which helps in performing machining operation also affects the cutting tool, in terms of deformation, bend, wear, which leads to the vibration in the machining system [7]. Abdullah Aslan [8], investigated variations in cutting forces and vibration have a direct impact on flank wear. Yong Wu [9] mentioned one of the most frequently accepted reasons for machine tool chatter is surface regeneration theory, the machined surface becomes wavy as a result of relative vibrations between the tool and the workpiece as a result, delay effects emerge in metal cutting operation models because the cutting force is controlled by the chip thickness, which is dependent on both the present tool position and the delayed position from the preceding cut, in result, the delay-differential equations are employed to describe machine tool vibrations, and regenerative machine tool chatter can be viewed as the manifestation of self-excited oscillations in a time-delay system. Zerti et al. [10], applied the Taguchi approach to reduce cutting forces and other machinability parameters. Turning experiments were carried out on AISI D3 steel using CC650 grade ceramic inserts without coolant. Haibo X. and Zhanjiang W. [11], [12] investigated how EVC factors such as vibration frequency, amplitude, and cutting speed affect cutting forces. The feed force is responsible for the cutting in machining operation therefore the feed rate influences the cutting forces which results in vibration. U. Şeker et al. [5], investigated that increasing feed rate, increases cutting forces in turning operations, while cutting force decreases with increasing speed. K. Kotaiah et al. [13], studied feed has a marked effect on stability in turning due to force variation. Rashid Ali Laghari et al. [6] studied that higher depth of cut, followed by feed rate, increases the cutting force, while higher cutting speed reduces it. Kagde and Deshmukh [14], studied optimization and effect of cutting parameters on numerous performance variables (work piece surface roughness, spindle load) obtained during

turning operations. Experiments were conducted using a CNMG 090308 PF carbide insert as a tool and HCHC steel as the workpiece material. The results highlights that spindle speed and feed rate were the most important parameters for numerous cutting performance metrics. Shunmugesh. K. [15]. results suggest that the key factor influencing surface roughness is depth of cut, followed by cutting speed and feed. Sharma V. et al. and Al-Ahmari [3], [16], studied the machinability of turning operations using input parameters such as cutting speed, feed, depth of cut, and nose radius, and response parameters such as cutting forces and surface roughness. Dong Y. [17] study demonstrate that cutting conditions such as cutting speed, feed rate, depth of cut, tool geometry, and material qualities of both the tool and the workpiece, have a considerable impact on the surface quality of machined parts. Monitoring quality indicators such as tool wear, surface integrity, cutting power, and vibration, among others, contributes to consistent development for best results. Monitoring process parameters improves productivity and increases tool life. To make these parameters more efficient, additional investigations on cutting forces and vibration components are critical for complete understanding. Not only should the significance of their weight be understood, but so should their correlation with one another, several studies on cutting forces and vibrations is undertaken, however study of the components and their relationship with machining parameters is still lacking.

This article aims to study the correlation between feed, components of cutting forces and components of vibration in turning of 11SMn30 steel grade using dynamometer and MPU6050 sensor. To check the significance of the regression model, analysis of variance (ANOVA) was used.

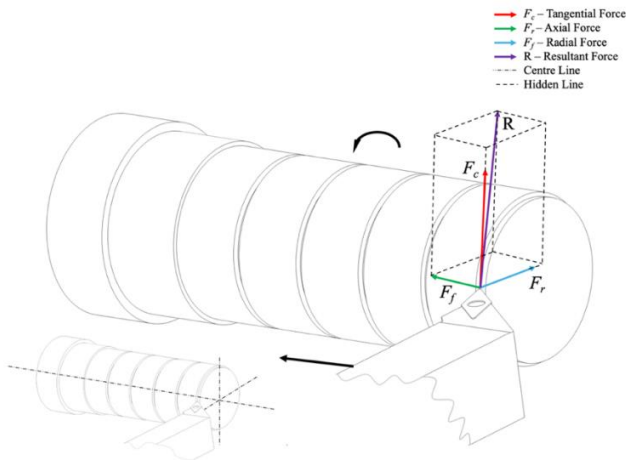


Figure 1. Components of cutting force in turning operation

## 2. Material and Methods

The workpiece shaft used to conduct the experiment is 11SMn30 grade steel, non-alloy quality, and not suitable for heat treatment, according to EN 10277-3 [18]. The chemical composition and mechanical properties of the workpiece material are shown in Table 1.

Table 1. Chemical composition in weight% and Mechanical properties of steel 11SMn30 (1.0715)

C	Si	Mn	P	S
max 0.14	max 0.05	0.9 – 1.3	max 0.11	0.27 – 0.33
Nominal thickness (mm)	$R_m$ – Tensile strength (MPa) (+C)	$R_{p0.2}$ 0.2% proof strength (MPa) (+C)	Min. elongation at fracture (%) (+C)	
40 – 63	400 – 650	305	9	

The workpiece was parted in 5 equal parts as shown in Fig. 2. It is to understand the relation between feed, components of cutting forces and vibration with varied feed in all the surfaces as mentioned in Table 2. [19]. Other machining parameters like depth of cut was kept 1 mm, spindle speed was 2000 rpm, for all the machining passes. Using these parameters, cutting forces and vibration data was recorded.

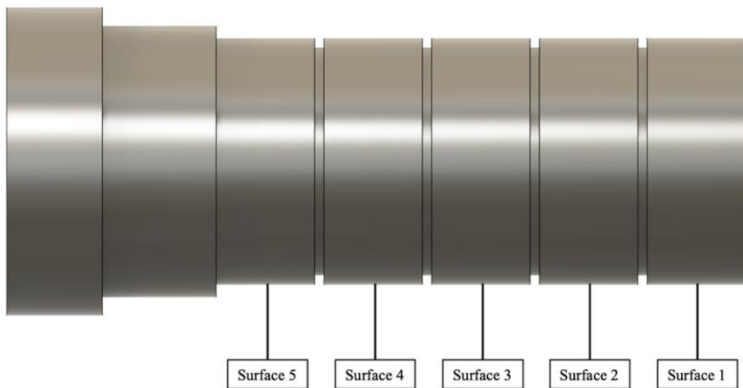


Figure 2. Partition of surfaces for the experiment.

The machining operation was repeated two times to collect more data on cutting forces and vibration, resulting in good correlation accuracy. The diameter of the workpiece specimen was 42 mm before machining, and it was reduced to 40 mm in first machining pass, after final pass it is 38 mm as shown in Fig. 3.

Table 2. Machining Parameters according to surface partition.

Surface No.	5	4	3	2	1
Feed ( $f_z$ ) mm/r	0.3	0.25	0.2	0.15	0.1
Depth of Cut ( $a_p$ ) mm	1	1	1	1	1
Spindle Speed RPM	2000	2000	2000	2000	2000

The specimen was divided into 5 equal parts of 16 mm length, each partitioned by a 1.5 mm groove, to test the vibrational signals and cutting forces at different feed rates and to draw the relationship between feed, cutting forces and vibration, Fig. 3. represents the final machined part to analyse the correlation between feed, cutting forces, and vibration.

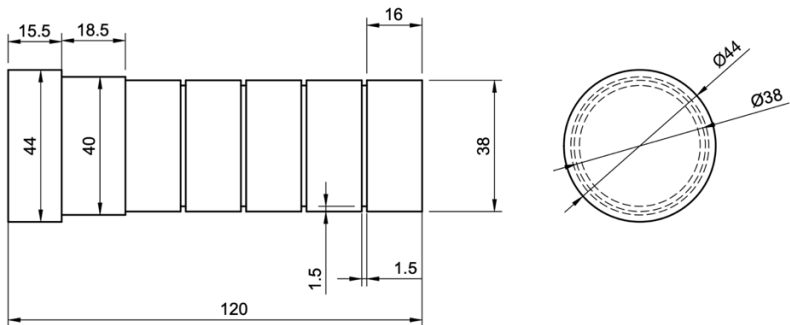


Figure 3. Drawing final machined part.

The tool used was the SVHBR2020K11 Walter Turn shank tool with screw clamping (S), as shown in Fig. 4. This tool has positive basic form insert and is appropriate for small-diameter shafts or low cutting pressures. The tool and insert specification for the VCGX style, used for the cutting operation, are listed in Table 3, [20].

Table 3. Tool & Insert Specification

Des.	Shank height	Shank width	Functiona l width	Functiona l length	Max Projectio n length	Orth. Rake angl e	Inclinatio n angle
Symbol	$h = h_1$	$b$	$f$	$l_1$	$l_4$	$\gamma$	$\lambda_s$
Value	20 m m	20 m m	25 mm	125 mm	19 mm	$0^\circ$	$0^\circ$
Insert Style	Insert Shape	Clearance Angle			Size	Corner Radius (Re)	
VCGX	35° Diamond	7° Positive			0.25	0.016	
Insert Material	Work Material	Machining Application			Insert Coating	Insert Thickness (S)	
Carbide	High Temp+Cast Iron+Non-Ferrous	Roughing & Finishing			Uncoated	0.125	

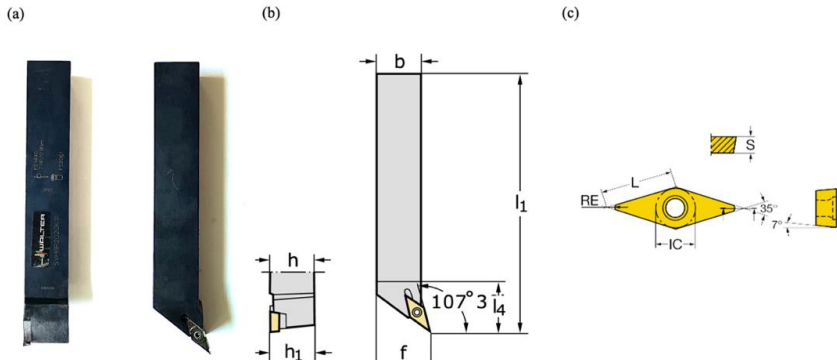


Figure 4. (a) Tool (b) Tool Specification (c) Insert specification [20]

The cylindrical turning operation was conducted in a dry condition using the Optimum Opti Turn S600 CNC machine Fig. 5(a). The vibrational data was collected by connecting the MPU6050 sensor to the tool, as seen in Fig. 5(c). MPU6050 sensor, the comprehensive 6-axis motion tracking device which integrates a 3-axis gyroscope, 3-axis accelerometer, and digital motion processor with ESP32 microcontroller comprised of two 240MHz cores [36, 37], each housing a Tensilica

Xtensa 32-bit LX6 microprocessor were used to measure the vibrational signal during each machining pass. The microcontroller was used to upload the code, and an SD card module connected to the microcontroller was used to gather the data. Sensor was attached to the tool with the help of a clip, the electronic setup was attached with the help of a screw to the tool holder in CNC machine, in case of movement of tool the electronic setup will also move to keep the connection secure between sensor and microcontroller, the microcontroller was attached to monitor to provide the power supply and also to visualise real time output vibration signals.

Fig. 5(b), depicts the electronic configuration. The orientation of sensor with respected to tool is shown in Fig. 5(c).

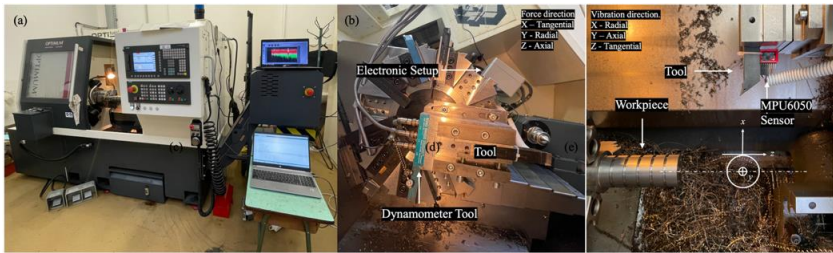


Figure 5. Experimental Setup (a) CNC Machine, (b) Dynamometer Setup, (c) Accelerometer Setup.

The cutting force components were measured using a three-component piezoelectric dynamometer, from Kistler Corporation 9257-A, Fig. 8(a) and 8(b). The dynamometer's output was amplified using a charge meter Kistler Corporation Model 5015A for three force components i.e.,  $F_x$ ,  $F_y$ ,  $F_z$ , has been connected to National Instruments Compact DAQ-9171 four-channel data acquisition unit (USB), The amplified signals from the charge amplifier are supplied into the data acquisition system, where they are transformed to digital output, which is then transferred to the computer. This setup allowed for the installation of a dynamometer between the tool holder of the CNC lathe and the tool without interacting with other parts. The three cutting force components were measured, as seen in Fig. 5(b). Tool, dynamometer and sensor position is defined in Fig. 5(b) and 5(c) respectively, monitor allows to validate the data during the process to avoid any error it is recommended to visualise the real time data. This configuration allowed the experiment to be conducted cleanly and without errors. Two boxes were fabricated using machining and 3D printing processes as shown in Fig. 5(b), and an outer wire casing was used to protect wires. These casings served as a shield to protect electronic setup from chips generated during the machining process.

### 3. Results

The results represents the calculated data of Force RMS (F RMS) for each components, for tangential cutting force (F RMS T), Radial cutting force (F RMS R) and axial cutting force (F RMS A), In Table 4. RMS calculation of force components is presented, it can be seen that active forces are the tangential and axial force as mentioned in article [23], the force RMS value measured for the tangential are much higher than radial and axial, and in comparison the significance of radial forces are much lower which is understandable because radial direction the tool is stationary and do not apply the force downwards. The results also presents the calculated values of vibration RMS for each components, Vibration RMS in tangential (Vb RMS T), Vibration RMS in Radial (Vb RMS R) and Vibration RMS in Axial (Vb RMS A), It can be concluded from Table 4. That tangential vibration RMS values is much higher in compared to radial and axial vibration.

Table 4. Forces RMS and Vibrations RMS data.

Individual							
Ex. No.	Feed Rate	F RMS T	F RMS R	F RMS A	Vb RMS T	Vb RMS R	Vb RMS A
EX1S1	0.1	216.63	2.3	111.34	9.09	5.23	1.51
EX1S2	0.15	315.01	3.26	161.4	9.09	5.24	1.67
EX1S3	0.2	395.4	5.16	181.98	9.14	5.25	1.49
EX1S4	0.25	473.69	7.46	191.19	9.28	5.32	1.78
EX1S5	0.3	532.61	10.91	183.74	9.43	5.31	1.75
EX2S1	0.1	206.59	4.39	114.63	9.08	5.22	1.47
EX2S2	0.15	303.55	6.7	164.73	9.12	5.24	1.48
EX2S3	0.2	366.82	11.71	178.89	9.1	5.25	1.41
EX2S4	0.25	425.64	19.03	182.08	9.3	5.31	1.79
EX2S5	0.3	Tool Break					

The active vibration considered is tangential and radial because it has much greater impact than the axial. It is understandable, because tool is moving in axial direction, so the vibration values can be ignored in axial direction. In terms of force

the axial force is much higher in comparison to radial because of the contact between workpiece and tool. Table 5. represents the correlation between individual directional forces and vibration, it can be concluded that feed has high influence on tangential and axial force which is considered as active force and weak correlation with radial forces. In terms of vibration feed has strong correlation on tangential and radial and weak correlation on axial. tangential and radial vibration are considered as active vibration.

Table 5. Correlation Analysis Feed, Forces RMS & Vibrations RMS.

	Feed Rate	F RMS T	F RMS R	F RMS A	Vb RMS T	Vb RMS R	Vb RMS A
Feed Rate	1	.989**	.693*	.864**	.899**	.918*	.681*
Force RMS Tangential	.989**	1	0.59	.890**	.871**	.900*	.674*
Force RMS Radial	.693*	0.59	1	0.581	0.607	.672*	0.446
Force RMS Axial	.864**	.890**	0.581	1	0.593	.731*	0.477
Vibration RMS Tangential	.899**	.871**	0.607	0.593	1	.914*	.794*
Vibration RMS Radial	.918**	.900**	.672*	.731*	.914**	1	.850*
Vibration RMS Axial	.681*	.674*	0.446	0.477	.794*	.850*	1
** Correlation is significant at the 0.01 level (2-tailed).							
* Correlation is significant at the 0.05 level (2-tailed).							

The one streak sign in table “\*”, Suggests correlation is significant at the 0.05 level (2-tailed). This indicates a moderately strong piece of evidence that the observed correlation is not due to chance. There's a 95% chance that a real relationship exists between the variables. tangential force also shows strong

relationship with tangential and radial vibration and comparatively weak relationship with axial, which can be understood by the above results of active vibration and active force. radial force shows weak relationship with vibration because it has very low value in compared with the other directional forces. There is a strong correlation between force components and vibration components which suggests that with change in value of force will influence the as well vibration induced. The analysis of force and vibration components as well as the correlation between the variables explains the influence of variables on one another, which can be used to overlook the variables with the less effect on the machining process.

#### **4. Conclusions**

The introduced approach can be used to understand the machinability of material and relationship between cutting forces and vibration, and several findings can be drawn from this study.

Individual forces and vibration data allows us to understand the impact and dependency of one variable on others. Tangential values in forces and vibration calculations are much higher compared to radial and axial values, which implies that tangential direction has significant impact on both forces and vibration.

The direction of active forces and active vibration differs, active force is the sum of tangential and axial, whereas active vibration considers the sum of tangential and radial direction.

Correlation analysis results.

Feed Rate shows strong correlation with F RMS tangential and F RMS axial with 98.9% and 86.4% correlation respectively, also with the Vibration RMS Tangential and Vibration RMS Radial with 89.9% and 91.8% correlation.

Components of forces also show the strong correlation with components of vibration which suggests that the with change in value of cutting force value influences the vibration, which can be used to predict the vibration in tool.

**References:** **1.** Joy, B. & Kumar, P. M. Optimization in Turning of 11sMn30 Through Process Capability Index. Materials Today: Proceedings vol. 11 [www.sciencedirect.com](http://www.sciencedirect.com) (2019). **2.** Varghese, L. Multi-Objective Optimization of Machining Parameters during Dry Turning of 11SMn30 Free Cutting Steel Using Grey Relational Analysis. [www.sciencedirect.com/www.materialstoday.com/proceedings](http://www.sciencedirect.com/www.materialstoday.com/proceedings) 2214-7853 (2017). **3.** Sharma, V., Kumar, P. & Misra, J. P. Cutting force predictive modelling of hard turning operation using fuzzy logic. in Materials Today: Proceedings vol. 26 740–744 (Elsevier Ltd, 2019). **4.** Tansel, I. N. et al. Tool Wear Estimation in Micro-Machining. Part I: Tool Usage-Cutting Force Relationship. International Journal of Machine Tools & Manufacture vol. 40 (2000). **5.** Şeker, U., Kurt, A. & Çiftçi, I. The effect of feed rate on the cutting forces when machining with linear motion. J Mater Process Technol 146, 403–407 (2004). **6.** Laghari, R. A., Li, J. & Mia, M. Effects of turning parameters and parametric optimization of the cutting forces in machining SiCp/Al 45 wt% composite. Metals (Basel) 10, 1–22 (2020). **7.** Yu, Q., Li, S., Zhang, X. & Shao, M. Experimental study on correlation between turning temperature rise and turning vibration in dry turning on aluminum alloy. International Journal of Advanced Manufacturing Technology 103, 453–469 (2019). **8.** Aslan, A. Optimization and analysis of

process parameters for flank wear, cutting forces and vibration in turning of AISI 5140: A comprehensive study. Measurement (Lond) 163, (2020). **9.** Wu, Y., Song, Q., Liu, Z. & Wang, B. Stability of turning process with a distributed cutting force model. International Journal of Advanced Manufacturing Technology 102, 1215–1225 (2019). **10.** Zerti, O., Yallese, M. A., Khettabi, R., Chaoui, K. & Mabrouki, T. Design optimization for minimum technological parameters when dry turning of AISI D3 steel using Taguchi method. International Journal of Advanced Manufacturing Technology 89, 1915–1934 (2017). **11.** Xie, H. & Wang, Z. Study of cutting forces using FE, ANOVA, and BPNN in elliptical vibration cutting of titanium alloy Ti-6Al-4V. International Journal of Advanced Manufacturing Technology 105, 5105–5120 (2019). **12.** Huang, W. T. & Wu, Z. X. Research on optimization of cutting force in AISI D2 hardened steel ultrasonic vibration-assisted turning. in Journal of Physics: Conference Series vol. 2345 (Institute of Physics, 2022). **13.** Rama Kotaiah, K., Srinivas, J. & Sekar, M. Force Feed Effects on Process Stability in Turning. Bangladesh J. Sci. Ind. Res vol. 45 [www.banglajol.info](http://www.banglajol.info) (2010). **14.** Kagade, V. R. & Deshmukh, R. R. Experimental investigation of turning operation using carbide inserts. International Journal of Applied Research in Mechanical Engineering 87–89 (2011) doi:10.47893/IJARME.2011.1017. **15.** Kumar, S., Gupta, M. & Satsangi, P. S. Multiple-response optimization of cutting forces in turning of UD-GFRP composite using Distance-Based Pareto Genetic Algorithm approach. Engineering Science and Technology, an International Journal 18, 680–695 (2015). **16.** Al-Ahmari, A. M. A. Predictive machinability models for a selected hard material in turning operations. J Mater Process Technol 190, 305–311 (2007). **17.** Jang, D. Y., Choi, Y. G., Kim, H. G. & Hsiao, A. Study of the correlation between surface roughness and cutting vibrations to develop an on-line roughness measuring technique in hard turning. Int. J. Mach. Tools Manuf. 36, 453–464 (1996). **18.** EU Steel and Alloy Grades Number. Preprint at <http://www.steelnumber.com/en/> (2024). **19.** Ridwan, F. & Xu, X. Advanced CNC system with in-process feed-rate optimisation. Robot Comput. Integr. Manuf. 29, 12–20 (2013). **20.** Walter. Preprint at <https://www.walter-tools.com/en-us> (2024). **21.** Cameron, N. ESP32 Microcontroller BT – ESP32 Formats and Communication: Application of Communication Protocols with ESP32 Microcontroller. 1–54 (2023). **22.** Cameron, Neil. ESP32 formats and communication : application of communication protocols with ESP32 microcontroller. 646 (2023). **23.** Rizal, M., Ghani, J. A. & Mubarak, A. Z. Design and Development of a Tri-Axial Turning Dynamometer Utilizing Cross-Beam Type Force Transducer for Fine-Turning Cutting Force Measurement. Sensors 22, (2022).

Тануй Намбудрі, Чаба Фельхо, Мішкольц, Угорщина

## **АНАЛІЗ КОРЕЛЯЦІЇ МІЖ СКЛАДОВИМИ СИЛИ І ВІБРАЦІЇ ПРИ ТОКАРНІЙ ОБРОБЦІ СТАЛІ 11SMN30**

**Анотація.** Технологічність матеріалу визначається як зручність його обробки. Сталь марки 11SMn30 є широко використовуваним матеріалом в автомобілебудуванні. Відомо, що зусилля різання є найбільш ефективним показником для розуміння процесів обробки металу. Для успішної реалізації токарної обробки вивчення сил різання є критично важливим, оскільки сили різання сильно корелюють з такими показниками різання, як точність поверхні, знос інструменту, поломка інструменту, температура різання. Сила різання є однією з найбільш значущих характеристичних змінних для контролю за операціями різання, оскільки її зміна прямо пропорційна умовам різання. Сили, які допомагають при виконанні операції механічної обробки, впливають і на ріжучий інструмент, в плані деформації, вигину, зносу, що призводить до вібрації в системі обробки. Компоненти сили різання у цьому дослідженні були виміряні за допомогою трикомпонентного п'єзоелектричного динамометра фірми Kistler Corporation 9257-A. Вихідний сигнал динамометра був посилений за допомогою підсилювача Kistler Corporation моделі 5015A для трьох силових складових, а саме,  $F_x$ ,  $F_y$ ,  $F_z$ , був підключений до чотириканального блоку збору даних (USB) National Instruments CompactDAQ-9171, Посилені сигнали від підсилювача надходять в систему збору даних, де перетворюються на цифровий вихід, який потім передається на

комп'ютер. Ця установка дозволила встановити динамометр між тримачем інструменту токарного верстата з ЧПУ та інструментом без взаємодії з іншими деталями. Було виміряно три складові сили різання. Положення інструменту, динамометра і датчика визначено відповідно, монітор дозволяє перевіряти дані в процесі для уникнення будь-яких помилок, рекомендується візуалізувати дані в реальному часі. Така конфігурація дозволила провести експеримент чисто і без помилок. Дана стаття має на меті вивчити взаємозв'язок між подачею, складовими сил різання і складовими вібрації в токарній обробці сталі марки 11SMn30 з використанням динамометра і MPU6050 датчика.

**Ключові слова:** операція токарної обробки; сили різання та вібрації; кореляція; дисперсний аналіз.

## **PROGRESS AND CHALLENGES IN PLUNGE MILLING: A REVIEW OF CURRENT PRACTICES AND FUTURE DIRECTIONS**

Afraa **Khattab** [0009-0001-8698-1043], Csaba **Felhő** [0000-0003-0997-666X]

University of Miskolc, 3515 Miskolc-Egyetemváros, Hungary  
[csaba.felho@uni-miskolc.hu](mailto:csaba.felho@uni-miskolc.hu)

**Received: 23 October 2024 / Revised: 14 November 2024 / Accepted: 27 November 2024 /  
Published: 15 December 2024**

**Abstract.** *This review examines recent advancements and ongoing challenges in plunge milling. It is an increasingly utilised machining process renowned for its high material removal rates, particularly with hard-to-machine materials like hardened steels and titanium alloys. Plunge milling's unique perpendicular tool path offers enhanced stability and reduced lateral cutting forces, making it valuable for applications that demand precision and efficiency, such as aerospace and automotive manufacturing. The paper systematically analyses and synthesises research on critical areas of plunge milling optimization, including tool geometry, material selection, coating technologies, and process parameters, highlighting strategies to mitigate common issues like rapid tool wear and chip evacuation difficulties. In this comprehensive overview, the review introduces theoretical and experimental findings on optimizing plunge milling tools and process parameters—such as cutting speed, feed rate, and coolant delivery—that are essential for improving performance and achieving desirable surface finishes. The paper also explores innovative trends, including AI-driven optimization algorithms and hybrid machining systems, which hold promise for addressing persistent limitations and enhancing plunge milling's industrial applicability. By consolidating findings from recent studies, this review contributes to a deeper understanding of plunge milling's role in high-precision manufacturing and identifies future research directions for advancing the process. The insights presented offer practical and strategic implications, aiming to guide ongoing developments in plunge milling technology and its adoption across various precision-oriented industries.*

**Keywords:** *Plunge milling; material removal; tool optimization; cutting tool coatings.*

### **1. Introduction**

The role of machining in modern manufacturing cannot be overstated. It enables the production of complex, precise components across various industries [1-3]. Among the diverse machining techniques, milling has remained a staple, particularly in aerospace, automotive, and tooling sectors, where precision and efficiency are paramount [1]. Traditional methods like end and face milling typically involve sweeping the tool horizontally across the workpiece, making them effective but sometimes less efficient for high-volume material removal [2].

© A. Khattab, C. Felhő, 2024

Plunge milling has emerged as a powerful alternative, especially for machining hard materials such as titanium alloys and hardened steels [3].

Characterized by a unique vertical, perpendicular tool path, plunge milling distinguishes itself by moving directly downward into the material, substantially improving tool stability and cutting efficiency [4]. This approach minimizes lateral cutting forces, extending tool life and reducing the likelihood of tool deflection—a benefit crucial for applications requiring deep cavity cuts or roughing operations. The technique's effectiveness has been demonstrated in demanding applications like the production of Kaplan turbine blades, where removing material rapidly without compromising precision is essential [5].

Beyond its practical benefits, plunge milling has prompted extensive research efforts to optimize tool geometry, material selection, and process parameters, including coating technologies and cutting speeds. However, challenges persist, particularly in managing rapid tool wear and optimizing chip evacuation [6,7]. This review synthesizes current advancements and presents a detailed analysis of optimization strategies, exploring emerging technology systems. By addressing these critical factors, plunge milling will continue evolving, meeting the growing demands of high-precision, high-efficiency manufacturing environments.

## **2. A Comprehensive Exploration**

Precision milling hardened steel components, such as dies, molds, and press tools, often rely on monolithic milling cutters [8]. In this context, plunge milling has gained significant attention due to its ability to produce complex shapes and intricate features [2] accurately. Driven by the need for greater productivity, high-speed machining has also gained traction across industries [1]. This approach typically uses small feed per tooth and minimal pick feed, which effectively produce precise surface textures and are widely adopted for end-milling operations in manufacturing die/mold components and precision mechanical parts [7,9]. For milling complex surfaces, specific parameters, like axial cutting depth, play a critical role in ensuring surface quality and dimensional accuracy [8], [10]. Furthermore, advancements in tool steel properties have supported the broader adoption of plunge milling, as these developments enable achieving a high surface hardness while maintaining a softer core structure advantageous for applications such as machinery parts and specialty fasteners [11,12]. The precision and adaptability of plunge milling make it an effective technique for accurately producing complex shapes and narrow apertures, enhancing its relevance across manufacturing sectors focused on intricate part production [13-15].

## **3. Process Optimization of plunge milling**

### 3.1. Cutting tool optimization

Tool optimization is essential in plunge milling, where high mechanical stresses and thermal loads, especially with rugged materials, impact cutting efficiency, tool life, and overall performance. Adjusting tool geometry and material selection is critical to these improvements [1]. In particular, tool failure due to wear is a significant concern that requires carefully selecting cutting parameters, cooling strategies, and tool designs [6].

#### 3.1.1. Optimization of Tool Geometry

The geometry of a cutting tool plays a critical role in plunge milling, particularly in how it handles cutting forces and heat generation. Key geometric aspects include the rake angle, clearance angle, and cutting-edge shape [2]. Plunge milling tools typically feature a positive rake angle to reduce cutting resistance and a large clearance angle to facilitate better chip evacuation, thereby minimizing the risk of tool clogging. A study by Ding et al. [16] showed that optimizing the cutting-edge radius and tool profile can significantly reduce tool wear by distributing cutting forces more evenly across the tool surface [6]. This is particularly important for maintaining tool stability during the high-impact forces of plunge milling, as shown in Figure 1 [7].

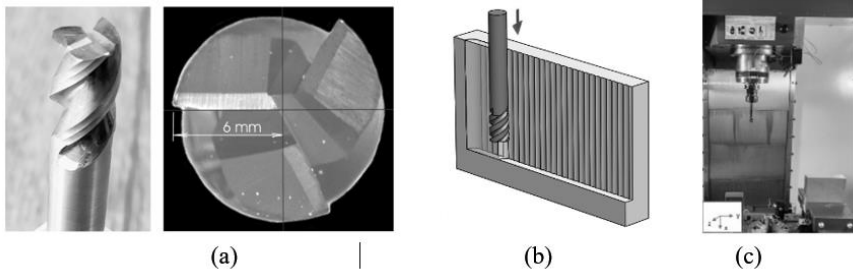


Figure 1. Used cutting tool, the strategy scheme, and Machining setup [7].

**Edge Preparation:** To reduce wear, the cutting-edge plunge milling tools can be tailored with micro-polishing or edge rounding techniques. These techniques help prevent chipping and fracture, which are common issues in plunge milling due to the aggressive vertical plunge of the tool into the material [6].

**Corner Design:** Tools used in plunge milling often have rounded or chamfered corners to increase strength and prevent the tool from fracturing at the corners under heavy loads. However, the tool tip's rounded corners can wear significantly during plunge milling, leading to potential failure. Common wear types include crater, flank, and notch wear. Understanding these can enhance tool life and performance, as is shown in Figure 2 [6]. Optimizing tool geometry increases tool life and improves chip

formation and surface finish [7]. Effective chip evacuation is critical in plunge milling. Chips generated during the plunge motion can obstruct the tool path, leading to tool damage and poor surface quality [4,5].

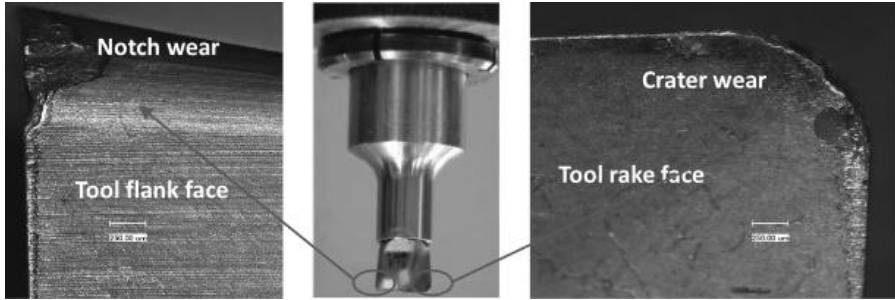


Figure 2. Plunge tool wear morphology [6].

### **3.1.2 Optimization of the Cutting Tool Design**

The tools used in plunge milling have distinct features compared to those used in other techniques. Plunge milling cutters are designed with robust cutting edges and reinforced corners to handle the high stresses generated during vertical cutting. Due to their strength and heat resistance, these tools are typically made from carbide or high-speed steel (HSS) [2, 17]. Cutting tool design plays a critical role in the efficiency and performance of plunge milling operations. Recent advancements in materials technology, as is shown in Figure 3, have enabled the development of high-strength and ultra-hard materials that are challenging to machine using conventional methods [18–20]. Appropriate selection is also crucial in plunge milling, as it directly impacts the tool's wear resistance, thermal stability, and overall service life [6, 21, 22]. Cemented carbide, diamond-coated tools, and polycrystalline diamonds are among the materials extensively studied for their suitability in applications [8, 17, 23]. Recent research has focused on material selection and the optimization of cutter geometry. Investigations into the effects of axial and radial rake angles and the impact of interference during helical milling have provided valuable insights into the design of high-performance milling cutters [10, 22, 24, 25].

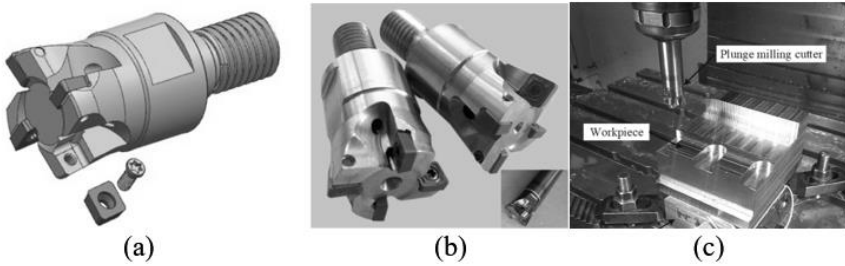


Figure 3. Optimizing the (a) Design, (b) Manufactured, (c) Experiment, plunge milling cutting tool [20].

### 3.1.3. Optimizing Cutter Geometry and Material Selection

Due to the significant differences in scale, traditional design methods for milling cutters are no longer applicable to micro-scale tools [26], [27]. Researchers have explored new micro-mill design approaches to address this challenge, focusing on optimizing cutting processes and integrating them with the tool design process, as shown in Figure 4 [21, 28]. One such approach is the development of parametric design systems for micro-mills, which leverage computer-aided design tools and programming techniques to establish a flexible and accurate tool design process [29–31]. This enables the creation of customized tool designs tailored to specific machining requirements by deconstructing the geometric features of micro-mills and connecting them through expression functions [1, 32, 33].

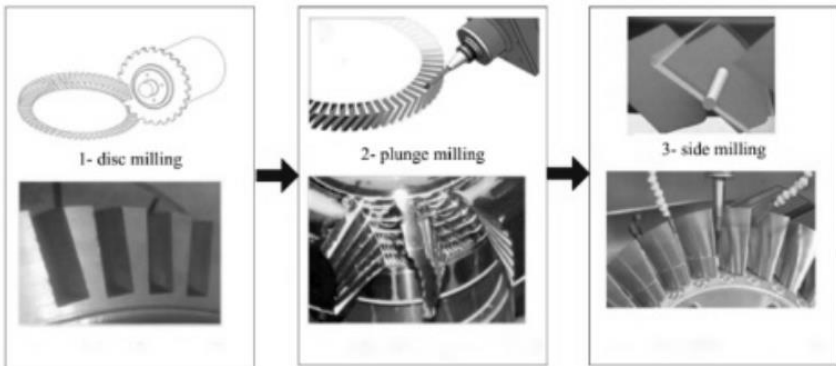


Figure 4. Optimizing cutting processes in plunge milling [28].

## 3.2. Tool Materials and Coatings Optimization

The choice of tool material is critical to ensuring high-performance plunge milling. Cemented carbide is the most commonly used material for plunge milling tools due to its high hardness and wear resistance [7, 23]. High-speed steel (HSS) is also used in some applications, though it is less wear-resistant than carbide [17, 34]. In recent years, research has focused on advanced coatings to enhance tool performance further [35, 36]. Coated carbide tools have significantly improved wear resistance and thermal stability compared to uncoated tools. Typical coating materials include:

- **Titanium Nitride (TiN)** is a widely used coating that provides wear resistance and reduces friction during cutting [37, 38]
- **(Sweatt et al., 2008) Titanium Aluminum Nitride (TiAlN)** offers superior oxidation and thermal degradation resistance, making it ideal for high-speed plunge milling in materials that generate significant heat during cutting [7, 34, 39].
- **Diamond-like Carbon (DLC) Coatings:** These coatings provide extreme hardness and low friction, improving tool life when machining abrasive materials like composites and hardened steels [1, 40]. Zagórski et al. show that TiAlN coatings, especially with AlTiN, enhance plunge milling by creating a thermal barrier that reduces adhesive wear and stabilises cutting forces. TiAlN-coated tools lower cutting forces under high-speed machining (HSM) conditions, boosting tool durability and milling efficiency in demanding applications [34, 41].

### **3.3. Process Parameter Optimization**

Optimizing cutting parameters such as cutting speed, feed rate, and depth of cut is essential for minimising tool wear and maximising machining performance [1, 2]. Finite Element Modeling (FEM) has become a vital tool in predicting how different cutting parameters affect tool performance in plunge milling. By simulating the forces, temperatures, and stresses acting on the tool during machining, FEM helps identify the optimal cutting conditions that will reduce wear while maintaining high MRR [21, 42, 43].

– **Cutting Speed:** Increasing the cutting speed improves MRR but generates more heat, leading to thermal wear. Balancing speed with appropriate cooling strategies is critical for maintaining tool life [5, 12, 44].

– **Feed Rate:** High feed rates lead to increased cutting forces, which can cause tool deflection and wear. Optimizing the feed rate helps maintain tool stability and reduces cutting-edge chipping [6, 12, 45].

– **Depth of Cut:** In plunge milling, the cut's depth directly affects the tool's load. Guo et al. found that reducing the cut depth in combination with coated tools can significantly lower tool wear, especially when machining hard materials like Inconel and titanium alloys [1, 20].

– **Workpiece Materials and Geometries:** Advances in materials technology have led to the development of high-performance composites, ceramics, and other difficult-to-machine materials, which pose unique challenges for conventional machining [1, 24]. Plunge milling has emerged as a viable solution for effectively machining these advanced materials. It leverages the direct application of energy to remove material without the limitations of traditional chip-removal methods [2]. The geometry of the workpiece, as shown in Figure, can significantly impact the tool path planning, cutter accessibility, and overall machining efficiency [1, 26, 46]. Research has explored using CAD-based visualization techniques and cutter accessibility maps to optimize the process for complex workpiece geometries, such as those encountered in the aerospace and automotive industries [2, 26, 47, 48]

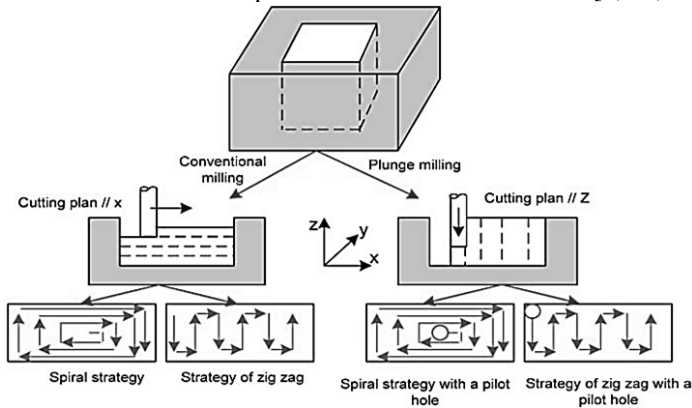


Figure 5. Machining strategies [26].

### 3.4. Optimized Chip Management and Coolant Delivery:

In plunge milling, efficient and coolant delivery is vital due to the high intensity cutting process that can result in rapid chip accumulation [18, 19]. Researchers have developed innovative methods such as air-jet-assisted chip removal, high-pressure coolant systems, and optimized tool geometries. These techniques significantly improve chip evacuation, preventing tool interference, machine damage, and surface quality degradation [7, 19]. Moreover, cutting fluid and coolant delivery is crucial in plunge milling to extend tool life, avoid thermal damage, and preserve surface integrity [23, 49]. Advanced fluid delivery techniques, like minimum quantity lubrication (MQL) and cryogenic cooling, have been investigated to optimize cooling and lubrication. These advanced methods can enhance stability and improve surface quality and efficiency [35, 50].

### **3.5. Optimization Algorithms for Plunge Milling**

Optimizing operations is a complex task that requires considering various parameters, including tool geometry, material properties, and process conditions [29, 51]. Recent research has focused on developing advanced Optimization to improve the efficiency and productivity of plunge milling [52, 53]. These algorithms leverage computational models and simulation tools to predict and analyze the performance of plunge milling processes, enabling the selection of optimal cutting parameters, tool paths, and machining strategies, as shown in Figure 6 [1, 54, 55, 56,58]. Integrating these Optimization algorithms with CAD/CAM systems has further enhanced plunge milling capabilities, allowing for the integration of design, planning, and machining operations [51, 54, 55, 57].

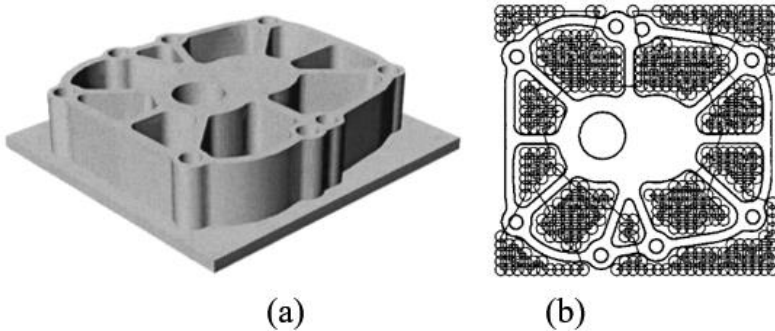


Figure 6. (a) Rendering of CAD drawing, (b) toolpoint path design(right) for a plunge milling example[58].

#### **4. Advantages of plunge milling:**

Plunge milling stands out in industrial machining for its high material removal rates (MRR), improved productivity, and efficient chip evacuation [1, 12, 59]. It is ideal for applications like mold and die-making, where precision is paramount [21, 28]. Unlike conventional methods, plunge milling directs the tool vertically into the material, reducing machining time and generating less heat, which extends tool life and enhances surface finish [55, 60]. It minimizes issues like tool deflection and vibration, allowing for better dimensional accuracy and control over the cuts, which is critical in complex geometries and intricate designs [22, 61]. Plunge milling enables advanced strategies like trochoidal tool paths and high-speed machining, reducing cutting forces and vibrations, enhancing tool life, and improving efficiency [1, 5]. Optimal parameters—such as cut depth and feed rate—help prevent surface and subsurface defects, especially in sensitive materials [4]. Its force control, tool

stability, and cost-effective precision make plunge milling suitable for complex, high-tolerance designs across industries [4, 41, 62].

## **5. Challenges and Limitations / Current Challenges:**

Critical challenges include rapid tool wear when machining superalloys, chip evacuation, and high tool costs [4, 20]. Grzesik et al. identified the need for better materials and cooling strategies to overcome limitations [5, 1].

### **5.1. Barriers to Adoption:**

The high initial cost of specialised plunge milling tools and the complexity of process Optimization have limited its adoption in smiles [4,1]. She pointed out the need for cost-effective solutions.

### **5.2. Technical challenges:**

Tool wear, particularly when machining abrasive materials, remains a significant challenge in plunge milling [27, 63]. Herbert et al. address the challenge of achieving near damage-free surfaces while minimising material removal during finishing operations [64], which can lead to cost savings and improved efficiency in manufacturing processes [4, 46].

### **5.3. Material-specific challenges:**

Plunge milling of superalloys such as titanium poses heat generation and tool life challenges. Due to machine capacity or tool wear, high-temperature alloys and lightweight materials may limit high-speed machining and high-performance cutting [63, 65].

### **5.4. Surface quality and integrity:**

Ensuring high-quality and consistent surface finish and integrity is crucial for the long-term performance of some components [51, 66]. Xin et al. note that multi-milling technology can increase cutting forces and vibrations, leading to surface defects like burrs, scratches, and micro-cracks that may weaken blisks over time by creating stress concentrators [28, 51, 66]. Guo et al. discovered that using the wavy-edge cutter reduced vibration amplitude by over 90% and cutting force by about 50% compared to straight-edge cutters [20].

## **6. Future Trends and Research Directions**

### **6.1. Smart Machining Systems:**

The study mentions the use of AI technology in intelligent machining, which includes various applications such as Optimization of machining parameters, real-time monitoring, and process control [21]. Hashmi et al. integrate sensors and AI in plunge milling to improve efficiency. Accelerometers on the spindle head measure forces, while AI processing detects and mitigates chatter, boosting material removal rates (MRR) and reducing machining time [64, 67]. Exploring advanced techniques to further optimise the tool path planning process, improve the selection of optimal plunger centres, and adapt the approach to various manufacturing scenarios [68].

### **6.2. Hybrid method:**

Researchers have explored enhancing plunge milling's capabilities by combining it with high-speed milling, laser-assisted machining, and additive manufacturing [1], which improve surface finish, boost material removal rates, and allow component repair or modification [64]. Effective integration requires advanced process planning, control algorithms, and coordination of multiple machining systems [42]. Xni et al. present a multi-milling technology for blisk processing that combines disc, plunge, and side milling to boost efficiency and reduce costs. Simulations reveal a 91.2% material removal rate, surpassing plunge and side milling (86.5%) and side milling alone (81.8%) [28, 51]. Omari et al. demonstrated that the Medial Axis Transformation can improve machining efficiency by expanding the milling area and converting shapes into efficient, tree-like structures for easier manipulation [31]. Also, using multi-axis milling machines could potentially revolutionise complex layered contour plunging processes, further enhancing the efficiency of plunge milling [31, 42, 69, 22].

### **6.3. Tool material development:**

Future advancements in tool materials will likely focus on hybrid composites and nanostructured coatings for improved durability and performance [7, 42]. Researchers focus on eco-friendly, energy-efficient plunge milling practices such as alternative cutting fluids, optimised energy use, and dry machining to reduce environmental impact, resource use, and costs while ensuring quality and productivity [1, 4].

### **6.4. Sustainability and Eco-Friendly Approach**

Altıntaş et al. developed a model to predict and reduce energy consumption in milling, aiding sustainable manufacturing through energy-efficient process planning

and parameter selection [27, 70]. Therefore, the study implicitly supports the idea that Optimizing milling contributes to sustainability goals [52]. Researchers aim to enhance machining while minimising the environmental impact, carbon emissions, and production costs associated with the grinding process [4, 51]. Awale et al. examine the grindability of AISI H13 tool steel using eco-friendly nano-lubricants under minimum quantity lubrication (MQL), aiming to enhance sustainability in tooling by improved surface integrity, reduced energy consumption, carbon emissions, and cost savings [50].

## 7. Conclusion

This review highlights plunge milling as a valuable machining method that enables high-efficiency material removal in hard-to-machine materials. By emphasising vertical cutting, plunge milling achieves significant improvements in tool stability and force reduction, proving especially beneficial for intricate and high-precision applications. Through an analysis of the latest research, this paper presents advancements in tool design, material selection, and process Optimizations that collectively address core challenges, such as tool longevity and effective chip evacuation. The findings underscore that, while plunge milling has established its place in the industry, continued research is essential to unlock its full capabilities and overcome existing limitations. This review provides a consolidated resource for current practices and future directions, supporting the evolution of plunge milling into a more versatile and sustainable manufacturing solution.

**References:** 1. *W. Grzesik*, Advanced machining processes of metallic materials: theory, modelling and applications, 2nd edition. Amsterdam Boston: Elsevier, 2017. 2. *S. Tichkiewitch, M. Tollenaere, and P. Ray, Eds.*, Advances in Integrated Design and Manufacturing in Mechanical Engineering II. Dordrecht: Springer Netherlands, 2007. doi: 10.1007/978-1-4020-6761-7. 3. *G. Madhavulu, S. V. N. A. Sundar, and B. Ahmed*, 'CAD/CAM solutions for efficient machining of turbo machinery components by Sturz milling method', in Proceedings of the 1996 IEEE IECON. 22<sup>nd</sup> International Conference on Industrial Electronics, Control, and Instrumentation, Taipei, Taiwan: IEEE, 1996, pp. 1490–1495. doi: 10.1109/IECON.1996.570604. 4. *L. Dong and M. Chen*, 'A comparative experimental study on the rough machining methods of centrifugal three-dimensional impellers', *Adv. Mech. Eng.*, vol. 16, no. 4, Apr. 2024, doi: 10.1177/16878132241244923. 5. *M. Bey, H. Bendifallah, Z. Tchanchane, A. Driouech, and D. L. Cherif*, '3-Axis Roughing of Complex Parts Using Plunge Milling Strategy'. 6. *J. Li, W. Yu, Q. An, and M. Chen*, 'A modelling and prediction method for plunge cutting force considering the small displacement of cutting layer', *Proc. Inst. Mech. Eng. Part B J. Eng. Manuf.*, vol. 234, no. 11, pp. 1369–1378, Sep. 2020, doi: 10.1177/0954405420921739. 7. *F. J. G. Silva et al.*, 'A Comparative Study of Different Milling Strategies on Productivity, Tool Wear, Surface Roughness, and Vibration', *J. Manuf. Mater. Process.*, vol. 8, no. 3, p. 115, May 2024, doi: 10.3390/jmmp8030115. 8. *M. Grabowski, J. Gawlik, J. Krajewska-Śpiewak, S. Skoczypiec, and P. Tyczyński*, 'Technological Possibilities of the Carbide Tools Application for Precision Machining of WCLV Hardened Steel', *Adv. Sci. Technol. Res. J.*, vol. 16, no. 1, pp. 141–148, Jan. 2022, doi: 10.12913/22998624/144340. 9. *S. H. Ryu, D. K. Choi, and C. N. Chu*, 'Roughness and texture generation on end milled surfaces', *Int. J. Mach. Tools Manuf.*, vol. 46, no. 3–4, pp. 404–412, Mar. 2006, doi:10.1016/j.jmachtools. 2005.05.010. 10. *T. L. Schmitz and K. S. Smith*, *Machining Dynamics: Frequency Response to Improved Productivity*. Cham: Springer International

Publishing, 2019. doi: 10.1007/978-3-319-93707-6. **11.** N. Yuvaraj, R. Arshath Raja, P. Palanivel, and N. V. Kousik, 'EDM Process by Using Copper Electrode with INCONEL 625 Material', IOP Conf. Ser. Mater. Sci. Eng., vol. 811, no. 1, p. 012011, Apr. 2020, doi: 10.1088/1757-899X/811/1/012011. **12.** A. A. Latif, M. R. Ibrahim, A. Z. Amran, and E. A. Rahim, 'A study on the effect of feed rate and cutting speed on surface roughness and material removal rate of mild steel', IOP Conf. Ser. Mater. Sci. Eng., vol. 257, p. 012025, Oct. 2017, doi: 10.1088/1757-899X/257/1/012025. **13.** Y. Altintas and J. H. Ko, 'Chatter Stability of Plunge Milling', CIRP Ann., vol. 55, no. 1, pp. 361–364, 2006, doi: 10.1016/s0007-8506(07)60435-1. **14.** Y. Altintas and M. Weck, 'Chatter Stability of Metal Cutting and Grinding', CIRP Ann., vol. 53, no. 2, pp. 619–642, 2004, doi: 10.1016/s0007-8506(07)60032-8. **15.** S. Liu, J. Xiao, Y. Tian, S. Ma, H. Liu, and T. Huang, 'Chatter-free and high-quality end milling for thin-walled workpieces through a follow-up support technology', J. Mater. Process. Technol., vol. 312, p. 117857, Mar. 2023, doi: 10.1016/j.jmatprotec.2023.117857. **16.** Y. Ding, R. Dwivedi, and R. Kovacevic, 'Process planning for 8-axis robotized laser-based direct metal deposition system: A case on building revolved part', Robot. Comput.-Integr. Manuf., vol. 44, pp. 67–76, Apr. 2017, doi: 10.1016/j.rcim.2016.08.008. **17.** G. T. Smith, CNC Machining Technology. London: Springer London, 1993. doi: 10.1007/978-1-4471-2053-7. **18.** D. Baffari, G. Buffa, D. Campanella, L. Fratini, and A. P. Reynolds, 'Process mechanics in Friction Stir Extrusion of magnesium alloys chips through experiments and numerical simulation', J. Manuf. Process., vol. 29, pp. 41–49, Oct. 2017, doi: 10.1016/j.jmapro.2017.07.010. **19.** J. A. Garcia-Barbosa, J. M. Arroyo-Ororio, and E. Córdoba-Nieto, 'Influence of tool inclination on chip formation process and roughness response in ball-end milling of freeform surfaces on Ti-6Al-4V alloy', Mach. Sci. Technol., vol. 21, no. 1, pp. 121–135, Jan. 2017, doi: 10.1080/10910344.2016.1260434. **20.** M. Guo, Z. Wei, Z. Zhang, M. Wang, and D. Zhai, 'Study on wavy-edge plunge milling cutter with chip split and cutting load reduction function', J. Manuf. Process., vol. 102, pp. 1059–1068, Sep. 2023, doi: 10.1016/j.jmapro.2023.08.020. **21.** Y. Cheng, J. Yang, D. Zuo, X. Song, and X. Feng, 'Tool design and cutting parameters Optimization for plunge milling blisk', Int. J. Manuf. Res., vol. 15, no. 3, p. 266, 2020, doi: 10.1504/ijmr.2020.108192. **22.** C. Sun, Y. Wang, and N. Huang, 'A new plunge milling tool path generation method for radial depth control using medial axis transform', Int. J. Adv. Manuf. Technol., vol. 76, no. 9–12, pp. 1575–1582, Feb. 2015, doi: 10.1007/s00170-014-6375-5. **23.** H. Chen, Z. Chen, and L. Li, 'Wear and Life of K40 Carbide Tool for Plunge Milling GH4169', J. Phys. Conf. Ser., vol. 2566, no. 1, p. 012058, Aug. 2023, doi: 10.1088/1742-6596/2566/1/012058. **24.** G. F. Barbosa and J. O. Savazzi, 'Influency of cutting tool's angle on milling of composite materials performed by robots', Braz. J. Oper. Prod. Manag., vol. 13, no. 2, p. 226, Jun. 2016, doi: 10.14488/bjopm.2016.v13.n2.a9. **25.** M. Fujiki, J. Ni, and A. J. Shih, 'Tool Path Planning for Near-Dry EDM Milling With Lead Angle on Curved Surfaces', J. Manuf. Sci. Eng., vol. 133, no. 5, Oct. 2011, doi: 10.1115/1.4004865. **26.** M. Al-Ahmad, A. d'Acunto, and P. Martin, 'Identification of Plunge Milling Parameters to Compare with Conventional Milling', in Advances in Integrated Design and Manufacturing in Mechanical Engineering II, S. Tichkiewitch, M. Tollenaere, and P. Ray, Eds., Dordrecht: Springer Netherlands, 2007, pp. 461–474. doi: 10.1007/978-1-4020-6761-7\_31. **27.** M. Reznicek and C. Horava, 'The Influence of the Choice of Machining Strategy on Production Technology', Manuf. Technol., vol. 24, no. 1, pp. 117–130, Feb. 2024, doi: 10.21062/mft.2024.014. **28.** H. Xin, Y. Shi, and T. Zhao, 'Compound efficient and powerful milling machine tool of blisk', Int. J. Adv. Manuf. Technol., vol. 98, no. 5–8, pp. 1745–1753, Sep. 2018, doi: 10.1007/s00170-018-2225-1. **29.** S. Cafieri, F. Monies, M. Mongeau, and C. Bes, 'Plunge milling time optimization via mixed-integer nonlinear programming', Comput. Ind. Eng., vol. 98, pp. 434–445, Aug. 2016, doi: 10.1016/j.cie.2016.06.015. **30.** J. Dong, Z. Chang, Y. Chang, Z. C. Chen, and N. Wan, 'A novel approach to modeling of multi-axis plunge milling and its application on the simulation of complex part plunging', Int. J. Adv. Manuf. Technol., vol. 102, no. 5–8, pp. 1141–1151, Jun. 2019, doi: 10.1007/s00170-018-2952-3. **31.** M. A. Omari, M. M. Rababah, and M. M. AlFakheh, 'A novel approach for plunging using plungers of predefined geometry', Int. J. Interact. Des. Manuf. IJIDeM, Sep. 2024, doi: 10.1007/s12008-024-02079-4. **32.** J. Fu, S. B. Joshi, and J. M. Catchmark, 'Sputtering rate of micromilling on water ice with focused ion beam in a cryogenic environment', J. Vac. Sci. Technol. Vac. Surf. Films, vol. 26, no. 3, pp. 422–429, May 2008, doi: 10.1116/1.2902962. **33.** M. Yeakub, R. Mehruz,

- A. Ali, and A. Faris, 'Micro Electro Discharge Milling for Microfabrication', in *Micromachining Techniques for Fabrication of Micro and Nano Structures*, M. Kahrizi, Ed., InTech, 2012, doi: 10.5772/38721. **34.** L. Roucoules, *Advances on Mechanics, Design Engineering and Manufacturing III: Proceedings of the International Joint Conference on Mechanics, Design Engineering & Advanced Manufacturing, JCM 2020, June 2-4, 2020*, in *Lecture Notes in Mechanical Engineering*. Erscheinungsort nicht ermittelbar: Springer Nature, 2021. **35.** P. Das, P. Bandyopadhyay, and S. Paul, 'Finish form grinding of thermally sprayed nano-structured coatings', *Adv. Mater. Process. Technol.*, vol. 5, no. 1, pp. 39–52, Jan. 2019, doi: 10.1080/2374068x.2018.1510680. **36.** M. Rettig et al., 'Carbide Brake Rotor Surface Coating Applied by High-performance-laser Cladding', in *EuroBrake 2020 Technical Programme, FISITA, 2020*, doi: 10.46720/eb2020-mds-025. **37.** P. J. Blau, B. C. Jolly, J. Qu, W. H. Peter, and C. A. Blue, 'Tribological investigation of titanium-based materials for brakes', *Wear*, vol. 263, no. 7–12, pp. 1202–1211, Sep. 2007, doi: 10.1016/j.wear.2006.12.015. **38.** J. Qu, P. J. Blau, and B. C. Jolly, 'Oxygen-diffused titanium as a candidate brake rotor material', *Wear*, vol. 267, no. 5–8, pp. 818–822, Jun. 2009, doi: 10.1016/j.wear.2008.12.044. **39.** P. Sivaprakasam, E. Abebe, R. Čep, and M. Elangovan, 'Thermo-Mechanical Behavior of Aluminum Matrix Nano-Composite Automobile Disc Brake Rotor Using Finite Element Method', *Materials*, vol. 15, no. 17, p. 6072, Sep. 2022, doi: 10.3390/ma15176072. **40.** W. C. Sweatt, D. D. Gill, D. P. Adams, M. J. Vasile, and A. A. Claudet, 'Diamond milling of micro-optics', *IEEE Aerosp. Electron. Syst. Mag.*, vol. 23, no. 1, pp. 13–17, Jan. 2008, doi: 10.1109/aes-m.2008.4444483. **41.** I. Zagorski, 'Cutting force components in rough milling of magnesium alloys with a TiAlN-coated carbide tool', in *2022 IEEE 9th International Workshop on Metrology for AeroSpace (MetroAeroSpace)*, Pisa, Italy: IEEE, Jun. 2022, pp. 64–69, doi: 10.1109/MetroAeroSpace54187.2022.9856171. **42.** F. Monies, I. Danis, C. Bes, S. Cafieri, and M. Mongeau, 'A new machining strategy for roughing deep pockets of magnesium-rare earth alloys', *Int. J. Adv. Manuf. Technol.*, vol. 92, no. 9–12, pp. 3883–3901, Oct. 2017, doi: 10.1007/s00170-017-0444-5. **43.** Y. S. Zhai, H. L. Song, and J. S. Hu, 'Study on Plunge Milling Cutter Design with Finite Element Analysis', *Mater. Sci. Forum*, pp. 836–837, pp. 425–429, Jan. 2016, doi: 10.4028/www.scientific.net/MSF.836-837.425. **44.** S. Wakaoka, Y. Yamane, K. Sekiya, and N. Narutaki, 'High-speed and high-accuracy plunge cutting for vertical walls', *J. Mater. Process. Technol.*, vol. 127, no. 2, pp. 246–250, Sep. 2002, doi: 10.1016/s0924-0136(02)00151-6. **45.** Y. Liang, D. Zhang, J. Ren, and Y. Xu, 'Feedrate scheduling for multi-axis plunge milling of open blisks', *Proc. Inst. Mech. Eng. Part B J. Eng. Manuf.*, vol. 229, no. 9, pp. 1525–1534, Sep. 2015, doi: 10.1177/0954405415555741. **46.** C. R. J. Herbert, J. Kwong, M. C. Kong, D. A. Axinte, M. C. Hardy, and P. J. Withers, 'An evaluation of the evolution of workpiece surface integrity in hole making operations for a nickel-based superalloy', *J. Mater. Process. Technol.*, vol. 212, no. 8, pp. 1723–1730, Aug. 2012, doi: 10.1016/j.jmatprotec.2012.03.014. **47.** A. Damir, 'Modelling the dynamics of plunge milling with workpiece vibrations consideration'. **48.** G. J. Deng, S. L. Soo, R. Hood, K. Marshall, A. L. Mantle, and D. Novovic, 'Assessment of workpiece surface integrity and dimensional/geometrical accuracy following finish plunge end milling of holes drilled with worn tools in PM-processed nickel based superalloy', *Procedia CIRP*, vol. 123, pp. 398–403, 2024, doi: 10.1016/j.procir.2024.05.070. **49.** E. Y. T. Adesta, Avicenna, I. Hilmy, and M. R. H. C. Daud, 'Toolpath strategy for cutter life improvement in plunge milling of AISI H13 tool steel', *IOP Conf. Ser. Mater. Sci. Eng.*, vol. 290, p. 012040, Jan. 2018, doi: 10.1088/1757-899X/290/1/012040. **50.** A. S. Awale, A. Chaudhari, A. Kumar, M. Z. Khan Yusufzai, and M. Vashista, 'Synergistic impact of eco-friendly nano-lubricants on the grindability of AISI H13 tool steel: A study towards clean manufacturing', *J. Clean. Prod.*, vol. 364, p. 132686, Sep. 2022, doi: 10.1016/j.jclepro.2022.132686. **51.** T. Huang, X.-M. Zhang, J. Leopold, and H. Ding, 'Tool Orientation Planning in Milling With Process Dynamic Constraints: A Minimax Optimization Approach', *J. Manuf. Sci. Eng.*, vol. 140, no. 11, p. 111002, Nov. 2018, doi: 10.1115/1.4040872. **52.** R. S. Altıntaş, M. Kahya, and H. Ö. Ünver, 'Modelling and optimization of energy consumption for feature based milling', *Int. J. Adv. Manuf. Technol.*, vol. 86, no. 9–12, pp. 3345–3363, Oct. 2016, doi: 10.1007/s00170-016-8441-7. **53.** L. Dong and J. Wang, 'A study of interferential tool position correcting algorithms in 3D impeller variable-axis rough plunge milling', *Proc. Inst. Mech. Eng. Part B J. Eng. Manuf.*, vol. 237, no. 1–2, pp. 122–133, Jan. 2023, doi: 10.1177/09544054221098609. **54.**

*M. Bey, Z. Tchantchane, L. Khaidri, and N. Benhenda*, 'Toward the automation of the plunge milling strategy for roughing sculptured surfaces from stl models'. 15th International Research/Expert Conference "Trends in the Development of Machinery and Associated Technology", TMT 2011, 12-18 September 2011/Prague, Czech Republic/ pp. 97–100. **55.** *F. Y. Han, D. H. Zhang, M. Luo, and B. H. Wu*, 'Optimal CNC plunge cutter selection and tool path generation for multi-axis roughing free-form surface impeller channel', *Int. J. Adv. Manuf. Technol.*, vol. 71, no. 9–12, pp. 1801–1810, Apr. 2014, doi: 10.1007/s00170-014-5608-y. **56.** *S. Perumalsamy and V. Kaliyamurthy*, 'Leveraging Blockchain with Optimal Deep Learning-Based Drug Supply Chain Management for Pharmaceutical Industries', *Comput. Mater. Contin.*, vol. 77, no. 2, pp. 2341–2357, 2023, doi: 10.32604/cmc.2023.040269. **57.** *K. Zhuang, X. Zhang, X. Zhang, and H. Ding*, 'Force Prediction in Plunge Milling of Inconel 718', in *Intelligent Robotics and Applications*, vol. 7507, C.-Y. Su, S. Rakheja, and H. Liu, Eds., in *Lecture Notes in Computer Science*, vol. 7507, Berlin, Heidelberg: Springer Berlin Heidelberg, 2012, pp. 255–263. doi: 10.1007/978-3-642-33515-0\_26. **58.** *H. Tawfik*, 'A New Algorithm to Calculate the Optimal Inclination Angle for Filling of Plunge-milling'. *International Journal of CAD/CAM / v.6, no.1, 2006*, pp. 193-198. **59.** *H. Wang and K. Tao*, 'Study on material removal and cutting analysis in ball helical milling process', *Proc. Inst. Mech. Eng. Part C J. Mech. Eng. Sci.*, vol. 236, no. 24, pp. 11493–11504, Dec. 2022, doi: 10.1177/09544062221110463. **60.** *K. Zhuang, X. Zhang, D. Zhang, and H. Ding*, 'On cutting parameters selection for plunge milling of heat-resistant-super-alloys based on precise cutting geometry', *J. Mater. Process. Technol.*, vol. 213, no. 8, pp. 1378–1386, Aug. 2013, doi: 10.1016/j.jmatprotec.2013.03.007. **61.** *V.-H. Bui, P. Gilles, G. Cohen, and W. Rubio*, 'Develop Model for Controlled Depth Milling by Abrasive Water Jet of Ti6Al4V at Jet Inclination Angle', in *Advances on Mechanics, Design Engineering and Manufacturing III*, L. Roucoules, M. Paredes, B. Eynard, P. Morer Camo, and C. Rizzi, Eds., in *Lecture Notes in Mechanical Engineering*, Cham: Springer International Publishing, 2021, pp. 21–27. doi: 10.1007/978-3-030-70566-4\_5. **62.** *I. Danis, F. Monies, P. Lagarrigue, and N. Wojtowicz*, 'Cutting forces and their modelling in plunge milling of magnesium-rare earth alloys', *Int. J. Adv. Manuf. Technol.*, vol. 84, no. 9–12, pp. 1801–1820, Jun. 2016, doi: 10.1007/s00170-015-7826-3. **63.** *Q. Cheng et al.*, 'Study on tool wear for efficient grooving blisk with disc milling cutter', *J. Mech. Sci. Technol.*, vol. 37, no. 10, pp. 5335–5348, Oct. 2023, doi: 10.1007/s12206-023-0935-2. **64.** *Y. Shi and G. Zheng*, 'The algorithm of layering calculation for corner plunge milling tool path', *Int. J. Adv. Manuf. Technol.*, vol. 91, no. 5–8, pp. 2059–2075, Jul. 2017, doi: 10.1007/s00170-016-9942-0. **65.** *R. Neugebauer, W. Drossel, R. Wertheim, C. Hochmuth, and M. Dix*, 'Resource and Energy Efficiency in Machining Using High-Performance and Hybrid Processes', *Procedia CIRP*, vol. 1, pp. 3–16, 2012, doi: 10.1016/j.procir.2012.04.002. **66.** *J. X. Ren, C. F. Yao, D. H. Zhang, Y. L. Xue, and Y. S. Liang*, 'Research on tool path planning method of four-axis high-efficiency slot plunge milling for open blisk', *Int. J. Adv. Manuf. Technol.*, vol. 45, no. 1–2, pp. 101–109, Nov. 2009, doi: 10.1007/s00170-009-2153-1. **67.** *A. W. Hashmi, H. S. Mali, A. Meena, I. A. Khilji, M. F. Hashmi, and S. N. B. M. Saffe*, 'Artificial intelligence techniques for implementation of intelligent machining', *Mater. Today Proc.*, vol. 56, pp. 1947–1955, 2022, doi: 10.1016/j.matpr.2021.11.277. **68.** *X. Q. Wang, Z. C. Wei, D. Wang, D. B. Zhang, X. Y. Wang, and M. J. Wang*, 'A supplementary processing method of residual material in impeller plunge milling', *J. Manuf. Process.*, vol. 108, pp. 1–11, Dec. 2023, doi: 10.1016/j.jmapro.2023.10.076. **69.** *Z. C. Chen and S. Abdelkhalik*, 'A New Approach to Planning Plungers Paths for Efficient 2½-Axis Computer Numerically Controlled Plunge Milling of Complex Pockets With Islands', *J. Manuf. Sci. Eng.*, vol. 136, no. 4, Aug. 2014, doi: 10.1115/1.4027538. **70.** *G. Urbikain Pelayo, D. Olvera-Trejo, M. Luo, K. Tang, L. N. López De Lacalle, and A. Elías-Zuñiga*, 'A model-based sustainable productivity concept for the best decision-making in rough milling operations', *Measurement*, vol. 186, p. 110120, Dec. 2021, doi: 10.1016/j.measurement.2021.110120.

Афраа Хаттаб, Чаба Фельхо, Мішкольц, Угорщина

## **ПРОГРЕС І ПРОБЛЕМИ ВРІЗНОГО ФРЕЗЕРУВАННЯ: ОГЛЯД ПОТОЧНОЇ ПРАКТИКИ ТА МАЙБУТНІХ НАПРЯМКІВ**

**Анотація.** У цьому огляді літератури розглядаються останні досягнення та поточні проблеми в врізного фрезерування. Це все більш часто використовуваний процес обробки, відомий своєю високою швидкістю видалення матеріалу, особливо з важкооброблюваними матеріалами, такими як загартовані сталі та титанові сплави. Унікальна перпендикулярна траєкторія інструменту врізного фрезерування забезпечує підвищену стабільність і зменшує поперечні сили різання, що робить його цінним для застосувань, які вимагають точності та ефективності, таких як аерокосмічне та автомобільне виробництво. У статті системно аналізуються та узагальнюються дослідження з критично важливих областей оптимізації врізного фрезерування, включаючи геометрію інструменту, вибір матеріалу, технології покриття та параметри процесу, висвітлюючи стратегії пом'якшення поширених проблем, таких як швидкий знос інструменту та труднощі з евакуацією стружки. У цьому всеосяжному огляді в огляді представлені теоретичні та експериментальні висновки щодо оптимізації інструментів для врізного фрезерування та параметрів процесу, таких як швидкість різання, швидкість подачі та подача охолоджуючої рідини, які мають важливе значення для підвищення продуктивності та досягнення бажаної обробки поверхні. У статті також досліджуються інноваційні тенденції, включаючи алгоритми оптимізації на основі штучного інтелекту та гібридні системи обробки, які є перспективними для вирішення постійних обмежень і підвищення промислової застосовності врізного фрезерування. Узагальнюючи результати нещодавніх досліджень, цей огляд сприяє глибшому розумінню ролі врізного фрезерування у високоточному виробництві та визначає майбутні напрямки досліджень для вдосконалення цього процесу. Представлені ідеї мають практичні та стратегічні наслідки, спрямовані на спрямування поточних розробок у технології врізного фрезерування та її впровадження в різних галузях, орієнтованих на точність.

**Ключові слова:** врізне фрезерування; видалення матеріалу; оптимізація інструменту; покриття ріжучого інструменту.

## ASSESSMENT OF THE ROOT MEAN SQUARE DEVIATION ON SURFACES MACHINED BY HIGH-FEED TANGENTIAL TURNING

István Sztankovics [0000-0002-1147-7475], István Pásztor [0000-0002-6971-3063],

University of Miskolc, 3515 Miskolc-Egyetemváros, Hungary

[istvan.sztankovics@uni-miskolc.hu](mailto:istvan.sztankovics@uni-miskolc.hu)

Received: 29 October 2024 / Revised: 12 November 2024 / Accepted: 27 November 2024 /  
Published: 15 December 2024

**Abstract.** *Recent advancements in machining focus on precision, efficiency, and handling harder materials, driven by sectors like aerospace and automotive. Hard machining, or processing materials over 45 HRC, presents challenges such as rapid tool wear, intense heat, and maintaining dimensional accuracy. Innovations in cutting tool materials and CNC technology have improved these processes, but tool degradation and high forces still complicate machining hardened materials. Surface roughness is a key quality metric, impacting performance factors like wear resistance and fatigue life. By optimizing cutting parameters, manufacturers aim to achieve consistent surface finishes, essential for durability in demanding applications. In this paper, the effect of the input parameters (depth of cut, feed, and cutting speed) are analysed on selected surface roughness parameters. The setup parameters were selected according to the full factorial design of experiment method. The results showed that higher feed rates resulted in rougher finishes, leading to greater spacing between profile elements and steeper surface profiles in the studied range.*

**Keywords:** *design of experiments; mean spacing of profile; root mean square deviation; root mean square slope; surface roughness; tangential turning.*

### 1. Introduction

In recent years, the field of machining has undergone significant advancements due to the increasing demand for precision, efficiency, and cost-effectiveness in manufacturing processes [1, 2]. Development trends in machining are largely driven by innovations in material science, tool design, and automation. Modern machining procedures have evolved to handle not only traditional soft and medium-hard materials but also a range of harder materials, such as hardened steels, superalloys, and composites [3–5]. This shift is driven by industries like aerospace, automotive, and medical manufacturing, which require components with high wear resistance and structural integrity. As a result, machining processes have adapted to achieve these demanding specifications through innovations in cutting tools, machining centres, and process control systems [7–9]. The development of advanced tooling materials, such as carbide, cermet, ceramic, and cubic boron nitride (CBN), The development of advanced tooling materials, such as carbide, cermet, ceramic, and

© I. Sztankovics, I. Pásztor, 2024

cubic boron nitride (CBN), has significantly enhanced the machinability of hard materials. In addition, high-speed machining, adaptive control, and computer numerical control (CNC) technologies allow for greater precision and reduced cycle times, improving productivity. The integration of digital technologies, including real-time monitoring and data analytics [10, 11], further refines these processes, enabling manufacturers to predict tool wear, optimize cutting parameters, and minimize downtime. However, despite these technological advancements, hard machining remains a challenging area due to the inherent difficulties associated with processing hardened materials.

Hard machining, specifically the machining of materials with a hardness level exceeding 45 HRC, poses several challenges. The primary difficulty is the increased wear and failure rate of cutting tools [12, 13], which leads to frequent tool replacements and higher production costs. The elevated hardness of materials generates intense heat and cutting forces during the machining process, resulting in rapid tool degradation. Heat dissipation in hard machining is also problematic; as cutting temperatures rise, tool wear accelerates, impacting surface finish and dimensional accuracy [14, 15]. Additionally, achieving desired geometrical tolerances and surface finishes in hard materials requires precise control over cutting parameters, including feed rate, depth of cut, and cutting speed. The presence of hard carbides and other abrasive constituents within these materials can further complicate the machining process, making it challenging to achieve consistent results.

Surface roughness is a critical quality parameter in machining [16–18] and is particularly important in the context of hard machining. Surface roughness affects the functional performance of machined components, influencing properties such as fatigue resistance, friction, wear, and corrosion resistance [19, 20]. In applications where components must withstand high stress or operate in harsh environments, a smooth and consistent surface finish is essential. Consequently, evaluating and controlling surface roughness has become a central aspect of machining research. Surface roughness evaluation typically involves measuring parameters like the Average Roughness ( $R_a$ ), Root Mean Square Roughness ( $R_q$ ), and Mean Spacing of Profile elements ( $R_{ms}$ ), which provide insights into the micro-topography of the machined surface [21, 22]. Various methods are used to assess surface roughness, including contact and non-contact measurement techniques [23]. Contact methods, such as stylus profilometers, physically trace the surface to record roughness values, while non-contact methods, such as optical and laser-based systems, offer faster measurements with less risk of damaging the surface. Advanced software tools and three-dimensional surface analysis have made it possible to obtain detailed topographical information, enabling engineers to better understand the effects of machining parameters on surface quality. With these methods, researchers can optimize machining processes by examining the impact of cutting speed, feed, depth

of cut, and tool geometry on surface roughness. By improving control over surface quality in hard machining, manufacturers can enhance the reliability, durability, and performance of critical components.

In summary, while advancements in machining technology have enabled significant progress in processing hard materials, challenges remain. The optimization of surface roughness through careful selection and control of cutting parameters is essential for achieving high-quality finishes in hard machining applications. In this paper, an innovative machining procedure (tangential turning) is studied, which could provide solutions for the challenges of hard machining. The surface roughness of the machined workpieces was assessed by the evaluation of Mean Spacing of Profile, Root Mean Square Deviation, Root Mean Square Slope roughness parameters. The study aims to find connections between the input technological parameters (feed, depth of cut, cutting speed), and the selected roughness parameters.

## **2. Experimental conditions and methods**

In this study, the tangential turning process was performed using a specialized tool designed for precision and durability. The tool setup included a SANDVIK Coromant CNMG 12 04 12-PM 4314 cutting insert for initial turning, followed by a tangential turning tool from HORN Cutting Tools Ltd., with a 45° inclination angle. The tangential tool assembly consisted of an S117.0032.00 insert and an H117.2530.4132 holder. The cutting edge used for tangential turning was an uncoated carbide insert of MG12 grade, selected for its ability to maintain sharpness under demanding cutting conditions.

The study focused on three primary technological parameters: cutting speed ( $v_c$ ), feed per revolution ( $f$ ), and depth of cut ( $a$ ). A 2<sup>3</sup> factorial design was employed to systematically vary these parameters and analyse their effects on cutting forces. For each parameter, two levels were defined. Cutting speed was set at 200 m/min as the lower level and 250 m/min as the upper level. Feed rates were chosen at 0.6 mm and 0.8 mm, while the depth of cut was varied between 0.1 mm and 0.2 mm. In total, eight different parameter setups were tested, as shown in Table 1. These ranges allowed for a comprehensive assessment of the analysed parameters.

Table 1 – Experimental setups

Setup	1	2	3	4	5	6	7	8
$f$ [mm]	0.6	0.8	0.6	0.8	0.6	0.8	0.6	0.8
$v_c$ [m/min]	200	200	250	250	200	200	250	250
$a$	0.1	0.1	0.1	0.1	0.2	0.2	0.2	0.2

[mm]								
------	--	--	--	--	--	--	--	--

The workpiece material selected for these experiments was 42CrMo4 alloyed steel, which was heat-treated to a hardness of 410 HV10 to replicate typical conditions encountered in hard machining applications. Cylindrical workpieces with an outer diameter of 65 mm were prepared for the tests, providing a consistent geometry for evaluating the surface roughness.

All experiments were conducted on an EMAG VSC 400 DS hard machining centre. This advanced machining centre enabled precise control of parameters and consistent conditions across each setup, ensuring accurate and reliable data collection for the analysis.

An AltiSurf 520 3D topography instrument equipped with a confocal chromatic probe was used for measurements following the machining tests. Measurement parameters were chosen in accordance with ISO 21920:2021 standards. Roughness profiles for each surface were recorded along three generatrix lines and subsequently analysed with AltiMap Premium 6.2.7487 surface analysis software.

The evaluated 2D surface texture parameters [X] were the following (ISO 21920:2021):

- $R_q$  – Root Mean Square Deviation of the assessed profile corresponds to the standard deviation of the height distribution on the sampling length. [ $\mu\text{m}$ ]
- $R_{sm}$  – Mean Spacing of profile elements, defined on the evaluation length. This parameter is interesting on surfaces having periodic or pseudo-periodic motifs, such as turned or structured surfaces, where this parameter approximates their spacing. [mm]
- $R_{dq}$  – Root Mean Square Slope of the assessed profile, defined on the sampling length. A low value is found on smooth surfaces while higher values can be found on rough surfaces with microroughness. [ $^\circ$ ]

Polynomial equations were also developed to calculate and represent the factors under study according to the design of experiments method, as shown in Equation 1. This equation incorporates variables ( $f, v_c, a_p$ ) and their interactions, with constants ( $k_i$ ) representing the influence of each factor. In this study, roughness parameters are expressed as the function  $y(f, v_c, a_p)$ . These equations provide a quantitative and visual means to assess the effects of each factor, offering a structured approach to optimize machining processes for enhanced dimensional accuracy and surface quality.

$$y(v_c, f, a) = k_0 + k_1v_c + k_2f + k_3a + k_{12}v_c f + k_{13}v_c a + k_{23}fa + k_{123}v_c fa \quad (1)$$

### 3. Experimental results

The experiments were carried out and the selected surface roughness parameters are measured for each setup three times on three separate directrix of the workpiece. The measurement results than averaged for each setup for the evaluation. The values of Root Mean Square Deviation are shown in Table 2, the results of Mean Spacing are presented in Table 3, and Table 4 contains the data of Root Mean Square slope. Equation 2-4 present the deducted calculation formulas of the previously declared roughness parameters, which are determined in the form of Equation 1 based on the design of experiments methodology.

$$R_q(f, v_c, a) = -0.0412fv_c a + 0.00661fv_c + 4.55fa + 0.877f + 0.0402v_c a - 0.00569v_c - 6.09a + 0.388 \quad (2)$$

$$R_{sm}(f, v_c, a) = -0.00463fv_c a + 0.000480fv_c + 1.17fa - 0.0967f + 0.00297v_c a - 0.00035v_c - 0.773a + 0.119 \quad (3)$$

$$R_{dq}(f, v_c, a) = -2.19fv_c a + 0.017fv_c + 380.3fa + 28.3f + 1.57v_c a + 0.005v_c - 272.6a - 6.70 \quad (4)$$

Table 2 – Measurement results of the Root Mean Square Deviation

$R_q$ [ $\mu\text{m}$ ]	Setup							
No.	1	2	3	4	5	6	7	8
1	0.55	0.89	0.55	0.92	0.52	0.82	0.57	0.81
2	0.53	0.90	0.54	0.95	0.52	0.83	0.58	0.87
3	0.55	0.93	0.52	0.91	0.52	0.79	0.62	0.91
Avg.	0.54	0.91	0.54	0.93	0.52	0.81	0.59	0.86

Table 3 – Measurement results of the Mean Spacing

$R_{sm}$ [mm]	Setup							
No.	1	2	3	4	5	6	7	8
1	0.0452	0.0510	0.0440	0.0480	0.0428	0.0510	0.0440	0.0470
2	0.0452	0.0460	0.0450	0.0460	0.0428	0.0520	0.0390	0.0460
3	0.0471	0.0550	0.0420	0.0520	0.0430	0.0550	0.0420	0.0480
Avg.	0.0458	0.0507	0.0437	0.0487	0.0429	0.0527	0.0417	0.0470

Table 4 – Measurement results of the Root Mean Square Slope

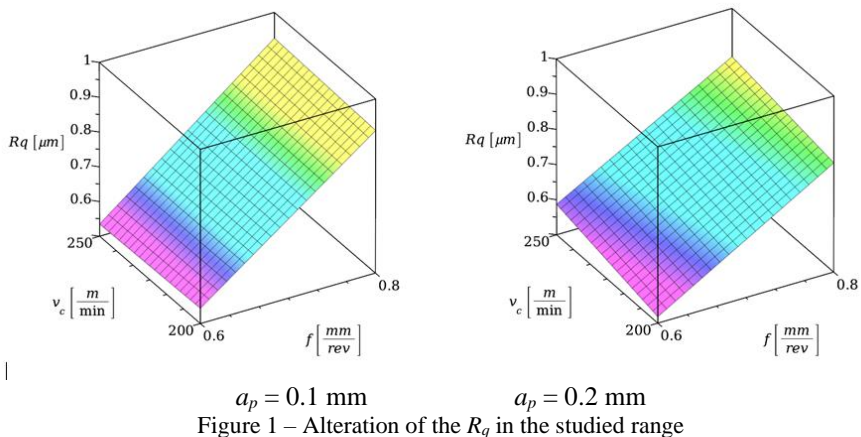
$R_{dq}$ [ $^\circ$ ]	Setup							
No.	1	2	3	4	5	6	7	8

1	14.5	18.6	15.9	19.1	14.6	18.4	17.7	17.5
2	14.3	20.3	16.9	20.6	14.7	19.7	18.8	18.1
3	13.7	19.2	15.9	18.6	15.3	18.5	18.3	18.5
Avg.	14.2	19.3	16.2	19.4	14.9	18.9	18.2	18.0

#### 4. Discussion

The paper continues with the analysis of the experimental results and the deduced equations. The three surface roughness parameter will be evaluated separately based on surface graphs based on Equation 2-4.

Figure 1 shows the alteration of the Root Mean Square Deviation in the studied range. When the feed rate increases from 0.6 mm to 0.8 mm, we observe an overall increase in Root Mean Square Deviation values, suggesting a rougher surface finish. For example, in the setups with a cutting speed of 200 m/min and depth of cut of 0.1 mm (Setups 1 and 2), the average pf Root Mean Square Deviation rises from 0.54  $\mu\text{m}$  to 0.91  $\mu\text{m}$  as the feed increases from 0.6 mm to 0.8 mm. This trend is consistent across different combinations of cutting speed and depth of cut, indicating that higher feed rates contribute to greater surface roughness due to the increased material removal rate per revolution, which results in more pronounced feed marks on the surface.

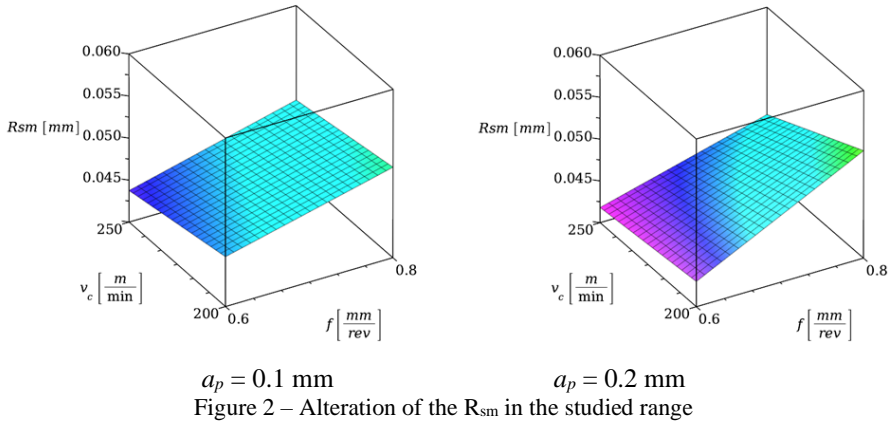


The influence of cutting speed on surface finish is less straightforward, with variations in effect depending on feed and depth of cut. In cases where the feed is 0.6 mm, increasing cutting speed from 200 m/min to 250 m/min (for example Setups 1 to 3 and 5 to 7) leads to a minor decrease in Root Mean Square Deviation, suggesting a slight improvement in surface quality. However, for experiments where

the feed rate is 0.8 mm, a similar increase in cutting speed results in only a slight reduction in Root Mean Square Deviation. This suggests that higher cutting speeds may reduce surface roughness, likely due to reduced tool vibration and heat generation, although the effect is moderated by the feed rate.

The impact of depth of cut on Root Mean Square Deviation appears significant. In both feed rate conditions, increasing the depth of cut from 0.1 mm to 0.2 mm generally leads to a reduction in Root Mean Square Deviation. For instance, at a cutting speed of 200 m/min and feed rate of 0.8 mm, the Root Mean Square Deviation drops from 0.91  $\mu\text{m}$  (Setup 2) to 0.81  $\mu\text{m}$  (Setup 6) when the depth of cut is increased. This could be due to the deeper cut stabilizing the tool's engagement with the material, thereby reducing the Root Mean Square Deviation.

The change in the measurement results of Mean Spacing of the profile elements can be seen in Figure 2. The depth of cut has a noticeable impact on Mean Spacing values, particularly at higher feed rates. For instance, at a feed rate of 0.8 mm and a cutting speed of 200 m/min, increasing the depth of cut from 0.1 mm (Setup 2) to 0.2 mm (Setup 6) results in an increase in MSP from 0.0507  $\mu\text{m}$  to 0.0527  $\mu\text{m}$ . This suggests that a deeper cut creates a more pronounced surface profile with wider spacing between elements, potentially due to increased material removal per pass, which emphasizes surface features.



An increase in feed rate from 0.6 mm to 0.8 mm generally results in higher Mean Spacing values, indicating greater spacing between surface profile elements. For instance, in experiments with a cutting speed of 200 m/min and a depth of cut of 0.1 mm (Setup 1 and Setup 2), the MSP average increases from 0.0458  $\mu\text{m}$  to 0.0507  $\mu\text{m}$  as the feed increases. Similarly, under a cutting speed of 250 m/min and a depth of cut of 0.2 mm (Setup 7 and Setup 8), Mean Spacing increases from 0.0417  $\mu\text{m}$  to 0.047  $\mu\text{m}$  with the higher feed rate. This pattern suggests that as feed increases, the

distance between profile peaks on the surface also grows, which is likely due to the larger increments in material removed per revolution, creating more distinct peaks and valleys.

The effect of cutting speed on Mean Spacing is less pronounced than that of feed, but some trends can be observed. When the feed rate is held constant at 0.6 mm, increasing the cutting speed from 200 m/min to 250 m/min results in a slight decrease in Mean Spacing. For example, in Setups 1 and 3, Mean Spacing drops from 0.0458  $\mu\text{m}$  to 0.0437  $\mu\text{m}$ . This reduction could be attributed to higher speeds improving tool stability, leading to a finer and more closely spaced surface profile. However, when the feed is increased to 0.8 mm, the effect of cutting speed is less consistent, suggesting that the interaction between cutting speed and feed rate influences Mean Spacing more complexly.

The last analysed roughness parameter (Root Mean Square Slope) is presented in Figure 3. The cutting speed also influences Root Mean Square Slope but to a lesser extent than feed rate. When the feed is held constant, increasing the cutting speed from 200 m/min to 250 m/min generally causes a slight increase in Root Mean Square Slope. For instance, in Setups 1 and 3, with a feed rate of 0.6 mm and depth of cut of 0.1 mm, the Root Mean Square Slope increases from 14.2  $\mu\text{m}$  to 16.2  $\mu\text{m}$  with a higher cutting speed. This suggests that higher speeds can contribute to steeper surface profiles, potentially due to the increased energy in the cutting process, which may amplify surface irregularities.

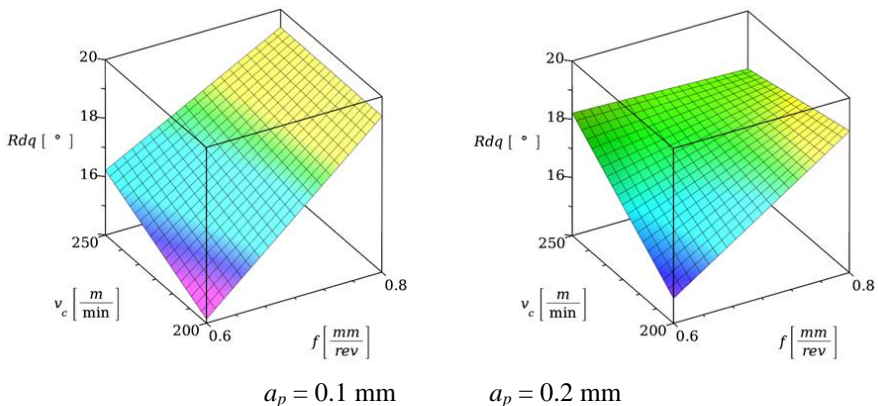


Figure 3 – Alteration of the  $R_{dq}$  in the studied range

Increasing the feed rate from 0.6 mm to 0.8 mm generally results in a higher Root Mean Square Slope, indicating steeper surface features. For example, in Setups 1 and 2, where the cutting speed is 200 m/min and the depth of cut is 0.1 mm, the RMS Slope increases from an average of 14.2  $\mu\text{m}$  to 19.3  $\mu\text{m}$  as the feed rate is

raised from 0.6 mm to 0.8 mm. This trend is consistent across different cutting speeds and depths of cut, suggesting that higher feed rates lead to sharper surface peaks and valleys due to the increased volume of material removed per revolution.

The depth of cut appears to have a moderate impact on the Root Mean Square Slope values. In both feed rate conditions, increasing the depth of cut from 0.1 mm to 0.2 mm leads to a general increase in Root Mean Square Slope. For example, at a feed rate of 0.6 mm and a cutting speed of 200 m/min, the Root Mean Square Slope rises from 14.2  $\mu\text{m}$  (Setup 1) to 14.9  $\mu\text{m}$  (Setup 5) with a deeper cut. This effect is more noticeable at higher feed rates, as seen in Setups 2 and 6, where the Root Mean Square Slope increases from 19.3  $\mu\text{m}$  to 18.9  $\mu\text{m}$ . A deeper cut likely results in more pronounced surface features due to the larger material removal.

## 5. Conclusions

The development of machining procedures requires the assessment of the produced surfaces in the point of view of geometric errors among many things. Surface roughness is a widely studied characteristic of the cutting processes, since the machined surface should meet the strict requirements of the product design. The surface quality could be improved by the application procedures with unusual kinematics, from which the tangential turning is studied in this paper. Three selected roughness parameters (Root Mean Square Deviation, the Mean Spacing of Profile Elements and the Root mean Square Slope) were measured on workpieces machined by this technique. The full factorial design of experiment method is applied in the selection of input parameters and in the determination of calculation formulas.

In summary, the following conclusions can be highlighted from the study:

- Feed has the most direct impact on the Root Mean Square Deviation, the Mean Spacing of Profile Elements and the Root mean Square Slope.
- with higher feed rates resulting in rougher finishes, leading to greater spacing between profile elements and steeper surface profiles.
- Cutting speed and depth of cut have more subtle and less consistent effects, although higher speeds and depths generally contribute to more distinct surface textures.

**References:** 1. *Pawan, S.; Gupta, K.* A Review on Recent Advances in the Energy Efficiency of Machining Processes for Sustainability. *Energies* 2024, 17, 3659, <http://doi.org/10.3390/en17153659>. 2. *Wippermann, A.; Gutowski, T.G.; Denkena, B.; Dittrich, M. -a.; Wessargues, Y.* Electrical Energy and Material Efficiency Analysis of Machining, Additive and Hybrid Manufacturing. *Journal of Cleaner Production* 2019, 251, 119731, <http://doi.org/10.1016/j.jclepro.2019.119731>. 3. *Tayal, A.; Kalsi, N.S.; Gupta, M.K.* Machining of Superalloys: A Review on Machining Parameters, Cutting Tools, and Cooling Methods. *Materials Today Proceedings* 2020, 43, 1839–1849, <http://doi.org/10.1016/j.matpr.2020.10.815>. 4. *Ezugwu, E.O.* Key Improvements in the Machining of Difficult-to-Cut Aerospace Superalloys. *International Journal of Machine Tools and Manufacture* 2005, 45, 1353–1367,

- <http://doi.org/10.1016/j.ijmachtools.2005.02.003>. **5.** Benotsmane, R.; Kovács, G. Optimization of Energy Consumption of Industrial Robots Using Classical PID and MPC Controllers. *Energies* 2023, 16, 3499, <http://doi.org/10.3390/en16083499>. **6.** Imad, M.; Hopkins, C.; Hosseini, A.; Yussefian, N.Z.; Kishawy, H.A. Intelligent Machining: A Review of Trends, Achievements and Current Progress. *International Journal of Computer Integrated Manufacturing* 2021, 35, 359–387, <http://doi.org/10.1080/0951192x.2021.1891573>. **7.** Kundrač, J.; Morgan, M.; Mitsyk, A.V.; Fedorovich, V.A. The Effect of the Shock Wave of the Oscillating Working Medium in a Vibrating Machine's Reservoir during a Multi-Energy Finishing-Grinding Vibration Processing. *The International Journal of Advanced Manufacturing Technology* 2020, 106, 4339–4353, <http://doi.org/10.1007/s00170-019-04844-2>. **8.** Kundrač, J.; Fedorovich, V.; Markopoulos, A.P.; Pyzhov, I.; Ostroverkh, Y. Increasing the Reliability of a Bladed Tool Made from Synthetic Polycrystalline Diamonds. *International Journal of Refractory Metals and Hard Materials* 2022, 110, 106045, <http://doi.org/10.1016/j.jirmhm.2022.106045>. **9.** Pálmai, Z.; Kundrač, J.; Felhő, C. Analysis of the General Tool Life Function of Cutting Tools by Application of the Catastrophe Theory. *Proceedings of the Institution of Mechanical Engineers Part B Journal of Engineering Manufacture* 2022, 237, 873–884, <http://doi.org/10.1177/09544054221123480>. **10.** Hentz, J.-B.; Nguyen, V.K.; Maeder, W.; Panarese, D.; Gunnink, J.W.; Gontarz, A.; Stavropoulos, P.; Hamilton, K.; Hascoët, J.-Y. An Enabling Digital Foundation towards Smart Machining. *Procedia CIRP* 2013, 12, 240–245, <http://doi.org/10.1016/j.procir.2013.09.042>. **11.** Heo, E.; Yoo, N. Numerical Control Machine Optimization Technologies through Analysis of Machining History Data Using Digital Twin. *Applied Sciences* 2021, 11, 3259, <http://doi.org/10.3390/app11073259>. **12.** Felho, C.; Varga, G. Theoretical Roughness Modeling of Hard Turned Surfaces Considering Tool Wear. *Machines* 2022, 10, 188, <http://doi.org/10.3390/machines10030188>. **13.** Kundrač, J.; Pálmai, Z.; Varga, G. Analysis of Tool Life Functions in Hard Turning. *Tehnicki Vjesnik - Technical Gazette* 2020, 27, <http://doi.org/10.17559/tv-20190712153727>. **14.** Shi, J.; Liu, C.R. On Predicting Chip Morphology and Phase Transformation in Hard Machining. *The International Journal of Advanced Manufacturing Technology* 2005, 27, 645–654, <http://doi.org/10.1007/s00170-004-2242-0>. **15.** Chinchankar, S.; Choudhury, S.K. Machining of Hardened Steel—Experimental Investigations, Performance Modeling and Cooling Techniques: A Review. *International Journal of Machine Tools and Manufacture* 2014, 89, 95–109, <http://doi.org/10.1016/j.ijmachtools.2014.11.002>. **16.** Ferencsik, V. Analytical Analysis Of The Theoretical Surface Roughness In The Case Of Burnishing Of Cylindrical Workpiece. *Cutting & Tools in Technological System* 2023, 101–109, <http://doi.org/10.20998/2078-7405.2023.99.05>. **17.** Maros, Z.; Kun-Bodnár, K.; Fekete, V. Investigation Of Electro Discharge Machining Of Tool Steels Based On The Roughness Of The Machined Surfaces. *Cutting & Tools in Technological System* 2023, 46–57, <http://doi.org/10.20998/2078-7405.2023.99.04>. **18.** Nagy, A.; Kundrač, J. Roughness Investigation Of Single And Double Cutting Marks On Face Milled Surface. *Cutting & Tools in Technological System* 2023, 58–70, <http://doi.org/10.20998/2078-7405.2023.99.07>. **19.** Benardos, P.G.; Vosniakos, G. -c. Predicting Surface Roughness in Machining: A Review. *International Journal of Machine Tools and Manufacture* 2003, 43, 833–844, [http://doi.org/10.1016/s0890-6955\(03\)00059-2](http://doi.org/10.1016/s0890-6955(03)00059-2). **20.** Abellán-Nebot, J.V.; Pastor, C.V.; Siller, H.R. A Review of the Factors Influencing Surface Roughness in Machining and Their Impact on Sustainability. *Sustainability* 2024, 16, 1917, <http://doi.org/10.3390/su16051917>. **21.** Grzesik, W.; Wanat, T. Comparative Assessment of Surface Roughness Produced by Hard Machining with Mixed Ceramic Tools Including 2D and 3D Analysis. *Journal of Materials Processing Technology* 2005, 169, 364–371, <http://doi.org/10.1016/j.jmatprotec.2005.04.080>. **22.** Bazan, A.; Turek, P.; Sulkowicz, P.; Przeszlowski, L.; Zakrzęcki, A. Influence of the Size of Measurement Area Determined by Smooth-Rough Crossover Scale and Mean Profile Element Spacing on Topography Parameters of Samples Produced with Additive Methods. *Machines* 2023, 11, 615, <http://doi.org/10.3390/machines11060615>.

Іштван Станкович, Іштван Пастор, Мішкольц, Угорщина

## **ОЦІНКА СЕРЕДНЬОКВАДРАТИЧНОГО ВІДХИЛЕННЯ НА ПОВЕРХНЯХ, ОБРОБЛЕНИХ ТАНГЕНЦІЙНОЮ ТОКАРНОЮ ОБРОБКОЮ З ВИСОКОЮ ПОДАЧЕЮ**

**Анотація.** Нещодавні досягнення в галузі обробки зосереджені на точності, ефективності та обробці твердих матеріалів, що обумовлено такими секторами, як аерокосмічна та автомобільна промисловість. Жорстка обробка або обробка матеріалів понад 45 HRC пов'язана з такими проблемами, як швидкий знос інструменту, інтенсивне нагрівання та збереження точності розмірів. Інновації в різанні інструментальних матеріалів і технології ЧПУ покращили ці процеси, але деградація інструменту і високі зусилля все ще ускладнюють обробку загартованих матеріалів. Шорсткість поверхні є ключовим показником якості, що впливає на такі фактори продуктивності, як зносостійкість і термін служби. Оптимізуючи параметри різання, виробники прагнуть досягти стабільної обробки поверхні, необхідної для довговічності в складних умовах. У даній роботі аналізується вплив вхідних параметрів (глибина різання, подача і швидкість різання) на вибрані параметри шорсткості поверхні. Параметри установки вибиралися відповідно до повного факторіального дизайну методу експерименту. Результати показали, що вища швидкість подачі призвела до більш грубої обробки, що призвело до більшої відстані між профільними елементами та більш крутими профілями поверхні в досліджуваному діапазоні. Подача має найбезпосередніший вплив на середньоквадратичне відхилення, середнє значення відстані між елементами профілю та середньоквадратичний нахил. Більш висока швидкість подачі призводить до більш грубої обробки, що призводить до більшої відстані між елементами профілю та більш крутими профілями поверхні. Швидкість різання та глибина різання мають більш тонкий і менш стабільний ефект, хоча вищі швидкості та глибина зазвичай сприяють більш чіткій текстурі поверхні.

**Ключові слова:** планування експериментів; середня відстань між профілями; середньоквадратичне відхилення; середньоквадратичний нахил; шорсткість поверхні; тангенціальне точіння.

## COLOR VISUALIZATION OF 3D-MODELS FOR ENHANCED PREPARATION OF ADDITIVE MANUFACTURING PROCESSES

Yaroslav **Garashchenko** <sup>[0000-0003-2568-4763]</sup>, Vladimir **Fedorovich** <sup>[0000-0001-7015-8653]</sup>,  
Andrii **Poharskyi** <sup>[0000-0001-5040-9961]</sup>, Olena **Harashchenko** <sup>[0000-0002-9572-6095]</sup>, Andrii  
**Malyniak** <sup>[0009-0001-5837-414X]</sup>

National Technical University «Kharkiv Polytechnic Institute», Kharkiv, Ukraine  
[yaroslav.garashchenko@gmail.com](mailto:yaroslav.garashchenko@gmail.com)

**Received: 29 October 2024 / Revised: 15 November 2024 / Accepted: 26 November 2024 /  
Published: 15 December 2024**

**Abstract.** *The main aspects of color visualization of triangulated models of industrial products are presented. The implementation of visualization capabilities is based on RGB and HSV color models. The structure and key features of the software implementation of color visualization and the export of the displayed image in PLY, and AMF formats are discussed. Methods for transformations between RGB and HSV color models are described, as well as an algorithm for coloring the triangular faces of the model based on specified color ranges. The developed algorithms allow for a sufficiently informative representation of the desired areas of the product's surfaces by significantly altering one color component while minimally changing the other two. This is achieved by directing the assignment of functional dependencies and value ranges for each component of the color model. Examples of various methods for color shading of vertices and/or edges and/or faces of the model are provided. The visualization subsystem enables the analysis of the geometric characteristics of the polygonal model during the preparation phase of additive manufacturing processes. Significant advantages of these approaches to color visualization are evident when adapting the product design to technological requirements (design preparation) and when solving optimization tasks in technological preparation. The developed software is integrated into the technological preparation system for manufacturing enterprises in the machine engineering sector. This research was developed at the Department of "Integrated Technologies of Mechanical Engineering" named after M. Semko of NTU "KhPI".*

**Keywords:** *technology planning; additive manufacturing; triangulated model; color model; RGB; HSV.*

### 1. Introduction

There is a problem of the low efficiency of additive technologies, especially in the mass production of a group of 3D-models of complex products. Each technology has its rational scope of application, which is determined by the design features of the product [1]. Automation of determining the design features of the product by its triangulation model creates the basis for a rational choice of manufacturing strategy

and increases the efficiency of additive manufacturing [2]. An additional aspect of the problem is the visual verification of 3D-models of industrial products at the preliminary stage of technological planning of processes.

Geometric models in CAD systems are based on a specific data structure that ensures the topological integrity of the model. In order to unify the representation of information about the surfaces of 3D-models for their subsequent additive manufacturing, a transition is made from CAD-models to triangulation models. The triangulation representation of the product model (STL format) is approximate. The accuracy of the approximation of the triangulation model to the original CAD-model is ensured by a sufficient number of triangular faces (polygons) within the specified limits of the permissible error.

## **2. Review of the literature**

Color visualization of triangulated models plays an important role in preparation for additive manufacturing. Colors can be used to represent different properties of the model, such as surface curvature, wall thickness, or material stress. This helps to identify potential problem areas before printing.

The RGB and HSV color models are widely used in computer graphics and image processing. The HSV model is considered more user-friendly for human perception due to its intuitive separation into hue, saturation, and brightness. Conversions between RGB and HSV are actively investigated for computational optimization [3].

Exporting triangulated models to PLY, OBJ, OFF, and AMF formats is necessary for data exchange between different CAD and analytical systems. Much work has been done to develop efficient methods for transforming and simplifying polygonal meshes [4].

The use of color to encode geometric and physical properties of models helps in visual analysis and defect detection [5]. Various shading techniques have been developed that take into account curvature, slope, wall thickness, etc. [6, 7].

In general, color visualization is an important tool for the preparation and optimization of additive manufacturing processes, which is confirmed by numerous studies in this field [7-9].

The work aims to determine recommendations for color visualization of polygonal model elements when analyzing both topological indicators and design features of the product, affecting the implementation of technological preparation tasks for additive manufacturing processes.

## **3. Materials and methods**

When visualizing triangulation models, two approaches can be used to highlight the colors of the studied topological and geometric features: discrete assignment of colors according to given conditions or the use of color scales for the interval of change of the studied feature.

Primary analysis of product models manufactured by layered building shows that to solve color visualization tasks, it is sufficient to use the RGB, and HSV color models and their combination [10, 11].

**RGB color model.** The RGB model is based on the combination of three main colors (components): red, green, and blue. Each of these colors has a range of discrete brightness values of  $0 \div 255$ . The required color is achieved by adding three basic colors with given intensity levels (additive model). The RGB model is the basic one for computer devices and color visualization programs. The maximum number of reproducible color shades is  $256 \times 256 \times 256 \cong 16.7$  million colors [12].

The disadvantage of the RGB model is the impossibility of constructing color scales for visualizing changes in the studied features since it is difficult to predict the consequences of even small changes in the color components R, G, B [10, 11].

**HSV color model.** The HSV model is based on the assumption that color can be described by a single monochromatic wave – color tone (hue) H with an additional assignment of saturation S and lightness V [10]. The parameters of this color model are as follows:

H (Hue) – color tone, one of the main characteristics of color that determines its shade, varies within  $0^\circ \div 360^\circ$ ;

S (Saturation) – saturation, characterizes the quality of the purity of the chromatic color tone, the closer this parameter to zero, the lighter the selected color, varies within  $0 \div 255$  ( $0 \div 1$  or  $0 \div 100$ );

V (Value) – brightness, the closer this parameter to zero, the darker the selected color, varies within  $0 \div 255$  ( $0 \div 1$  or  $0 \div 100$ ).

In computer graphics, the parameters S and V are usually represented as an integer from 0 to 255.

The main advantage of the HSV model is the ability to construct color scales to visualize the features being studied.

The color scale displays the change in the studied feature using color shades for a given color model ( $S = S_{base}$ ,  $V = V_{base}$ ). The color scale is defined by the range from the initial value  $H = H_{Top}$  to the final value  $H = H_{End}$ , which contains all the shades corresponding to the spectrum. For the original HSV model, the values  $H_{Top} = 0^\circ$ ,  $H_{End} = 360^\circ$  ( $H_{Top} < H_{End}$ ), which provides a smooth transition between the six primary colors: red  $\Rightarrow$  yellow  $\Rightarrow$  green  $\Rightarrow$  blue  $\Rightarrow$  dark blue  $\Rightarrow$  purple [11]. When creating special color scales, the range of color shades can be reduced ( $H_{Left} > 0^\circ$

and/or,  $H_{Right} < 360^\circ$ ) or the order of shades can be reversed ( $H_{Left} > H_{Right}$ ). In color visualization of computer models,  $S_{Base} = V_{Base} = 255$  is usually taken, i.e. the maximum possible values of saturation and brightness (prismatic colors) [11, 12].

Color visualization taking into account the values of the studied feature  $X$  ( $x_{min} \leq x \leq x_{max}$ ) is performed in two stages:

1. transition  $x \Rightarrow H = f(x; x_{min}, x_{max}, H_{Left}, H_{Right})$ ;
2. transition HSV  $\Rightarrow$  RGB:  $R, G, B = f(H; S_{Base}, V_{Base})$ .

**Transition  $x \Rightarrow H$ .** The transition from the current  $x$  value visualized by color to the  $H$  color value of the HSV scale for linear scales is performed according to the following dependencies (proportion problem taking into account special cases):

- $H = H_{Left}$ , if ( $x = x_{min}$  and  $H_{Left} \leq H_{Right}$ ) or ( $x = x_{max}$  and  $H_{Left} \geq H_{Right}$ );
- $H = H_{Right}$ , if ( $x = x_{max}$  and  $H_{Left} \leq H_{Right}$ ) or ( $x = x_{min}$  and  $H_{Left} \geq H_{Right}$ );
- $H = [(x - x_{min}) / (x_{max} - x_{min})] \times (H_{Right} - H_{Left}) + H_{Left}$ , if  $H_{Left} < H_{Right}$ ;
- $H = [(x - x_{min}) / (x_{max} - x_{min})] \times (H_{Left} - H_{Right}) + H_{Right}$ , if  $H_{Left} > H_{Right}$ ,

where  $H_{Left}, H_{Right}$  – left and right values of the HSV color scale;

$x_{min}, x_{max}$  – minimum and maximum possible values of  $x$ .

**Transition HSV  $\Rightarrow$  RGB.** The transition diagram is shown in Fig. 1. The transition functions for each of the RGB components are piecewise linear and shifted relative to each other by  $120^\circ$ .

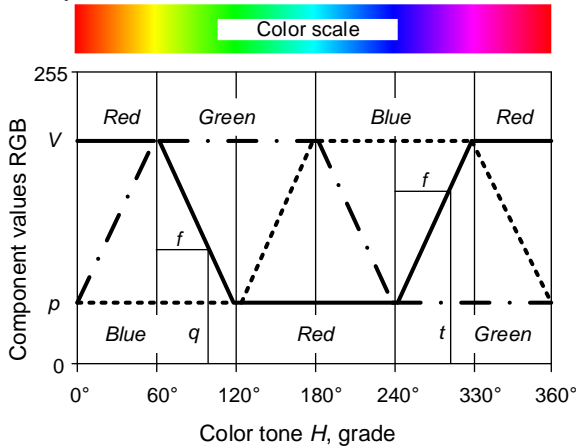


Figure 1 – Scheme of transition from HSV to RGB color model

The general algorithm for the HSV  $\Rightarrow$  RGB transition is presented in [12]. For the case of  $H = 0 \div 360^\circ$ ;  $S, V, R, G, B = 0 \div 255$ , the calculation is performed

according to the following dependencies in two stages (definition of auxiliary variables and directly the RGB components).

Definition of auxiliary variables:

- integer part of the expression  $H / 60 \Rightarrow H_i$ ;
- fractional part of the expression  $H / 60 \Rightarrow f$ ;
- maximum possible value  $R/G/B \Rightarrow V$ ;
- minimum possible value  $R/G/B \Rightarrow p: p = V(1 - S / 255)$ ;

amplitude (interval of change) of values  $R/G/B \Rightarrow A: A = V - p = VS / 255$ ;

$R/G/B$  value for downlink  $\Rightarrow t: q = A(V - f) = V(1 - fS / 255)$ ;

$R/G/B$  value for uplink  $\Rightarrow t: t = p + fA = V[1 - (1 - f)S / 255]$ .

Determining the values RGB components:

- |                         |      |           |           |           |
|-------------------------|------|-----------|-----------|-----------|
| • if $H_i = 0$ or $6$ , | then | $R = V$ , | $G = t$ , | $B = p$ ; |
| • if $H_i = 1$ ,        | then | $R = q$ , | $G = V$ , | $B = p$ ; |
| • if $H_i = 2$ ,        | then | $R = p$ , | $G = V$ , | $B = t$ ; |
| • if $H_i = 3$ ,        | then | $R = p$ , | $G = q$ , | $B = V$ ; |
| • if $H_i = 4$ ,        | then | $R = t$ , | $G = p$ , | $B = V$ ; |
| • if $H_i = 5$ ,        | then | $R = V$ , | $G = p$ , | $B = q$ . |

#### **4. Implementation of developments in the morphological analysis system**

The considered approaches to color visualization are implemented in the system of analysis of triangulation 3D models of products which was developed at the Department of "Integrated Technologies of Mechanical Engineering" named after M. Semko of NTU "KhPI" [13].

Color visualization of individual elements of triangulation models can be performed using discrete color assignment (RGB and/or HSV) or the HSV color scale (Fig. 2). The choice of color visualization strategy is determined by the features of the topological or design-technological analysis in the context of the production or educational task being solved.

The color of the model is assigned based on the data obtained during the morphological analysis of the components of the triangulation model surface. The subsystem allows coloring the following elements of the triangulation model: vertices, faces, or edges. Visual perception of the topological features of the model is achieved by comparing the specified color scale with the feature being studied.

For further work with the model, it is exported to formats that support color: PLY, AMF (new format for additive manufacturing), or XLS (analysis results). Vertex coloring during viewing is implemented as a gradient coloring of triangular faces by the color of adjacent vertices.

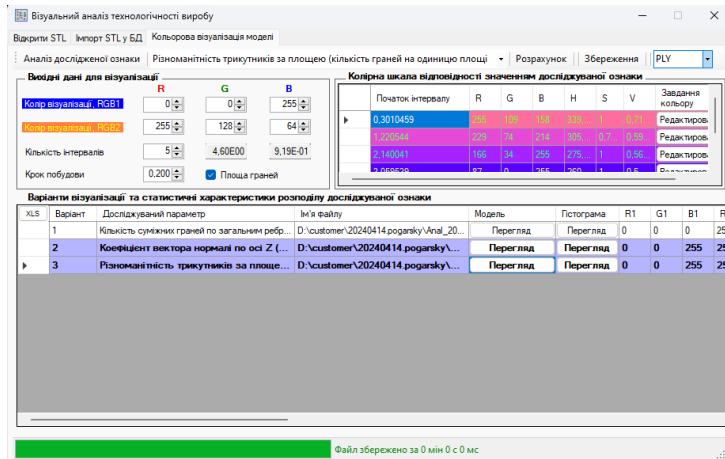


Figure 2 – Screen form of the color visualization subsystem

To view and edit the created files in the educational process, Materialise Magics program is used with a sufficient set of tools and is free, which is important for scientific research.

### 5. Examples of color visualization of triangulation models. Discussion

Let's consider several examples of color visualization of triangulation model elements.

- Color visualization of vertices by the value of adjacency of faces (Fig. 3). Vertices are assigned one of three specified colors. For example, if the adjacency of faces at a vertex is  $A_{Vert} < 3$ , then the color RGB 1 (red) is assigned, if  $A_{Vert} = 3 \Rightarrow$  RGB 2 (green),  $A_{Vert} > 3 \Rightarrow$  RGB 3 (gray). This allows us to visually identify missing edges that disrupt the closed nature of the model surface and lead to failure of the layer-by-layer materialization installations.

- Color visualization of faces (Fig. 4) relative to the x, y, z axes, where the orientation of the faces is determined by the direction cosines of the normal (HSV model).

- Color visualization of faces depending on the area value of triangles (HSV model). The studied feature that determines the color tone in this case is the area value of the face. The left border of the color scale of the color tone implies the

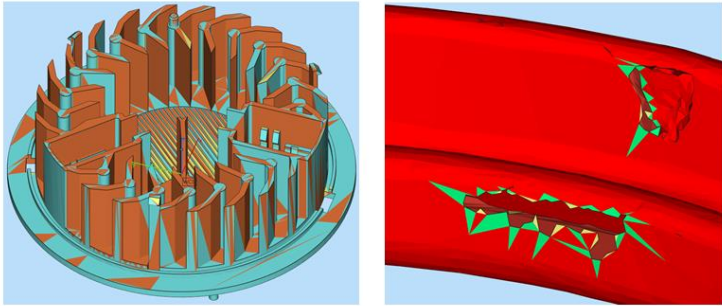


Figure 3 – Adjacency of faces

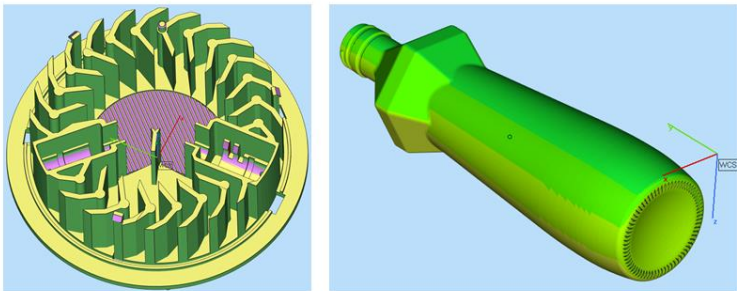


Figure 4 – Orientation of faces

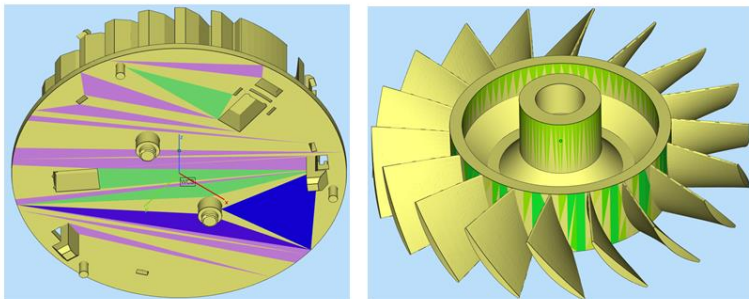


Figure 5 – Face area

largest value of the faces area, and the right one - the smallest (Fig. 5). Thus, the color scale gives a visual representation of the sizes of the triangles.

## 6. Conclusions

The research presents a comprehensive approach to color visualization of triangulation models for additive manufacturing using RGB and HSV color models. Key findings include:

- the HSV color model offers significant advantages over RGB for visualization, enabling - intuitive color scale construction, smooth representation of feature changes, flexible color mapping for various topological and geometric characteristics;
- developed color visualization techniques allow for discrete color assignment; interval-based color scaling, and detailed analysis of model elements (vertices, faces, edges);
- practical implementation demonstrates the effectiveness of color visualization in identifying surface topology issues, analyzing face orientation, evaluating triangle areas, and detecting potential manufacturing challenges.

The proposed methodology provides a flexible tool for morphological analysis of 3D models, supporting both scientific research and educational applications.

The developed color visualization approach enhances the preparatory stages of additive manufacturing by enabling comprehensive visual analysis of geometric and topological model features.

**References:** 1. Gibson I., Rosen D.W., Stucker B., Khorasani M., Rosen D., Stucker B., Khorasani M.: Additive manufacturing technologies. Cham, Switzerland: Springer. 2021. 675 p., doi: 10.1007/978-3-030-56127-7. 2. Garashchenko Y., Rucki M. Part decomposition efficiency expectation evaluation in additive manufacturing process planning. International Journal of Production Research. 2021. 14 p., doi: 10.1080/00207543.2020.1824084. 3. Kruse A., Alenin A., Vaughn I., Tyo J. Perceptually uniform color space for visualizing trivariate linear polarization imaging data. Optics Letters. 43. 2018. 2426. doi: 10.1364/OL.43.002426. 4. Yirci M., Ulusoy I. A comparative study on polygonal mesh simplification algorithms. 2009. pp. 736-739. doi: 10.1109/SIU.2009.5136501. 5. Zhou L. and Hansen C.D. A survey of colormaps in visualization. IEEE transactions on visualization and computer graphics, 22(8), 2015. pp. 2051-2069. doi: 10.1109/TVCG.2015.2489649. 6. Kannan R., Knapp G.L., Nandwana P., Dehoff R., Plotkowski A., Stump B., Yang Y., Paquit V. Data mining and visualization of high-dimensional ICME data for additive manufacturing. Integrating Materials and Manufacturing Innovation, 11(1), 2022. pp. 57-70. 7. Steed C.A., Halsey W., Dehoff R., Yoder S.L., Paquit V., Powers S., Falcon: Visual analysis of large, irregularly sampled, and multivariate time series data in additive manufacturing. Computers & Graphics, 63, 2017. pp. 50–64. 8. Nascimento R., Martins I., Dutra T.A., Moreira L. Computer vision based quality control for additive manufacturing parts. The International Journal of Advanced Manufacturing Technology, 124(10), 2023. pp. 3241–3256. 9. Kim H., Lin Y., Tseng T.L.B. A review on quality control in additive manufacturing. Rapid Prototyping Journal, 24(3), 2018. pp. 645–669. 10. Ibraheem N.A., Hasan M.M., Khan R.Z., Mishra P.K. Understanding color models: a review. ARPN Journal of science and technology, 2(3), 2012. pp. 265–275. 11. Loesdau M., Chabrier S., Gabillon A.

Hue and saturation in the RGB color space. In Image and Signal Processing: 6th International Conference, ICISP 2014, Cherbourg, France, June 30–July 2, 2014. Proceedings 6. pp. 203–212. **12.** *Süsstrunk S., Buckley R., Swen S.* Standard RGB color spaces. In Color and imaging conference. Society of Imaging Science and Technology. 1999. January. Vol. 7, pp. 127–134. **13.** *Garashchenko Y.M.* Improvement of technological preparation of additive production of folding viruses. Monograph. (in Ukrainian), Kharkiv: NTU «KhPI». 2023. 388 p.

Ярослав Гаращенко, Володимир Федорович, Андрій Погарський, Олена Гаращенко, Андрій Малиняк, Харків, Україна

## **КОЛІРНА ВІЗУАЛІЗАЦІЯ 3D МОДЕЛЕЙ ДЛЯ УДОСКОНАЛЕННЯ ПІДГОТОВКИ ПРОЦЕСІВ АДИТИВНИХ ТЕХНОЛОГІЙ**

**Анотація.** *Представлено комплексний підхід до кольорової візуалізації триангульованих моделей промислових виробів для адитивного виробництва. Дослідження базується на використанні RGB та HSV кольорових моделей, що дозволяють створювати інформативні та наочні зображення геометричних характеристик виробів. Розроблено структуру та методологію програмної реалізації кольорової візуалізації з можливістю експорту в стандартні формати PLY, AMF. Детально висвітлено алгоритми перетворення між кольоровими моделями RGB та HSV, включаючи математичні залежності для перетворення значень кольорових компонент з урахуванням специфіки комп'ютерної графіки та вимог щодо виконання задач технологічної підготовки процесів адитивних технологій. Запропоновано новий підхід до розфарбовування трикутних граней 3D-моделі, який дозволяє цілеспрямовано змінювати кольорові відтінки для виділення специфічних геометричних особливостей. Ключова перевага розробленої методики – можливість інформативного відображення топологічних характеристик поверхонь шляхом контрольованої зміни кольорових компонент. Це реалізовано шляхом візуалізації кольорів з гнучким налаштуванням дискретності призначення кольору за наданими інтервалами шкали кольорів. Представлення шкали кольорів у вигляді таблиці дає розширені можливості. Таблиця шкали кольорів формується автоматично за налаштуваннями, але можлива зміна як окремо по кожній компоненті кольору або візуально на основі палети (стандартного набору) кольорів. Шкала кольорів визначається діапазонами компонент RGB моделі кольору, залежностями зміни, зсувом значень між компонентами та кількістю інтервалів. Реалізовано можливість зміни кольору вершин, ребер та граней залежно від їх геометричних параметрів або відносного розташування. Представлено практичні приклади застосування різних стратегій кольорової візуалізації. Розроблена підсистема візуалізації забезпечує ефективний аналіз геометричних характеристик полігональних 3D-моделей на етапі підготовки адитивного виробництва, надаючи розширені можливості для комплексної конструкторської та технологічної підготовки адитивного виробництва. Дослідження виконувалося з використанням системи "Технологічна підготовка матеріалізації складних виробів адитивними методами" розробленої на кафедрі «Інтегровані технології машинобудування» ім. М.Ф. Семка НТУ «ХПІ».*

**Ключові слова:** технологічна підготовка; адитивні технології; триангуляційна модель; колірні моделі; RGB; HSV.

## INFLUENCE OF HELICAL CUTTING-EDGE ANGLE ON END-MILLING STABILITY

Sergei Dyadya <sup>[0000-0002-7457-7772]</sup>, Olena Kozlova <sup>[0000-0002-3478-5913]</sup>, Pavlo Tryshyn <sup>[0000-0002-3301-5124]</sup>, Denys Yakhno <sup>[0009-0009-2816-9397]</sup>, Denys Dziuba <sup>[0009-0006-1915-655X]</sup>

National University «Zaporizhzhya Polytechnic», Zaporizhzhya, Ukraine  
[kozlova@zntu.edu.ua](mailto:kozlova@zntu.edu.ua)

Received: 30 October 2024 / Revised: 13 November 2024 / Accepted: 26 November 2024 /  
Published: 15 December 2024

**Abstract.** *Increasing productivity, machining accuracy and efficient use of resources are important priorities for companies that manufacture competitive products. One of the main problems that hinders these processes is the vibration that occurs during cutting. Various methods are used to suppress vibration, one of which is the use of tools with a variable helical cutting-edge angle. However, when choosing the cutting-edge angle, it is important to consider the types of vibrations that occur during cutting, as they directly affect the efficiency of the milling process. In addition, the use of tools with different cutting-edge geometries, such as wavy, gives positive results in roughing, but becomes ineffective in finishing. The purpose of this paper is to study the effect of the helical cutting-edge angle on the stability of the end-milling at different cutting speeds. Both theoretical aspects and experimental data are considered, which make it possible to evaluate the effectiveness of using tools with different angles of inclination to ensure the stability of the machining process and increase productivity while minimizing vibrations in the most unfavorable third speed zone of oscillations for cutting. To conduct the experiments, a special stand was used to adjust the stiffness of the workpiece, record the vibrations that occur during cutting, and the time of contact between the workpiece and the tool. The milling was performed in the third high-speed oscillation zone using a tool whose design provides for the possibility of adjusting the angle of inclination of the helical cutting edge. Studies confirm that changing the angle of inclination can significantly affect the stability of the milling process, reducing the intensity of oscillations and improving machining accuracy. However, this effect depends on the initial cutting conditions, such as the cutting speed. With its increase, the amplitude of the accompanying free oscillations increases, regardless of the value of the angle of inclination. Ensuring the stability of the end-milling in the third speed zone by changing the angle of inclination is possible only at the speeds that determine the beginning of this zone. However, within the entire speed range covered by the third speed zone, it is impossible to ensure a stable milling process only due to the angle of inclination. The study emphasizes the importance of an integrated approach to selecting cutting parameters to achieve process stability.*

**Keywords:** *milling; milling cutter; thin-walled components; feed rate; oscillogram; accompanying free oscillations.*

### 1. Introduction

Increasing productivity, machining accuracy, and being economical with all types of resources are the top priorities for companies when manufacturing

© S. Dyadya, O. Kozlova, P. Tryshyn, D. Yakhno, D. Dziuba, 2024

competitive products. One of the reasons why this is difficult is the vibrations that occur during cutting. Small values of vibrations help to ease chip formation and have a minor impact on surface quality. But such conditions occur at low cutting speeds. With its increase, the intensity of vibrations increases and the cutting process may not be possible. Various measures are used to suppress vibrations. Paper [1] proposes to consider various cutting strategies that increase the rate of material removal without vibrations using the method of structural modification. The authors of [2, 3] propose to use the geometry of the cutting edge with a radius to dampen vibrations during cutting. They found out its effectiveness at low cutting speeds. When milling in the high-speed zone, it is proposed to use a tool with a variable helical cutting-edge angle [4, 5]. For machining the side surfaces of gas turbine impellers, which is accompanied by high cutting forces and vibrations, it is proposed to use variable pitch cutters [6]. At the same time, adaptive control of the cutting force by changing the tool orientation and depth of cut on a 5-axis machine allows it to be maintained at a constant level, which significantly reduces the machining cycle. The use of end mills with wavy grooves [7, 8] increases the stability of the cutting process, but due to their specific profile, they cannot be used for finishing machining.

Researchers S. Tobias and W. Fishwick [11] suggested using lobe diagrams of stability when assigning cutting modes, which would prevent the excitation of regenerative oscillations. The widespread use of carbide cutters in high-speed machining with the use of stability diagrams makes the cutting process highly productive [10]. When determining an unstable milling process, modal analysis is used to calculate the ratio between the frequency of free oscillations of a part and the frequency of forced oscillations [9].

Manufacturers of cutting tools such as LIHSING, DHM, SUMITOMO, NACHREINER, GUHRING, and others take into account the influence of the helical cutting-edge angle on reducing the intensity of vibrations. To ensure the stability of the cutting process when machining carbon, stainless, and hardened steels, they recommend using cutters with a helical cutting-edge angle of 30° to 60°. Cutting modes are also added to this. However, it is recommended to reduce the speed if excessive vibration occurs. According to GOSTs 17025-71 and 17026-71, domestic HSS milling cutters with a normal tooth are manufactured with helical cutting-edge angles of 30° to 35°, and with a large tooth - from 35° to 45°. According to GOST 18372-73, for carbide milling cutters, the helical cutting-edge angle for a number of 3 cutting teeth is 30-40°, and for a number of 4 and 5 teeth it is 30-35°.

In contrast to straight tooth cutter milling cutters, where cutting starts at the smallest layer thickness in counter milling and starts at the largest layer thickness in plunge milling, in helical cutting, when the helical cutting-edge angle is greater than zero, the cutting conditions are reversed and, in any feed direction, cutting starts at the smallest layer thickness to be cut and ends at the smallest layer thickness. Under these favorable conditions, the cutting force changes gradually. The research of A.

M. Rosenberg [12] found that in oblique milling, the normal component of the cutting force differs slightly in magnitude from the circumferential force and depends little on the angle of inclination. The friction force on the front surface of the cutting-edge increases with increasing tilt angle and reaches a significant value at an angle of 70°, which has a positive effect on oscillation damping [12]. However, to ensure the stability of the cutting process using helical cutting-edge angles, it is necessary to take into account the types of oscillations that occur. This issue for end milling is poorly understood. Therefore, the purpose of this work is to determine the effect of the cutting-edge angle on the stability of end milling at different cutting speeds.

## 2. Experiments and discussion of results

A special stand was used for the experiments, which allows adjusting the stiffness of the part, recording vibrations during cutting, and the time of contact between the part and the tool [12]. Milling was carried out in the third high-speed oscillation zone with a special cutter, the design of which provides for adjusting the angle of inclination of the helical cutting edge [12].

Table 1 shows the initial data for the study.

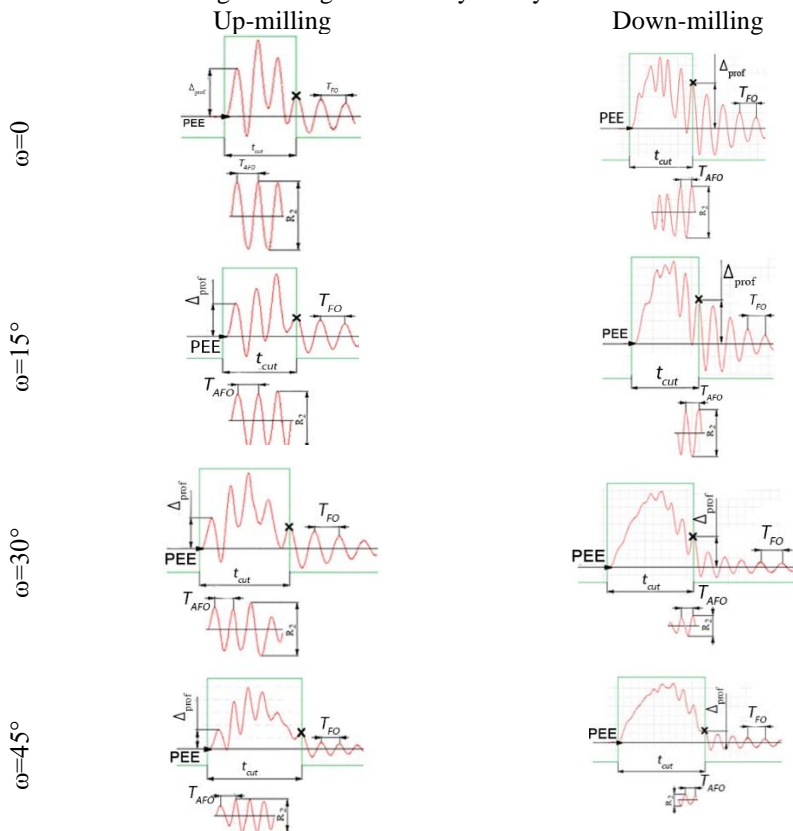
Table 1. Initial data for the research

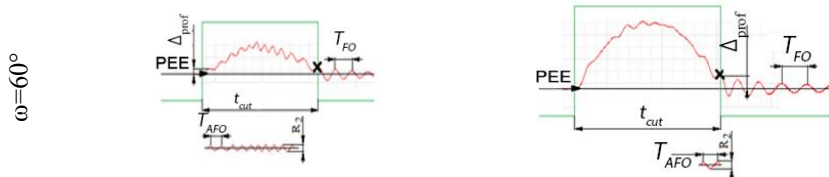
Radial depth of cut $a_e$ , mm	Axial depth of cut $a_p$ , mm	Feed rate $S_z$ , mm/tooth	Angle of inclination of the cutting edge $\omega$ , deg	Spindle speed $n$ , rpm (speed, $v$ , m/min)	Cutter diameter $D$ , mm/number of teeth $z$	Frequency of free oscillations of the part $f_{fo}$ , Hz	The period of free oscillation of the part, $T_{FO}, 10^{-3}$ s
0,5	4	0,1	0, 15, 30, 45, 60	280 (44)	50/1	455	2,19

First of all, it should be noted that during end-milling, due to the short cutting time, no self-oscillations occur [13]. Therefore, the main sources affecting tool life and machined surface quality are the accompanying free and forced oscillations. According to the ratio of the cutting time to the period of free oscillations, parts [12] divide the effect of possible oscillations into five speed zones [12]. Since different materials are processed at different cutting speeds, this distribution can be used to determine which types of vibrations need to be counteracted. It should be noted that the effect of these oscillations is a physical manifestation of the system's excitation

from the impact when the cutter plunges. While forced vibrations are always present during cutting, the accompanying free oscillations (AFO) are present only for a certain time, until the cutting time is less than the AFO period. It is the third speed zone of oscillations that is the most unfavorable for the accuracy of the machined surface shape, because it is the zone where the waviness from the cutting surface is transferred as a heredity and where the intensity of the AFO is the highest.

Fig. 1 shows fragments of the waveforms obtained during milling according to the initial data given in Table 1. To determine the period and magnitude of the AFO, the waveform was aligned using the Savitsky-Golay filter.





► - cutting into the workpiece, ✕ - exit of the cutter from the workpiece, PEE – position of elastic equilibrium,  $\Delta_{prof}$  – deviation of the AFO forming wave from the PEE,  $T_{AFO}$  – period of accompanying free oscillations of the part,  $T_{FO}$  – period of free oscillation of the part,  $t_{cut}$  – cutting time

Figure 1 - Fragments of oscillation waveforms of a workpiece during end-milling with cutters with different helical cutting-edge angles

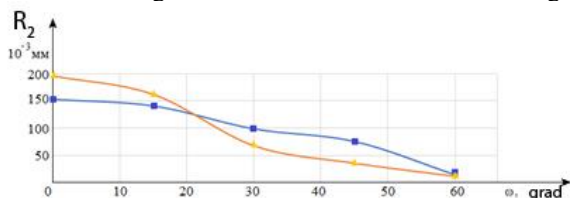
Changing the helical cutting-edge angle  $\omega$  changes the thickness of the layer to be cut. This affects the properties of the workpiece. With an increase in the angle of inclination during up- and down-milling, the period of the AFO and their span  $R_2$  decrease. Their values are shown in Table 2.

In Fig. 2 and Fig. 3 show graphs of the dependences of the span  $R_2$  and the period of the AFO on the angle of inclination of the helical cutting edge  $\omega$ .

Table 2 – Period and span of the AFO when milling with different angles of inclination of the cutting edge

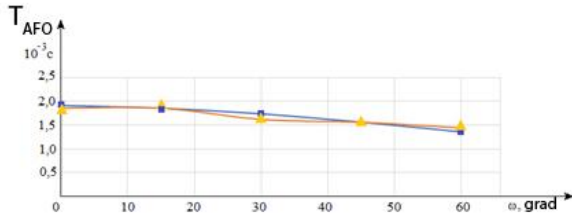
Feed direction	Span of the AFO $R_2$ , $10^{-3}$ mm					The period of the AFO $T_{AFO}$ , $10^{-3}$ s				
	0	15°	30°	45°	60°	0	15°	30°	45°	60°
Up-milling	153	141	99	76	15	1,92	1,86	1,74	1,56	1,35
Down-milling	196	162	68	36	12	1,86	1,86	1,62	1,56	1,44

In Fig. 2 and Fig. 3 show graphs of the dependences of the span  $R_2$  and the period of the AFO on the angle of inclination of the helical cutting edge  $\omega$ .



■ – up-milling; ▲ – down-milling

Figure 2 – Dependence of the AFO span  $R_2$  on the angle of inclination of the helical cutting edge  $\omega$



■ – up-milling; ▲ – down-milling

Figure 3 – Dependence of the period of the AFO on the angle of inclination of the helical cutting edge  $\omega$

The correlation coefficient between the AFO span  $R_2$  and of the angle of inclination helical cutting edge  $\omega$  is (-0.97), which is described by the regression equation:

$$R_2 = -0,0023 \cdot \omega + 0,165, \text{ (mm)}$$

The correlation coefficient between the period of the AFO and the slope angle  $\omega$  is (-0.98), which is described by the regression equation:

$$T_{AFO} = -1 \cdot 10^{-5} \cdot \omega + 0,002, \text{ (s)}$$

When milling with a spindle speed of  $n = 280$  rpm (cutting speed  $v = 44$  m/min), the period of the AFO decreases by more than 10 times, or by more than 90%, with an increase in the angle of inclination  $\omega$  from 0 to 60°. At all values of  $\omega$ , the period of the AFO is less than the period of free oscillations of the workpiece. In general, it decreases from 12% to 38%. However, provided that the oscillations have a favorable effect on the chip formation process, with an  $R_2/2$  amplitude of up to 20 microns, stable milling will occur only when  $\omega$  is greater than 60° for counter milling and greater than 45° for down milling.

When using the angle of inclination to ensure stable milling, it should be remembered that the intensity of the AFO depends on the initial cutting speed. In Fig. 4 shows fragments of the oscillation waveforms of a workpiece during end-milling with an inclination angle of  $\omega = 60^\circ$  at a spindle speed of  $n = 710$  rpm (cutting speed of  $v = 111$  m/min).

Up-milling

Down-milling

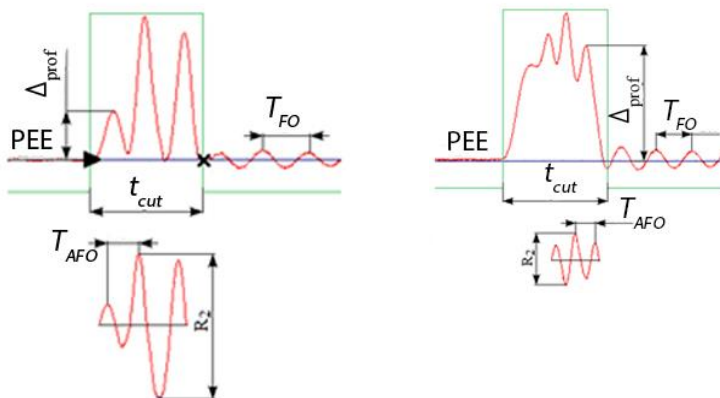


Figure 4 – Fragments of workpiece vibration waveforms during milling at a spindle speed of  $n = 710$  rpm

Table 3 shows the values of the swing and period of the AFO when milling at a speed of  $v = 111$  m/min with a cutter with an inclination angle of  $\omega = 60^\circ$ .

With a 2.5-fold increase in cutting speed, the AFO span during up-milling increases 11 times, and during down-milling it increases 7 times. That is, the process of milling with an end-mill with an inclination angle of  $\omega = 60^\circ$  in third speed zone of oscillations becomes unstable.

Table 3 – Period and span of the AFO during up- and down-milling at a cutting speed of  $v = 111$  m/min with a cutter with an inclination angle of  $\omega = 60^\circ$

Feed direction	Span of the AFO $R_2, 10^{-3}$ mm	The period of the AFO $T_{AFO}, 10^{-3}$ s
Up-milling	175	1,44
Down-milling	81	1,26

### 3. Conclusions

The study of the influence of the inclination angle  $\omega$  on the stability of end-milling shows that third speed zone of oscillations, where AFOs operate, the cutting speed plays an important role. An increase in the angle has a positive effect on reducing the intensity of the AFOs. But it depends on the initial conditions, which include the cutting speed. With its increase, the AFO amplitude increases. Ensuring the stability of end-milling in the third speed zone due to the angle of inclination  $\omega$  is possible at cutting speeds that determine the beginning of this zone. But in the

entire range of cutting speeds covering the third speed zone, it is impossible to ensure stable cutting due to the angle of inclination  $\omega$ .

**References:** 1. Alan S., Budak E., Ozguven H. Analytical Prediction of Part Dynamics for Machining Stability Analysis. International Journal of Automation Technology. 2010. 4(3). pp. 259–267. doi: 10.20965/ijat.2010.p0259. 2. Tunc L.T., Budak E. Effect of Cutting Conditions & Tool Geometry on Process Damping In Machining. International Journal of Machine Tools & Manufacture. 2012. 57. pp.10–19. doi: [10.1016/j.jmactools.2012.01.009](https://doi.org/10.1016/j.jmactools.2012.01.009). 3. Yusoff A.R., Turner S., Taylor C.M., Sims N.D. The Role of Tool Geometry in Process Damped Milling. International Journal of Advanced Manufacturing Technology. 2010. 50(9–12). pp. 883–895. doi: 10.1007/s00170-010-2586-6 4. Altintas Y., Engin S., Budak E. Analytical Stability Prediction & Design for Variable Pitch Cutters. Journal of Manufacturing Science & Engineering. 1999. 121(2). pp. 173–178. doi: [10.1115/1.2831201](https://doi.org/10.1115/1.2831201). 5. Sellmeier V., Denkena B. Stable Islands in the Stability Chart of Milling Processes Due To Unequal Tooth Pitch. International Journal of Machine Tools & Manufacture. 2010. 51(2). pp. 152–164. doi: [10.1016/j.jmactools.2010.09.007](https://doi.org/10.1016/j.jmactools.2010.09.007). 6. Budak E. Improving Productivity & Part Quality in Milling of Titanium Based Impellers by Chatter Suppression & Force Control. CIRP Annals. 2000. 49(1). pp. 31–36. doi: [10.1016/S0007-8506\(07\)62890-X](https://doi.org/10.1016/S0007-8506(07)62890-X) 7. Stone B.J. Chatter & Machine Tools, Springer International Publishing Switzerland, 2014. 260 p. 8. Wang J.J., Yang C.S. Angle & Frequency Domain Force Models for a Roughing End Mill with a Sinusoidal Edge Profile. International Journal of Machine Tools & Manufacture. 2003. 43. pp. 1509–1520. doi: [10.1016/S0890-6955\(03\)00163-9](https://doi.org/10.1016/S0890-6955(03)00163-9). 9. Munoa J., Zatarain M., Dombovari Z., Yang Y. Effect of Mode Interaction on Stability of Milling Processes. 12th CIRP Conference on Modelling of Machining Operations, San Sebastian, Spain. 2009. 10. Smith S., Tlustý J. Current Trends in High-Speed Machining. Journal of Manufacturing Science & Engineering. 1997. 119. pp. 664–666. doi: [10.1115/1.2836806](https://doi.org/10.1115/1.2836806). 11. Tobias S.A., Fishwick W. Theory of Regenerative Machine Tool Chatter. The Engineer. 1958. 205 p. 12. Vnukov Y.N., Dyadya S.I. I., Kozlova E.B., et al. Self-oscillations during milling of thin-walled parts elements. Zaporozhye: ZNTU, 2017. 208 p. 13. Dyadya S., Vnukov Y., Kozlova O., Trishyn P. [Regularities of Oscillations During Turning and End Milling](#). Grabchenko's International Conference on Advanced Manufacturing Processes. 2023. pp. 136–144.

Сергій Дядя, Олена Козлова, Павло Тришин, Денис Яхно, Денис Дзюба,  
Запоріжжя, Україна

## ВПЛИВ КУТА НАХИЛУ ГВИНТОВОЇ РІЗАЛЬНОЇ КРАЙКИ НА СТАЛІСТЬ КІНЦЕВОГО ФРЕЗЕРУВАННЯ

**Анотація.** Підвищення продуктивності, точності обробки та ефективного використання ресурсів є важливими пріоритетами для підприємств, що займаються виготовленням конкурентоспроможної продукції. Однією з основних проблем, що стримує ці процеси, є вібрації, які виникають під час різання. Невеликі коливання мають незначний вплив на якість поверхні деталі, однак, із збільшенням швидкості різання інтенсивність вібрацій зростає, що призводить до зниження точності обробки. Для пригнічення вібрацій використовують різні методи, одним з яких є використання інструментів зі змінним кутом нахилу гвинтової різальної крайки. Ці інструменти сприяють зменшенню амплітуди коливань, особливо при високих швидкостях різання. У роботах, що присвячені даній темі, пропонуються різні стратегії, які дозволяють підвищити швидкість видалення матеріалу без виникнення вібрацій за допомогою методів структурної модифікації. Однак при виборі кута нахилу різальної крайки важливо враховувати типи коливань, що виникають під час різання, оскільки вони безпосередньо впливають на ефективність процесу фрезерування. Крім того, використання інструментів з різними

геометріями різальної крайки, як, наприклад, з хвилеподібною формою, дає позитивні результати при чорновій обробці, але при оздоблювальній стає неефективним. Метою цієї роботи є дослідження впливу кута нахилу гвинтової різальної крайки на сталість кінцевого фрезерування при різних швидкостях різання. Розглядаються як теоретичні аспекти, так і експериментальні дані, що дають можливість оцінити ефективність застосування інструментів з різними кутами нахилу для забезпечення стабільності процесу обробки та підвищення продуктивності при мінімізації вібрацій в найбільш несприятливій для різання третій швидкісній зоні коливань. Для проведення експериментів використовувався спеціальний стенд, який дозволяє регулювати жорсткість деталі, записувати коливання, що виникають під час різання, та час контакту деталі з інструментом. Фрезерування проводилося в третій швидкісній зоні коливань за допомогою інструменту, конструкція якого передбачає можливість регулювання кута нахилу гвинтової різальної крайки. Дослідження підтверджують, що зміна кута нахилу може суттєво впливати на стабільність процесу фрезерування, знижуючи інтенсивність коливань і покращуючи точність обробки. Але цей ефект залежить від початкових умов різання, таких як швидкість різання. З її збільшенням амплітуда супроводжуючих вільних коливань зростає, незважаючи на величину кута нахилу. Забезпечення сталості кінцевого фрезерування в третій швидкісній зоні за рахунок зміни кута нахилу можливе лише при швидкостях, що визначають початок цієї зони. Однак, в межах всього діапазону швидкостей, що охоплює третя швидкісна зона, забезпечити стабільний процес фрезерування тільки за рахунок кута нахилу неможливо. Дослідження підкреслює важливість комплексного підходу до вибору параметрів різання для досягнення стабільності процесу.

**Ключові слова:** фрезерування; фреза; тонкоістинний елемент; напрям подачі; осцилограма; супроводжуючі вільні коливання.

## DETERMINATION OF THE STABILITY PERIOD OF TURNING CUTTERS FOR HEAVY MACHINE TOOLS

Galyna **Klymenko** <sup>[0000-0002-1022-6324]</sup>, Yana **Vasylichenko** <sup>[0000-0002-4566-8827]</sup>, Yevhen **Reva** <sup>[0009-0008-4723-9082]</sup>, Dmytro **Korchma** <sup>[0009-0000-1875-6285]</sup>, Roman **Boroday** <sup>[0009-0009-6730-9540]</sup>

Donbass State Engineering Academy (DSEA), bul. Mashinostroiteley, 39,  
Kramatorsk, Ukraine  
[wasilchenko.ua@gmail.com](mailto:wasilchenko.ua@gmail.com)

Received: 30 October 2024 / Revised: 14 November 2024 / Accepted: 26 November 2024 /  
Published: 15 December 2024

**Abstract.** *To determine the optimal cutting modes under conditions of increased requirements for the stability of technological processes, it is necessary to take into account the value of the tool life with a given probability. In this paper, the stability dependence for prefabricated cutters used on heavy machine tools with maximum diameters  $D_{max} = 1250-2500$  mm is specified using the group argumentation method. The study presents a new mathematical model that establishes the relationship between tool fracture resistance and key operational parameters. This model incorporates the probabilistic nature of tool performance, which allows for a more accurate assessment of the impact of part size variation, cutting conditions, and process variability. The proposed relationship facilitates the determination of cutting modes that not only increase tool stability but also ensure the reliability and efficiency of heavy machine tools in industrial environments. This mathematical dependence makes it possible to take into account the variation of workpiece parameters and cutting modes, which is especially important when working with large-sized parts on heavy-duty machine tools. The results of the study are of practical importance for industry, as they make it possible to increase the sustainability and productivity of technological processes.*

**Keywords:** *cutting tool; tool life; reliability; failure probability; cutting insert; cutting force.*

### 1. Introduction

The issues of wear and durability of cutting tools, machinability of various materials by cutting have been considered to a greater or lesser extent by many studies [1–13] and others. To obtain a mathematical model of the machining process for determining rational cutting modes, the initial dependence is  $T=f(V, S, t)$ . Therefore, for a number of years, a large number of researchers have been engaged in the study of tool wear patterns and resistance dependencies. At present, there are a large number of formulas derived from experimental data and linking durability with the elements of the cutting mode. Cutting speed has the strongest influence on the durability period. At present, empirical dependences of durability on the elements of the cutting mode have been established practically for all types of cutting tools and most tool machined materials. The most frequently used equation is:

$$S_p = C_p \cdot T_p^{-m_p}$$

However, the practice of using these formulas has shown that they are valid only in a limited range of changes in cutting modes.

The most complete studies of the stepped resistance dependence indices were performed in [6,11], which used multiplicative models of the resistance dependence, in which the degree indices are functions of the cutting tool parameters and machining conditions.

Despite the great variety of formulas describing the relationship between tool resistance and elements of the cutting mode, the required reliability and accuracy of the initial information for the calculation of cutting modes is not always ensured. The described dependencies are valid for those machining cases when tool failure occurs due to tool wear [3,8,9].

In real production conditions, carbide tool failure can occur not only as a result of wear of the cutting part, but also due to its destruction. In real production conditions, carbide tool failure can occur not only as a result of wear of the cutting part, but also due to its destruction. Therefore, for these cases, the steady-state dependences need to be clarified.

A number of works [12,13,14] have been devoted to the study of the tool fracture process. In works [12,13] the causes of cutting tool fracture on CNC machines are analysed. Failures of roughing cutters due to wear are only 60-70%, the remaining failures are related to tool breakages [13]. When turning on heavy machines, the percentage of cutting tool failures reaches 75% [14].

The most complete classification of the types of breakages of the working part of the tool is given in [14]. It is proved that during rough turning the destruction of a carbide plate mainly depends on the feed, and the wear depends on the cutting speed. The relationship between feed and the number of durability periods is expressed by the equation obtained on the basis of experimental and statistical data:

$$S_K = C_K \cdot K^{-m_k} \quad , \text{ where}$$

$S_K$  – the feed rate corresponding to a certain period of resistance;

$m_k$  – degree index;

In the same work, a similar relationship between the tool endurance to fracture and the breaking feed rate is given:

$$S_p = C_p \cdot T_p^{-m_p} \quad ,$$

where  $S_p$  is a coefficient characterising the average strength of the tool and depending on the processed material and working conditions;

$m_p$  – value characterising the degree of influence of  $T_p$  on  $S_p$ .

When machining steel parts with cutters  $m_p = 0,08-0,28$ . These dependencies relate feed rate to the tool life before fracture and the number of tool life periods and

are essentially similar to the  $V-T$  life dependencies. The former allows you to determine the tool life under conditions of wear, the latter – under conditions of its destruction. However, for practical use in the calculation of cutting modes, these dependences need to be clarified in relation to specific conditions, since the values of degree indices fluctuate in a wide range (especially  $m_k$ ) and have been studied mainly for medium-sized machine tools.

It was shown in [10] that the number of tool life periods can be considered with some approximation as a value inversely proportional to the probability of tool fracture.

The authors [3,9,12] pointed out the necessity of taking into account the probability of tool fracture when determining the feed rate. However, due to the lack of relations reflecting the probabilistic nature of the cutting process, taking into account both tool wear and tool fracture, this problem has not been completely solved.

In [11], an attempt was made to establish the dependence of tool life period numbers on the feed rate. However, the experiments were carried out on medium-sized machine tools. Therefore, the peculiarities of machining on heavy machine tools could not be fully taken into account.

Taking into account the large dispersion of the tool life period during its operation on heavy machine tools, the study of tool reliability and its relationship with the parameters of the operation process is of particular importance.

## **2. Applied methods**

The average tool life is a probabilistic value. It depends on the probability of a particular type of failure (wear or fracture). Tool life is defined as the time between failures of the corresponding type. In this case, these periods are conditional values that characterise the properties of a given tool. The average actual life of a cutting tool, which depends on its wear resistance and strength, is determined:

$$\bar{T} = q_s T_s + q_p T_p,$$

where  $T_s$ ,  $T_p$  are the periods of stability due to tool wear and fracture, respectively;  $q_s$ ,  $q_p$  are the probabilities of tool wear and fracture, respectively,  $q_s + q_p = 1$ .

To develop a mathematical model of the period of resistance to fracture of turning cutters for heavy machine tools, the method of group accounting of arguments was adopted [15].

This approach of self-organisation of models is fundamentally different from the commonly used deductive methods. It is based on inductive principles - finding the best solution by searching through various options.

By searching through different solutions, the role of assumptions about the modelling results is minimised. The algorithm determines the structure of the model

and the laws that apply to the object. It can be used to create artificial intelligence to resolve disputes and make decisions.

The group argumentation method consists of several algorithms for solving various tasks. It includes both parametric and clustering algorithms, analogue complexity and probabilistic algorithms. This self-organising approach is based on searching through gradually increasingly complex models and selecting the best solution according to a minimum external criterion. Not only polynomials but also nonlinear, probabilistic functions or clustering are used as basic models.

In this paper, we used the following types of functions:

$$f(x) = x, f(x) = 1/x, f(x) = \ln(x) .$$

The next step is to determine the optimal complexity of the model structure, adequate to the level of errors in the data sample. It is guaranteed to find the most accurate or unbiased model – the method does not miss the best solution when trying all options (in a given class of functions).

This method automatically finds the relationships interpreted in the data and selects the most effective input variables, neglecting the least influential elements. The method uses information directly from the data sample and minimises the influence of the author's a priori assumptions about the modelling results. This approach of this method can be used to improve the accuracy of other modelling algorithms and makes it possible to find an unbiased physical model of an object (law or clustering) - the same for all future samples.

### **3. Results and discussion**

According to laboratory tests (Figs. 1, 2), the type dependence was obtained for preliminary crust turning of steel with turning cutters with horizontally arranged T5K10 carbide inserts and for machining on machine tools with a maximum diameter of the workpiece above the bed (standard size)  $D_{max} = 1250-2500$  mm:

$$f(S_p) = f(C_1 \dots C_6, \ln V, \ln t, \ln D, \ln \sigma, t, V, D, \sigma),$$

where  $S_p$  is the average value of the fracturing feed, mm/rev;  $V$  is the cutting speed, m/min;  $t$  is the depth of cut, mm;  $D$  is the dimensional parameter of the machine tool, mm;  $\sigma$  is the tensile strength of the material being processed, MPa;  $C_1, \dots, C_6$  are approximation factors.

In many cases, the period of resistance to fracture of a cutting tool is directly proportional to the number of cycles before fracture. When turning under the specified conditions, the stress on the front surface of the cutting element

$$\sigma = C_y N^{-m_y} = C_y (fT_p)^{-m_y} = C'_y T_p^{-m_y}.$$

where:  $C_y$  is the coefficient characterising the strength of the tool,  
 $N$  is the number of fracture cycles,  
 $T_p$  is the period of resistance of the cutting tool to fracture.

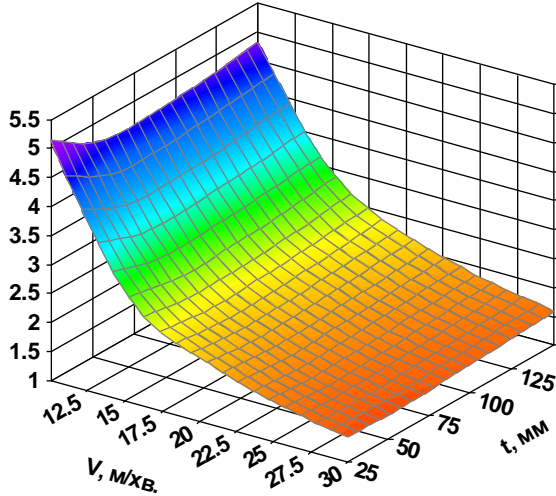


Fig. 1. Character of change in the breaking feed  $S_p$  with depth  $t$  and cutting speed  $V$  ( $D_{ma} = 1250$  mm, 90XF - T5K10 (P30), on the crust)

Maximum principal stress

$$\sigma_{max} = C''_y S_p,$$

$$S_p = \left( \frac{C'_y}{C''_y} \right) T_p^{-m_y}.$$

Based on the previous equation, the period of resistance to fracture can be determined by :

$$T_p = C_p \left( \frac{1.87 e^{\frac{1839.53 \ln V}{D} + 0.0336 \frac{D^2 \ln^2 t}{\sigma^2} \left( 1 + \frac{89.583}{V^2} \right)}}{e^{\frac{1071.21 \ln t}{\sigma} \left( 1 + 9 \cdot 10^{-9} \frac{D^3 V \ln^2 t}{\sigma^2} \right)}} \right)^{m_p},$$

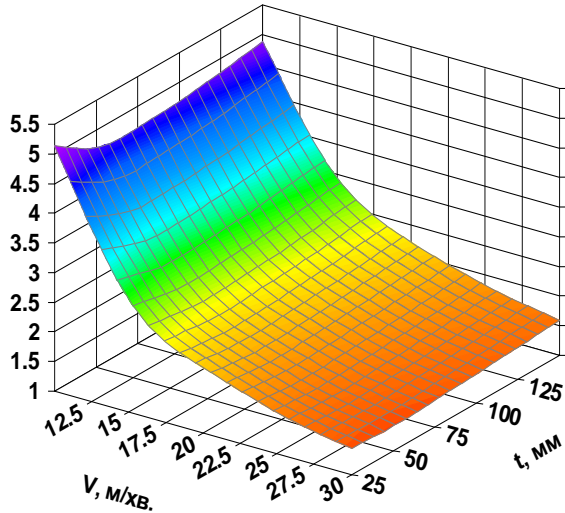


Fig. 1. Character of change in the breaking feed  $S_P$  with depth  $t$  and cutting speed  $V$  ( $D_{\text{ma}} = 2500$  mm, 90XF - T5K10 (P30), on the crust)

where  $C_P$  is a coefficient characterising the average strength of the tool, depending on the processed material and working conditions;  $m_P$  is a value characterising the degree of influence of the  $T_P$  on  $S_R$  ( $m_P = 1.6$  for  $S = 1.2\text{--}1.6$  mm/rev,  $m_P = 2.1$  for  $S = 1.61\text{--}2.05$  mm/rev.)

In developing the mathematical model, a sample ( $N = 240$ ) of statistical data from the information bank of failures of carbide tools on heavy machine tools with a maximum diameter of the workpiece  $D_{\text{max}} = 1250 - 2500$  mm was used. Mathematical processing of the data collected at different plants made it possible to determine the degree of dispersion of tool life and confirm the probabilistic nature of tool failures. This proves the need to take into account the destruction, not just the wear of the tool when determining its durability.

#### 4. Conclusions

The stability dependence for prefabricated cutters of heavy machine tools with  $D_{\text{max}} = 1250\text{--}2500$  mm is specified using the method of group argument accounting. The new mathematical dependence of tool fracture resistance on the most common operating conditions allows taking into account the probabilistic nature of tool operation, scattering of workpiece parameters, and cutting modes. Based on the research, a system of mathematical models and objective functions will be developed

to optimise cutting modes and tool consumption rates according to the following criteria: reduced costs, productivity, tool consumption, and the level of reliability of a prefabricated turning cutter when machined on heavy machine tools.

**References:** 1. *Gaddafee M., Satish S.*, An Experimental Investigation of Cutting Tool Reliability and its Prediction Using Weibull and Gamma Models: A Comparative Assessment, *Materials Today: Proceedings*, Volume 24, Part 2, 2020, pp.1478–1487, ISSN 2214-7853, <https://doi.org/10.1016/j.matpr.2020.04.467> 2. *Letot, C., Serra, R., Dossevi, M. et al.* Cutting tools reliability and residual life prediction from degradation indicators in turning process. *Int. J. Adv. Manuf. Technol.*, 86, 495–506 (2016). <https://doi.org/10.1007/s00170-015-8158-z> 3. *Liu, Erliang & An, Wenzhao & Xu, Zhichao & Zhang, Huiping.* (2020). Experimental study of cutting-parameter and tool life reliability optimization in inconel 625 machining based on wear map approach. *Journal of Manufacturing Processes*. 53. pp. 34–42. <https://doi.org/10.1016/j.jmapro.2020.02.006> 4. *Karimi, B., Niaki, S.T.A., Haleh, H. et al.* Reliability optimization of tools with increasing failure rates in a flexible manufacturing system. *Arab J Sci Eng*44, 2579–2596 (2019). <https://doi.org/10.1007/s13369-018-3309-9> 5. *Bakša, Tomáš & Kroupa, Tomáš & Hanzl, Pavel & Zetek, Miroslav.* (2015). Durability of Cutting Tools during Machining of Very Hard and Solid Materials. *Procedia Engineering*. <https://doi.org/10.1016/j.proeng.2015.01.51121> 6. *Jaydeep M. Karandikar, Ali E. Abbas, Tony L. Schmitz,* Tool life prediction using Bayesian updating. Part 2: Turning tool life using a Markov Chain Monte Carlo approach, *Precision Engineering*, Volume 38, Issue 1, 2014, pp.18–27, ISSN 0141-6359, <https://doi.org/10.1016/j.precisioneng.2013.06.007> 7. *Karimi, B., Niaki, S.T.A., Haleh, H. et al.* Reliability optimization of tools with increasing failure rates in a flexible manufacturing system. *Arab. J. Sci. Eng.* 44, 2579–2596 (2019). <https://doi.org/10.1007/s13369-018-3309-9> 8. *Astakhov V.*, The assessment of cutting tool wear, *International Journal of Machine Tools and Manufacture*, Volume 44, Issue 6, 2004, pp. 637–647, ISSN 0890-6955, <https://doi.org/10.1016/j.ijmactools.2003.11.006> 9. *Zhang, G., Wang, J., To, S.* (2023). Tool Fracture Wear Evaluation Method Using Cutting Chips. In: To, S., Wang, S. (eds) *Fly Cutting Technology for Ultra-precision Machining*. Precision Manufacturing, Springer, Singapore. [https://doi.org/10.1007/978-981-99-0738-0\\_9](https://doi.org/10.1007/978-981-99-0738-0_9) 10. *Vagnorius, Z., Rausand, M., & Sorby, K.* (2010). Determining optimal replacement time for metal cutting tools. *European Journal of Operational Research*, 206(2), 407–416. <https://doi:10.1016/J.EJOR.2010.03.023> 11. *Rathod N., Chopra M., Vidhate U., Gurule N., Saindane U.*, Investigation on the turning process parameters for tool life and production time using Taguchi analysis, *Materials Today: Proceedings*, Volume 47, Part 17, 2021, Pages 5830-5835, ISSN 2214-7853, <https://doi.org/10.1016/j.matpr.2021.04.199> 12. *Arif M., Rahman M., Wong Yoke San,* Analytical model to determine the critical feed per edge for ductile–brittle transition in milling process of brittle materials, *International Journal of Machine Tools and Manufacture*, Volume 51, Issue 3, 2011, pp. 170–181, ISSN 0890-6955, <https://doi.org/10.1016/j.ijmactools.2010.12.003> 13. *Klymenko G. Kvashnin V.* Reliability assurance technological systems exploitation of heavy lathe Cutting & tool in technological system 2019; 91: pp. 78–86 <https://doi.org/10.20998/2078-7405.2019.91.08> 14. *Klymenko G., Kovalov V., Vasylychenko, Korchma D., Boroday R.* Probabilistic approach to calculating the rational thickness of the tool’s cutting insert for heavy machine tools. *Cutting & tool in technological system 2023*; 99: pp 110–119 <https://doi.org/10.20998/2078-7405.2023.99.1> 15. *Ravskaya N., Kovaleva L.* Application of self-organisation methods for identification of processes and objects. *Lucrările științifice ale simpozionului internațional ‘UNIVERSITARIA ROPET 2002’ - INGINERIE MECANICĂ /*, Petroșani: Focus

Галина Клименко, Яна Васильченко, Євген Рева, Дмитро Корчма, Роман  
Бородай, Краматорськ, Україна

## **ВИЗНАЧЕННЯ ПЕРІОДУ СТІЙКОСТІ ТОКАРНИХ РІЗЦІВ ДЛЯ ВАЖКИХ ВЕРСТАТІВ**

**Анотація.** У статті доведено, що розробка регламентів експлуатації різальних інструментів на важких верстатах, формування цільових функцій оптимізації параметрів обробки деталей повинні здійснюватися виходячи із заданого рівня надійності різального інструменту. При цьому використовується велика кількість показників, що визначають окремо безвідмовність, довговічність та ремонтпридатність інструменту. На основі статистичних і теоретичних досліджень імовірного характеру властивостей різального інструменту і параметра розподілу навантаження на нього отримані кількісні залежності між параметрами розсіювання властивостей і товщиною інструментальної пластини збірного інструменту. Стохастичний характер процесу обробки на важких верстатах зумовлює великий розкид властивостей оброблюваних і інструментальних матеріалів та інших параметрів обробки. Це призводить до необхідності імовірного підходу до визначення конструктивно-технологічних параметрів різального інструменту. Надійність роботи збірного різця залежить як від його навантаження, так і від несучої здатності конструкції інструменту, яка є граничним напруженням, що характеризує міцність конструкції. Використовуючи імовірнісний підхід до розрахунку товщини ріжучої пластини різця, було визначено поправочний коефіцієнт на товщину з урахуванням рівня надійності інструменту. Під рівнем надійності розуміли ймовірність того, що максимальне напруження, яке виникає під дією навантаження, не перевищить тримальної здатності. Досліджувалися типові конструкції, які найчастіше використовуються на сучасних підприємствах важкого машинобудування. Закон розподілу сил різання визначався на основі статистичних даних про роботу твердосплавних різців. Товщина ріжучого елемента розраховувалася для релеївського закону розподілу навантаження, визначеного на основі статистичних даних про сили різання при токарній обробці для різних конструкцій різців. Розподіл тримальної здатності інструментального матеріалу пластин визначено на основі лабораторних випробувань.

**Ключові слова:** різальний інструмент; стійкість; надійність; ймовірність відмов; різальна пластина; сила різання.

UDC 621.7

doi: 10.20998/2078-7405.2024.101.10

## ADDITIVE TECHNOLOGIES IN CONSTRUCTION: TECHNICAL, ECONOMIC AND MANAGEMENT ANALYSIS

Yaroslav **Garashchenko** <sup>1</sup>[\[0000-0003-2568-4763\]](#), Olena **Harashchenko** <sup>1</sup>[\[0000-0002-9572-6095\]](#),  
Ruslan **Kucher** <sup>2</sup>[\[0009-0000-5835-4600\]](#)

<sup>1</sup>National Technical University «Kharkiv Polytechnic Institute», Kharkiv, Ukraine

<sup>2</sup>Mykolaiv National Agrarian University, Mykolaiv, Ukraine  
[yaroslav.garashchenko@gmail.com](mailto:yaroslav.garashchenko@gmail.com)

**Received: 29 October 2024 / Revised: 15 November 2024 / Accepted: 26 November 2024 /  
Published: 15 December 2024**

**Abstract.** *The study is devoted to a comprehensive analysis of the introduction of additive technologies into modern construction production, revealing the technical, economic, and managerial aspects of concrete 3D-printing of architectural structures. The work systematically analyzes the evolution of additive manufacturing technologies and identifies the main structural types of 3D-printers (an additive machine for layer-by-layer construction of objects), including portal, robotic, mobile, and hybrid systems. A detailed study of the technological parameters of concrete 3D-printing with concrete mixtures is presented, in particular, optimal printing speed modes, layer parameters, criteria for shaping and quality of building structures. A comparative analysis of the technological capabilities of leading world equipment manufacturers, such as ICON, COBOD International, Apis Cor, and WinSun, is conducted. The economic analysis demonstrates significant advantages of additive technologies: reduction of construction time by 2-6 times, reduction of construction cost by 20-35%, and increase in the load-bearing capacity of structures. The study comprehensively explores the structure of capital and operational expenses associated with technology implementation. Special emphasis is placed on the management aspects of introducing additive technologies, highlighting the critical need for an interdisciplinary approach and knowledge integration across architecture, engineering, management, and computer modeling. The study determines the prospects for the development of concrete 3D-printing technology in the construction industry and outlines the main directions of further scientific research and practical implementation of innovative solutions. This study was developed between the Department of "Integrated Technologies of Mechanical Engineering" named after M. Semko of NTU "KhPI" and "Geopolimer" LTD to implement innovative technologies in the construction industry.*

**Keywords:** *concrete 3D printing; construction; economic efficiency; project management; building materials.*

### 1. Introduction

The introduction of additive technologies (concrete 3D-printing) into construction is driven by many global challenges and industry needs. First, the global construction industry is facing an acute need for rapid and cost-effective housing construction [1].

Second, the construction sector is one of the largest consumers of natural resources. Additive technologies offer the potential for significant reduction of construction waste and optimization of material use. Third, there is a shortage of skilled labor in the construction sector. Automation of construction processes through concrete 3D-printing allows for partially addressing this issue. Moreover, the relevance of using additive technologies is underscored by the following factors:

- growing requirements for building energy efficiency;
- the need for rapid infrastructure restoration in post-conflict zones and disaster-affected areas;
- the requirement to create complex architectural forms while reducing their implementation costs;
- a trend towards individualization of housing construction and project adaptation to specific customer needs.

From a technological perspective, recent advancements in materials science, robotics, and CAD/CAM technologies create favorable conditions for the widespread implementation of additive technologies in construction. New construction mixtures optimized for concrete 3D-printing have been developed, along with improved quality control systems and automation of layer-by-layer forming processes [2–4].

However, despite the obvious potential, the widespread adoption of additive technologies in construction is constrained by several technical, economic, and managerial challenges that require comprehensive analysis and development of appropriate solutions. This necessitates a comprehensive study of the possibilities and limitations of additive technologies in the context of modern construction.

## **2. Review of the literature**

The state of studying additive technologies in construction is characterized by diverse and interdisciplinary approaches. Technical aspects of concrete 3D-printing of building structures have been explored in works [1–5], which focused on developing optimal construction mixture compositions [4] and technological printing parameters [5, 6]. In the work [7] presented the main scientific research directions for technological aspects of layer-by-layer construction using cement mixtures. Researchers from China, the United States, and Australia have been the most active in this research direction (in order of decreasing publication volume). Now Germany, France, Netherlands, and England are the leaders in Europe. The largest number of publications in journals: *Construction and Building Materials*, *Cement and Concrete Composites*, *Materials*, *Cement and Concrete Research*, *Automation in Construction*, *Additive Manufacturing* [8].

Economic aspects of additive technology implementation were examined in the work [9]. Studies [10] are dedicated to comparative cost analysis of traditional and additive construction. Project management issues using concrete 3D-printing were investigated in [11], focusing on the specifics of planning and organizing the construction process.

A particularly well-developed research direction is determining the rational composition of concrete mixtures depending on multiple factors and the physical-mechanical characteristics of concrete samples [12].

If we count by the number of publications in Google Scholar, the greatest scientific contributions to additive construction technologies were made by: Ma Guowei, Wang Li, Sanjayan Jay, Xiao Jianzhuang, Mechtcherine Viktor, Tan Ming Jen, Panda Biranchi, De Schutter Geert, Schlangen Erik, Zhang Yamei.

Despite the significant volume of research, there remains a need for a comprehensive analysis of the interconnections between technical and technological capabilities, economic efficiency, and management aspects of implementing additive technologies in construction.

The work aims to identify research directions for developing a comprehensive approach to evaluating the effectiveness of implementing additive technologies in construction, based on the integration of technical, economic, and management analysis.

### **3. Modern design solutions of 3D-printers for additive manufacturing of concrete structures**

Additive technologies in construction are currently experiencing a stage of active development, where specialized 3D-printers for working with concrete play a key role. The main structural types of such printers include [1, 2]:

- portal structures with a fixed frame (extruder movement along Cartesian X, Y, and Z axes; provide high printing accuracy and process stability; used for small architectural forms and construction structures);
- portal structures with fixed or movable vertical structures and displacement of two longitudinal and/or one transverse beam (provide sufficiently high precision and printing productivity; used for obtaining large building structures);
- robotic manipulators (based on multi-axis industrial robots, allowing printing of complex spatial structures. Have higher flexibility compared to portal systems, but require more complex software and have lower productivity);
- mobile concrete 3D printers (design allows autonomous movement and installation on various surfaces; for rapid construction of temporary structures);

- hybrid systems (combine properties of different concrete printer types, ensuring maximum adaptability to various architectural and construction tasks).

- All concrete printer types allow combining traditional construction methods with additive technologies.

Each printer type has specific advantages and limitations, the selection of which depends on specific project requirements, building geometry, and production conditions.

The main criteria for equipment selection and comparison include:

- printing accuracy (positioning and shape formation errors);
- workspace dimensions (possible building sizes);
- extruder movement productivity and speed (construction time);
- equipment mobility (preparation time for transportation, assembly time, transportation requirements);
- equipment and operational costs.

Research directions are aimed at improving concrete 3-D printer structural parameters, expanding their functional capabilities (parallel extruder or nozzle operation, reinforcement during extrusion), diversifying nozzle and leveling knife designs, reducing shape formation errors, and developing diagnostic and construction process monitoring systems.

The subsequent details are considered for portal printers (Fig. 1), which are among the most promising design solutions for rapidly restoring Ukraine's infrastructure.



Figure 1 – Concrete 3D-printer GP-1 (manufacturer "Geopolimer" LTD, Kharkiv)

#### **4. Technological parameters of the concrete 3D printing**

When determining the technological capabilities of additive technologies in construction, the primary focus was on the shape formation mode parameters [2].

Printing speed  $V$ . Based on the practical experience of large-format construction printer developers, the optimal printing speed range is  $V = 50\text{--}150$  mm/s. The maximum speed can reach up to 1000 mm/s (depending on mixture composition, layer width, and height [4]). Minimum speed: not less than 30 mm/s (to prevent material solidification). Speed is primarily determined by mixture composition and extruder productivity. Key factors influencing speed [13] include concrete mixture viscosity, cement setting time, mixture supply pressure, nozzle diameter, and ambient temperature.

Layer parameters: thickness  $h$  and width  $b$ .

Layer thickness  $h$ . The optimal range is considered to be 8–50 mm, with typical values for vertical walls being 15–20 mm;  $h$  mainly depends on layer width, nozzle diameter, and mixture rheological properties.

Layer width  $b$ . Recommended range is  $b = 20\text{--}60$  mm, ensuring a rational  $b/h$  ratio of 2.5–4.0. This  $b/h$  ratio is necessary to ensure a stable layer and overall structure dimensions. The maximum possible  $b$  value is 300 mm. The  $b$  values depend on nozzle diameter, supply pressure, printing speed, and surface inclination angle  $a$ .

Permissible wall surface inclination angle range (without additional support)  $a_c = 75^\circ\text{--}90^\circ$ , with vertical walls providing the greatest structural stability, i.e., at  $a_c = 90^\circ$ . With support, it is practically feasible across the entire  $a_c$  range.

Factors influencing the permissible angle  $a_c$  (without support): layer thickness, mixture setting speed, previous layer strength, structure height, temperature conditions, and mixture composition.

Additional technological parameters include:

- layer construction interval  $t_{\min,1}$  (necessary for ensuring stable shape formation), optimal interval  $t_{\min,1} = 1\text{--}10$  minutes, depending on mixture composition, structure height, and environmental conditions;

- environmental conditions: temperature (optimal  $-15^\circ\text{C} \dots -25^\circ\text{C}$ , recommended range  $5^\circ\text{C} \dots -40^\circ\text{C}$ ), humidity (optimal  $-50\% \dots -70\%$ ), protection from direct sunlight and wind.

#### **5. Comparative analysis of technological capabilities of concrete 3D printing equipment**

Analysis of the technological capabilities of market-leading additive equipment

reveals the following features:

ICON Technology:

- printing speed up to 2000 mm/s;

COBOD International:

- modular BOD2 system with broader scaling capabilities;
- printing speed up to 1000 mm/s;

Apis Cor:

- mobile printer with a printing radius of up to 8.5 meters;
- ability to print curved surfaces;

WinSun (Yingchuang):

- large-scale systems for extensive projects;
- capability to print multi-story buildings;
- material recycling;

Generally for most manufacturers:

- proprietary material developments;
- operation in challenging weather conditions (advantages for ICON);
- integrated quality control system (advantages for ICON);
- multifunctional extruder;
- ability to work with a wide range of materials (advantages for COBOD

International);

• high positioning accuracy (advantages for COBOD International and Apis Cor).

In cases of printing under extreme conditions (low or high temperature and/or humidity), key technological innovations can be separately highlighted:

Materials:

- special additives for rapid setting at low temperatures;
- viscosity modifiers for high-temperature operations;
- reinforcing components to increase early-stage strength;

Material supply system:

- thermal insulation of transport line;
- heating/cooling of material during transportation;
- moisture control system for components;
- automatic mixture composition adjustment;

Extruder:

- nozzle thermal stabilization system;
- protection against abrasive wear;
- dynamic extrusion diameter control;
- cleaning system during stops;

Control system (electronics):

- compensation for structural thermal deformations;
- adaptive calibration system;
- vibration and position correction sensors;
- enhanced drives for operation during strong winds;

Control system (software):

- external factor compensation algorithms;
- predictive print quality analytics;
- adaptive speed management;
- material structural integrity monitoring.

Due to these innovations, the working conditions are considered:

ICON (Vulcan system):

- temperature range from +2°C to +43°C;
- relative humidity 20–95% (with compensation systems);

COBOD (BOD2 system):

- temperature range from +5°C to +40°C;
- relative humidity 30–85%.

Research directions: optimizing extruder speed and acceleration depending on movement trajectory, mixture composition, and environmental conditions; predicting, monitoring, and preventing extruder movement jolts; optimizing building design for specific equipment technological capabilities; optimizing trajectory and construction time based on surface quality criteria.

## **6. Print quality criteria**

There are several important quality criteria for 3D printing of buildings, based on various technical standards. The main requirements include:

- verticality of the walls, the maximum deviation from the vertical should not exceed 1/200 of the wall height (for a 3 m high wall, the permissible deviation is approximately 15 mm);
- horizontality of the surfaces, the maximum deviation from the horizontal is 1/300 of the length (for a 6 m section, the permissible deviation is approximately 20 mm);
- wall thickness, the permissible deviation is  $\pm 5 \dots 10$  mm from the design thickness (it is important to ensure uniformity over the entire height);
- straightness (along the surface of the layer), on an arbitrary section of 2 meters the maximum deviation is no more than 10–12 mm, the total curvature along the length of the wall should not exceed 20 mm;

- corner joints, deviation of corners from the design position should not exceed 5–7 mm;
- minimum concrete strength, 20–40 MPa;
- bond strength between layers, not less than 1.5–2 MPa;
- absence of delaminations;
- homogeneity of the concrete mix (the mix should be free of pores and cavities, with a material density of no less than 97%, and a uniform distribution of reinforcing elements).

## **7. Economic Aspects of Implementing Additive Technologies**

According to research [14], the main capital costs associated with the implementation of additive technologies in construction are as follows:

- construction 3D printer – 40...60% of the total investment;
- material mixing and feeding systems – 15...25%;
- software and control systems – 10...20%;
- auxiliary equipment, tools and consumables – 5...15%.

The distribution of operating costs for such technologies typically follows this structure [15]:

- materials – 30...45%;
- labor costs – 20...35%;
- energy consumption – 5...10%;
- maintenance – 10...15%;
- logistics – 5...10%.

An analysis of the indicators for the most common construction technologies, based on the example of a 100 m<sup>2</sup> private house, has led to the following results, which are presented in Table 1.

A comparative analysis of construction technology characteristics (Table 1) highlights several advantages of 3D printing, particularly in constructing walls with a rectilinear configuration.

The fundamental advantages of the technology include:

- reduction of construction time (for example, 3D printing technology allows to reduce the duration of wall construction by 2–6 times compared to traditional methods – masonry, aerated concrete).
- reduced load on the foundation and greater bearing capacity (a comparative analysis shows that 3D printing technology provides significantly higher bearing capacity indicators (2457.2 kN) with lower specific material consumption (0.185–0.235 m<sup>3</sup> per 1 m<sup>2</sup> of wall)).

- economic efficiency (the cost of 1 m<sup>2</sup> of wall using 3D printing technology is 115–135 US dollars, which is 20–35% lower than traditional technologies). Additional technological advantages include:
  - the possibility of integrated insulation without the need for additional structural elements;
  - elimination of the need for external and internal finishing;
  - architectural variability, enabling the individualization of structural solutions.

Table 1 Comparison of indicators of the construction of the walls of the house per 100 m<sup>2</sup> obtained by different technologies

Construction technology	Relative indicators (with a wall height of 3.0 m)				Construction time (days)
	weight (kg / m <sup>2</sup> )	permissible load (kN)	volume per m <sup>2</sup> (m <sup>3</sup> )	min cost (\$/m <sup>2</sup> )	
Stone masonry – brick, 51 cm wide	918	881	0,51	180	25
Construction of aerated concrete	450	1500	0,4	150	10-12
3D printing of a wall, 40 cm wide	370	2457	0,185	115	4
3D printing of a wall, 60 cm wide	470	2457	0,235	135	5
3D printing of a wall, 50 cm wide, reinforced concrete (pouring)	1200	2 800–3 000	0,5	210	5
Monolithic house, formwork 50 cm wide, reinforced concrete (pouring)	1250	2 800–3 000	0,5	180–230	10-14

Note: The cost is indicated based on 2024 prices.

These advantages confirm the prospects of 3D printing technology in the construction industry, especially in countries with developed innovation infrastructure (USA, Netherlands, Western European countries).

Further research is needed on the issues of long-term operation, the influence of climatic factors, and the adaptation of the technology to various construction conditions.

## **8. Project Management for Additive Technologies in Construction**

The introduction of additive technologies into the construction industry necessitates a fundamentally new approach to project management that accounts for the specific requirements of 3D printing architectural structures.

The main components of project management include:

- planning and preparation (special tasks of 3D modeling of an architectural object, preliminary calculation of material consumption, selection of optimal printing technology, preparation of specialized equipment);
- technological features of management (control of printing mixture parameters, monitoring the accuracy of architectural form reproduction, printing management, ensuring printing conditions);
- resource provision (training of qualified personnel, maintenance of 3D printers, material logistics, equipment calibration);
- economic efficiency (optimization of construction time reduction, minimization of labor costs, production waste, and project estimates);
- risk management (forecasting possible technological limitations, insurance of project risks, ensuring the quality of the final design, testing of test samples).

A key aspect is the establishment of an integrated management system that combines technological innovations, economic efficiency, and engineering solutions.

Promising directions for further research include the development of unified management standards.

The implementation of additive technologies requires an interdisciplinary approach, integrating knowledge from architecture, engineering, management, and computer modeling.

## **9. Conclusions**

Additive technologies in construction are at the stage of active development, demonstrating significant potential for transforming this industry.

Modern 3D printers are represented by various design types: gantry, robotic, mobile, and hybrid systems, each with specific advantages and limitations.

The key technological parameters of concrete 3D printing are speed (50–1000 mm/s), layer thickness (5–50 mm), layer width (20–300 mm), and surface inclination angle (75°–90°).

Leading manufacturers of 3D printers (ICON, COBOD, Apis Cor, WinSun) demonstrate unique technological solutions, particularly high speed, mobility, and adaptability of equipment.

3D printing technology offers several advantages over traditional construction methods, including:

- a reduction in construction time by 2–6 times;
- a decrease in the load on the foundation;
- high load-bearing capacity of structures;
- economic efficiency, with cost reductions of 20–35%.

Clear quality requirements for 3D printing have been established, encompassing:

- permissible deviations from vertical and horizontal alignment;
- specifications for wall thickness;
- criteria for the strength and uniformity of the concrete mix.

The distribution of capital costs for implementing this technology has been analyzed, with the largest share attributed to equipment expenses. A distinctive feature of budgeting for additive technologies is the significant proportion of material costs, accounting for 30–45%.

The adoption of additive technologies necessitates a novel, integrated management approach that combines technological innovation, economic efficiency, and engineering solutions. An interdisciplinary effort is essential, requiring collaboration among specialists in architecture, various engineering disciplines (e.g., design, mechanics, electronics, technology, programming), management, and computer modeling.

Additive 3D printing technologies demonstrate revolutionary potential in the construction industry, offering more efficient, economical, and flexible solutions compared to traditional methods.

## **10. Acknowledgements**

This study was conducted as part of the project for the development of a 3D printer for large-scale construction by the team at "Geopolimer" LTD. Special gratitude is extended to the project manager, Elina Rudenko, for her invaluable assistance in collecting and providing informational materials for this study.

**References:** **1.** *El-Sayegh S., Romdhane L., Manjikian S.* A critical review of 3D printing in construction: Benefits, challenges, and risks. *Archives of Civil and Mechanical Engineering*, 20, 2020. pp. 1–25. **2.** *Tay Y.W.D., Panda B., Paul S.C., Noor Mohamed N.A., Tan M.J., Leong K.F.* 3D printing trends in building and construction industry: a review. *Virtual and physical prototyping*, 12(3), 2017. pp. 261–276. **3.** *Zhang Y., Zhang Y., Liu G., Yang Y., Wu M., Pang B.* Fresh properties of a novel 3D printing concrete ink. *Construction and Building Materials*, 174, 2018. pp. 263–271. **4.** *Paul S. C., Tay Y. W. D., Panda B., Tan M. J.* Fresh and hardened properties of 3D printable cementitious materials for building and construction. *Archives of Civil and Mechanical Engineering*, 18(1), 2018. pp. 311–319. **5.** *Panda B., Tan M. J.*

Experimental study on mix proportion and fresh properties of fly ash based geopolymer for 3D concrete printing. *Ceramics International*, 44(9), 2018. pp. 10258–10265. **6.** Zhou W., Zhang Y., Ma L., Li V.C. Influence of printing parameters on 3D printing engineered cementitious composites (3DP-ECC). *Cem. Concr. Compos.* 2022, 130, 104562. **7.** Buswell R.A., De Silva W.L., Jones S.Z., Dirrenberger J., 3D printing using concrete extrusion: A roadmap for research. *Cement and concrete research*, 112, 2018. pp.37–49. **8.** Wang J., Liu Z., Hou J., Ge M. Research Progress and Trend Analysis of Concrete 3D Printing Technology Based on Cite Space. *Buildings*, 14(4), 2024. 989 p. **9.** De Schutter G., Lesage K., Mechtcherine V., Nerella V.N., Habert G., Agusti-Juan I. Vision of 3D printing with concrete — Technical, economic and environmental potentials. *Cement and Concrete Research*, 112, 2018. pp. 25–36. **10.** Sakin M., Kiroglu Y.C. 3D Printing of Buildings: Construction of the Sustainable Houses of the Future by BIM. *Energy Procedia*, 134, 2017. pp. 702–711. **11.** Kazemian A., Yuan X., Meier R., Khoshnevis B., Sanjayan J.G., Nazari A., Nematollahi B. 3D Concrete Printing Technology. 2019. **12.** Overmeir A.L., Šavija B., Bos F.P., Schlangen E. 3D Printable Strain Hardening Cementitious Composites (3DP-SHCC), tailoring fresh and hardened state properties. *Construction and Building Materials*, 403, 2023. p. 132924. **13.** Roussel N. Rheological requirements for printable concretes. *Cement and Concrete Research*, 112, 2018. pp. 76–85. **14.** Tinoco M. P., de Mendonça É. M., Fernandez L. I. C., Caldas L. R., Reales O. A. M., Toledo Filho R. D. Life cycle assessment (LCA) and environmental sustainability of cementitious materials for 3D concrete printing: A systematic literature review. *Journal of building engineering*, 52, 2022. 104456. **15.** De Soto B. G., Agustí-Juan I., Hunhevicz J., Joss S., Graser K., Habert G., Adey B. T. Productivity of digital fabrication in construction: Cost and time analysis of a robotically built wall. *Automation in construction*, 92, 2018. pp. 297–311.

Ярослав Гаращенко, Олена Гаращенко, Харків, Україна  
Руслан Кучер, Миколаїв, Україна

## **АДИТИВНІ ТЕХНОЛОГІЇ В БУДІВНИЦТВІ: ТЕХНІЧНИЙ, ЕКОНОМІЧНИЙ ТА МЕНЕДЖМЕНТ-АНАЛІЗ**

**Анотація.** Дослідження присвячене комплексному аналізу впровадження адитивних технологій у сучасне будівельне виробництво, розкриваючи технічні, економічні та управлінські аспекти 3D-друку архітектурних конструкцій. Актуальність використання адитивних технологій підкреслюється наступними факторами: зростання вимог до енергоефективності будівель; необхідність швидкого відновлення інфраструктури в постконфліктних зонах та районах стихійних лих; потреба у створенні складних архітектурних форм при зниженні вартості їх реалізації; тенденція до індивідуалізації житлового будівництва та адаптації проектів під конкретні потреби замовників. У роботі системно проаналізовано еволюцію технологій адитивного виробництва, визначено основні конструктивні типи 3D-принтерів, включаючи портальні ліх, роботизовані, мобільні та гібридні системи. На сьогодні у світі відомо близько 500 виробників будівельних 3D принтерів. Представлено детальне дослідження технологічних параметрів 3D-друку бетонними сумішами, зокрема оптимальних режимів швидкості друку, параметрів шарів, критеріїв формоутворення та якості будівельних конструкцій. Проведено порівняльний аналіз технологічних можливостей провідних світових виробників обладнання, таких як ICON, COBOD International, Apis Cor та WinSun. Економічний аналіз демонструє значні переваги адитивних технологій по відношенню до інших, які широко поширені у будівництві: скорочення термінів будівництва у 2 – 6 разів, зниження собівартості будівництва на 20 – 35 %,

*підвищення несучої здатності конструкцій, зменшення навантаження на фундамент. Розкрито структуру капітальних та операційних витрат при впровадженні технології. Основними технологічними параметрами 3D-друку бетонними сумішами є швидкість друку (50 – 1000 мм/с), товщина шару (8 – 50 мм), ширина шару (20 – 300 мм) та кут нахилу поверхні (75° – 90°). Особливу увагу приділено управлінським аспектам впровадження адитивних технологій, необхідності міждисциплінарного підходу та інтеграції знань з архітектури, інженерії, менеджменту та комп'ютерного моделювання. Дослідження визначає перспективи розвитку технології 3D-друку в будівельній галузі, окреслює основні напрямки подальших наукових досліджень та практичного впровадження інноваційних рішень. Дослідження виконано в рамках науково-технічного співробітництва між кафедрою «Інтегровані технології машинобудування» ім. М.Ф. Семка» НТУ «ХПИ» та ТОВ «Геополімер» з метою впровадження інноваційних технологій в будівельну галузь.*

**Ключові слова:** 3D друк бетону; будівництво; економічна ефективність; управління проектами; будівельні матеріали.

## **THE ESSENCE OF THE PROCESS OF VIBRATIONAL FINISHING AND CLEANING, ITS TECHNOLOGICAL CAPABILITIES AND WAYS TO INCREASE EFFICIENCY**

Andrii Mitsyk <sup>[0000-0002-3267-8065]</sup>, Vladimir Fedorovich <sup>[0000-0001-7015-8653]</sup>, Natalia Kozakova <sup>[0000-0002-1891-4615]</sup>

National Technical University «Kharkiv Polytechnic Institute», Kharkiv, Ukraine  
[Volodymyr.Fedorovych@khp.edu.ua](mailto:Volodymyr.Fedorovych@khp.edu.ua)

**Received: 29 October 2024 / Revised: 15 November 2024 / Accepted: 26 November 2024 /  
Published: 15 December 2024**

**Abstract.** *The main provisions of the classification of the vibration processing process depending on the characteristics and composition of the processing medium are given. It is established that vibration processing is a mechanochemical removal of metal particles and its oxides, and plastic deformation of the microroughness of the surface of the part. It was found that vibration processing is related to mechanical dynamic processes, when using chemically active solutions it is related to mechanochemical processes, according to technological purpose to dimensionless processes, according to the type of tool – to processing with free abrasives. It was determined that vibration processing is characterized by the dynamic mechanochemical effect of abrasive medium granules on the treated surface and the acoustic effect of shock waves. It has been established that the features of mechanical and physicochemical phenomena of vibration processing differ in the physical properties of the granules of the medium, the characteristics of the material of the processed parts, the dynamic nature of the process, the composition and properties of the chemically active solution. A classification of defects in the formation of parts, controlled parameters and vibration processing operations is given. The technological capabilities of the processing are presented, these are micro-cutting and surface plastic deformation, the effect of variable accelerations and continuous application of micro-impacts to the surface being processed, which ensures the dynamic nature of the process and creates conditions for strengthening and stabilizing processing. The design of the vibration machines allows the use of various compositions of solid, liquid and mixed compositions of working media. To increase the efficiency of the process, a variable scheme for combining technical solutions of new varieties of the vibration processing process is proposed. It has been established that by combining various combinations of technological and design parameters it is possible to expand the scope of application of the vibration finishing and cleaning process based on the creation and implementation of its varieties.*

**Keywords:** *vibration finishing and cleaning; process classification; workpieces; classification of shaping defects; combination of technical solutions; area of application of the process; process varieties..*

### **1. General provisions for the classification of vibration machining processes**

© A. Mitsyk, V. Fedorovich, N. Kozakova, 2024

Vibration processing, depending on the characteristics and composition of the processing medium, is a mechanical or mechanochemical removal of the smallest particles of metal or its oxides and plastic deformation of microroughness as a result of mutual collisions of the granules of the medium with the processed surface of the parts caused by vibration of the tank in which the processing medium and the processed parts are placed.

In accordance with the accepted classification, vibration processing is related to mechanical processing processes, and when chemically active solutions are introduced into the working environment, it should be classified as a combined process, in particular, as a group of mechanochemical processing processes.

Vibration machining is a dynamic and, by its technological purpose, a dimensionless machining process. By the type of tool used, it is a free abrasive machining process [1].

## **2. Basic phenomena and features of the vibration processing process**

In general, vibration processing is characterized by the following phenomena:

- dynamic impact of the processing environment in the form of multiple collisions of its granules with the surface of the workpiece;
- mechanochemical interaction of the abrasive medium and the material of the part;
- acoustic impact of shock waves.

The features of mechanical and physical-chemical phenomena during vibration processing are as follows:

- physical properties of abrasive granules of the medium;
- characteristics of the material of the parts being processed;
- dynamic process parameters;
- composition, properties and quantity of chemically active solution.

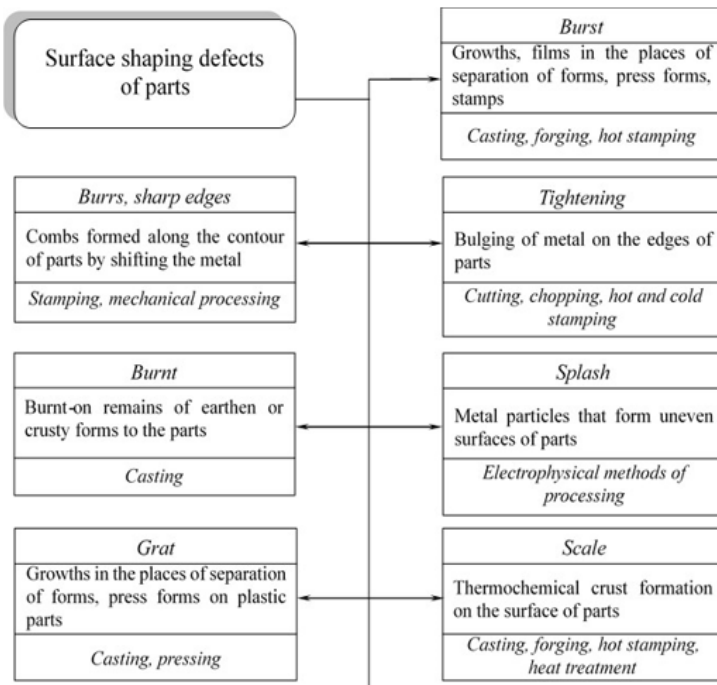
The efficiency of the vibration processing process, assessed by the weight removal of metal from a unit of surface area of the processed part per unit of time, depends on the intensity of mechanical and chemical effects and the ability of the part material to resist the action of these phenomena [2].

## **3. Classification of defects in the formation of parts, controlled parameters and operations of the vibration processing process**

The results achieved when performing various processes of processing a part are determined by the nature of the interaction of these parts with the working environment, as well as the processing modes. The interaction characteristics are considered as a general concept that includes the nature of the movements performed by the workpieces and the working environment and the forces that arise in this process.

Vibration processing and its varieties are considered as a combination of the effects of several types of energy and schemes during technological operations such as casting, pressing, forging, hot and cold stamping, processing on metal-cutting machines, which are accompanied by the formation of defects on the surface of the processed parts, causing deviations in their shape, accuracy and roughness from the specified values. These defects in the production of parts must be removed before assembly operations of the products and their further operation.

For the final processing of parts, defects acquired at various stages of their manufacture are classified from the standpoint of the structure and features of the technological processes for obtaining blanks of these parts (Fig. 1).



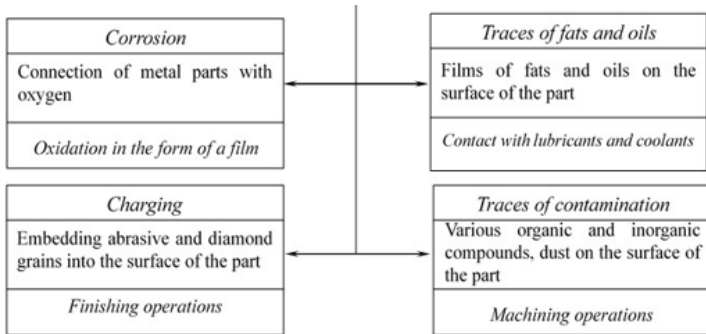


Fig. 1 Classification of surface shaping defects of parts subject to removal by finishing and cleaning treatment

All defects in the formation of the surface of a part in metalworking production are removed by carrying out various finishing and cleaning operations, the classification of which is given below (Fig. 2).



Fig. 2 Classification of vibration finishing and cleaning operations used in metalworking industries

When considering cleaning operations, the controlled parameter of the processing process is the degree of cleanliness of the parts from metallic and non-metallic defects physically and chemically connected to the material of the part. In addition, the effect of the duration of processing on the surface cleanliness is controlled, which is illustrated graphically (Fig. 3) [3].

#### **4. Technological capabilities of the vibration processing process**

An examination of the technological capabilities of the vibration processing process shows that they consist of a complex effect of a number of factors on the processed surfaces of parts [4]:

- multiple micro-impacts of the working medium granules, ensuring uniform impact on the surfaces of the parts being processed;
- variable accelerations causing shock wave processes and bending stress in the workpieces;
- chemically active solutions that cause physical and chemical processes;
- intensive movement of the working environment and workpieces.

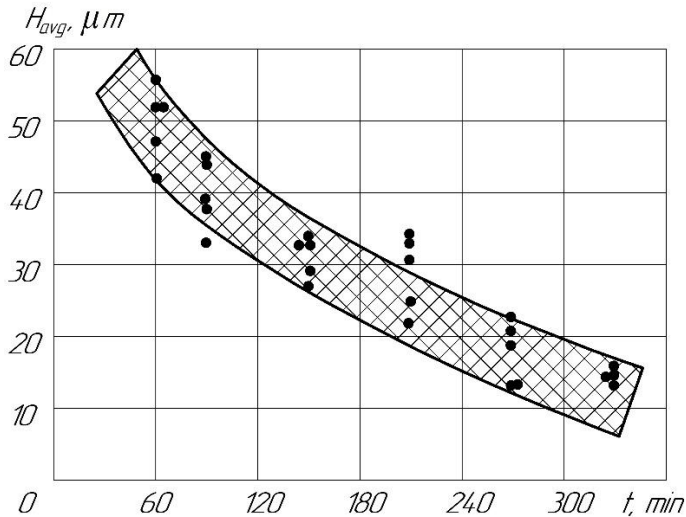


Fig. 3 Effect of processing time on the surface finish of castings

By analyzing the values of each of the listed process factors, we can imagine its technological capabilities, which are as follows:

– Micro cutting and surface plastic deformation are the main elements of the vibration machining process. The absence of a rigid connection between the part and the tool eliminates the possibility of effective and controlled influence on the geometric dimensions and shape of the part. Therefore, the vibration processing process is dimensionless, i.e. does not determine the shape and dimensions of the parts being processed.

– The effect of variable accelerations at different orientations of the workpieces and continuous application of micro-impacts to the workpiece surface ensures the dynamic nature of the process, shock-wave phenomena and the performance of such operations as removal, alignment and creation of optimal residual stresses ensure its stabilization at a certain level. Conditions are created for the implementation of strengthening and stabilizing treatment.

The design of the vibration machines and the long-term vibration processing process allow for the placement and use of various compositions of solid, liquid and mixed compositions of working media, as well as changing their temperature. This creates conditions for both mechanical processing processes and physical-mechanical processes of their combination by introducing powder materials, solutions, suspensions, and electrolytes into the working environment, which intensifies the processing process.

## **5. Improving the efficiency of the vibration machining process**

Consideration of the issue of increasing the efficiency of the vibration processing process made it possible to propose a variable scheme for combining technical solutions for new types of vibration processing processes (Fig. 4) [5].

When implementing process variations, according to the hardware design options of the technological system "tank with working medium - device with workpieces" in the tank of the vibratory machine, an energy effect is formed that creates a general circulation character of the cyclonic movement of granules of the working medium, freely penetrating to all hard-to-reach areas of the surface of the workpiece, which leads to high intensity of processing, the control of which is carried out by choosing rational combinations of the values of the amplitude-frequency parameters of the oscillatory movement of the tank and the device with workpieces, as well as the rotational movement of the spindle and impeller of the vibratory machine.

The workpieces are given additional types of oscillatory and rotary motion by installing them in machine tools, spindles and other devices. By combining various

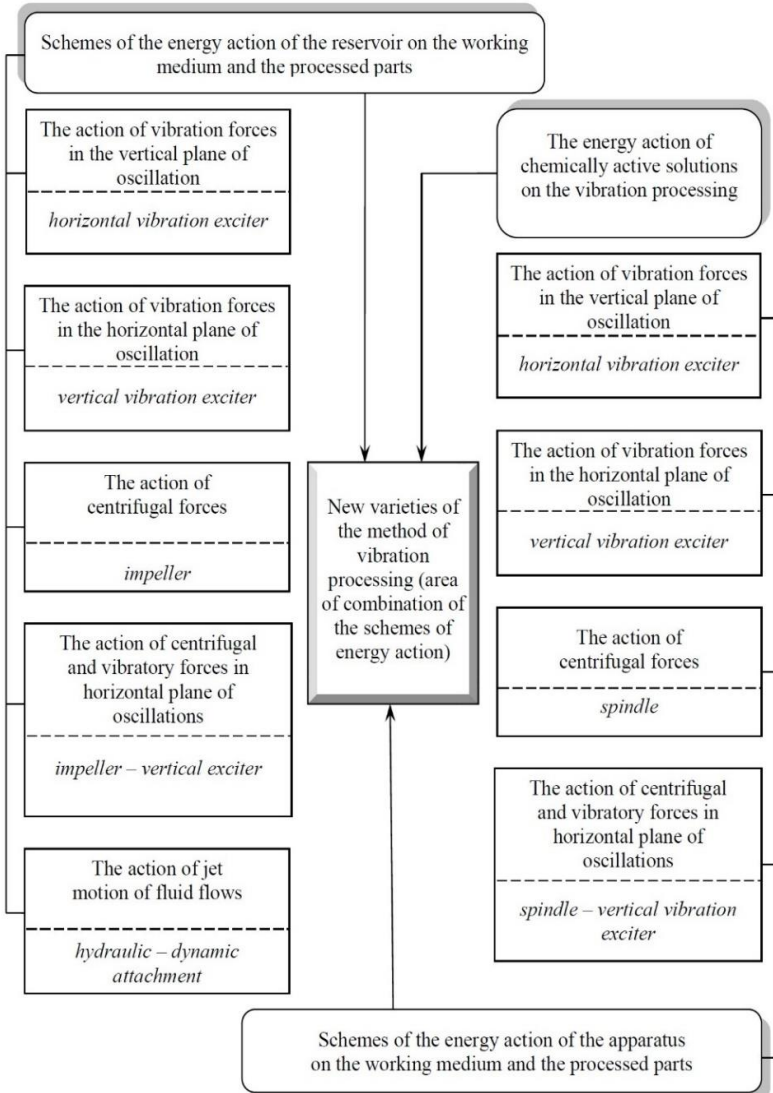


Fig. 4 Variable scheme of combining energy impacts and design elements of technical solutions of new types of vibration processing methods

combinations of technological and design parameters, it is possible to significantly expand the scope of application of the vibration finishing and cleaning process based on the creation and implementation of its new varieties [6].

Of all the problematic, from the point of view of finishing and cleaning processing, nomenclature of parts of drive and distribution mechanisms, as well as parts of the type of body of revolution, such as disks, bushings, coils, pulleys, gear wheels and others, having a symmetrical surface shape and central through holes, which can be used for basing and fixing in devices of working bodies of vibratory machines.

## 6. Conclusions

1. It has been revealed that the process of vibration processing is a complex of interrelated phenomena involving: microcutting; elastic-plastic deformation; activation of the surface layer of the metal; formation and destruction of secondary structures, repeating with the frequency of the action of the disturbing force.

2. It has been established that chemically active solutions perform the following functions during vibration processing: intensification of the process by chemical action on the processed surfaces of the part; cooling of the part during processing; removal of wear products from the reservoir; prevention of sticking of flat parts.

3. A variable scheme of hardware design of the technological system “tank with working medium – device with workpieces” is proposed, the use of which creates favorable conditions for processing parts with complex-profile surfaces with a free abrasive medium.

**References:** 1. Kang YS, Hashimoto F, Johnson SP, Rhodes JP (2017) Discrete element modeling of 3D media motion in vibratory finishing process. *CIRP Ann* 66:313–316. <https://doi.org/10.1016/j.cirp.2017.04.092> 2. Tools for machining parts with free abrasives (in Ukrainian): monografija / M.O. Kalmykov, T.O. Shumakova, V.B. Strutins'kij, L.M. Lubens'ka. Kyiv – Luhans'k: «Noulidzh», 2010. 214 p. 3. Uhlmann, E., Dethlefs, A. & Eulitz, A. Investigation into a geometry-based model for surface roughness prediction in vibratory finishing processes. *Int. J. Adv. Manuf. Technol.* 75, pp. 815–823 (2014). <https://doi.org/10.1007/s00170-014-6194-8> 4. Mitsyk A.V., Fedorovich V.A., Ostroverkh Y.V. Purpose and technological properties of granular media for vibration finishing and grinding processing. *Cutting & Tools in Technological System*. Kharkiv, NTU «KhPI». 2023. № 99. pp. 85 – 93. <https://doi:10.20998/2078-7405.2023.99.10> 5. Kundrák, J., Morgan, M., Mitsyk, A., Fedorovich, V. The effect of the shock wave of the oscillating working medium in a vibrating machine's reservoir during a multi-energy finishing-grinding vibration processing. *Int. J. Adv. Manuf. Technol.*, 106, pp. 4339–4353 (2020). <https://doi.org/10.1007/s00170-019-04844-2> 6. Kundrák, J.; Mitsyk, A.V.; Fedorovich, V.A.; Morgan, M.; Markopoulos, A.P. The Use of the Kinetic Theory of Gases to Simulate the Physical Situations on the Surface of Autonomously Moving Parts During Multi-Energy Vibration Processing. *Materials* 2019, 12, 3054. <https://doi.org/10.3390/ma12193054>

Андрій Міцик, Володимир Федорович, Наталія Козакова, Харків, Україна

## **СУТНІСТЬ ПРОЦЕСУ ВІБРАЦІЙНОЇ ОЗДОБЛЮВАЛЬНО-ЗАЧИЩУВАЛЬНОЇ ОБРОБКИ, ЇЇ ТЕХНОЛОГІЧНІ МОЖЛИВОСТІ ТА ШЛЯХИ ПІДВИЩЕННЯ ЕФЕКТИВНОСТІ**

**Анотація.** *Наведено основні положення класифікації процесу вібраційної обробки залежно від характеристик та складу обробного середовища. Встановлено, що вібраційна обробка є механохімічним зніманням частинок металу та його оксидів, та пластичним деформуванням мікронерівностей поверхні деталі. Виявлено, що вібраційна обробка відноситься до механічних динамічних процесів, при використанні хімічно-активних розчинів її відносять до механохімічних процесів, за технологічним призначенням до безрозмірних процесів, за видом інструменту до обробки вільними абразивами. Визначено, що вібраційна обробка характеризується динамічною механохімічною дією гранул абразивного середовища на оброблювану поверхню та акустичним впливом ударних хвиль. Встановлено, що особливості механічних та фізико-хімічних явищ вібраційної обробки відрізняються фізичними властивостями гранул середовища, характеристикою матеріалу оброблюваних деталей, динамічним характером процесу, складом та властивостями хімічно-активного розчину. Дана класифікація дефектів формоутворення деталі, контрольованих параметрів та операцій вібраційної обробки. Представлені технологічні можливості процесу обробки, це мікрорізання та поверхневе пластичне деформування, вплив змінних прискорень та безперервне нанесення мікроударів по оброблюваній поверхні, що забезпечує динамічний характер процесу та створює умови зміцнювальної та стабілізаційної обробки. Конструктивне виконання вібростатів дозволяє застосовувати різні склади твердих, рідких та змішаних складів робочих середовищ. Для підвищення ефективності процесу запропоновано варіативну схему комбінування технічних рішень нових різновидів процесу вібраційної обробки. Встановлено, що комбінуючи різні поєднання технологічних та конструкторських параметрів, можливо розширити область використання процесу вібраційної оздоблювально-зачищувальної обробки на основі створення та впровадження її різновидів.*

**Ключові слова:** *вібраційна оздоблювально-зачищувальна обробка; класифікація процесу; оброблювані деталі; класифікація дефектів формоутворення; комбінування технічних рішень; область використання процесу.*

## CONTENT

<i>A. G. Tirnovean, N. D. Csoregi, C. Borzan, G. Varga.</i> A review of additive manufacturing technologies and their applications in the medical field.....	3
<i>V. Lavrinenko, V. Solod, V. Tyshchenko, Y. Ostroverkh.</i> The influence of different hardness of the tool material on the wear of SHM grinding wheels and the specific energy intensity of grinding.....	18
<i>V. Ferencsik.</i> Influence of diamond burnishing on core height an ten-point height.....	28
<i>T. Namboodri, C. Felhő.</i> Correlation analysis between components of force and vibration in turning of 11SMN30 steel.....	39
<i>A. Khattab, C. Felhő.</i> Progress and challenges in plunge milling: a review of current practices and future directions.....	51
<i>I. Sztankovics, I. Pásztor.</i> Assessment of the root mean square deviation on surfaces machined by high-feed tangential turning.....	66
<i>Y. Garashchenko, V. Fedorovich, A. Poharskyi, O. Harashchenko, A. Malyniak.</i> Color visualization of 3D-models for enhanced preparation of additive manufacturing processes.....	77
<i>S. Dyadya, O. Kozlova, P. Tryshyn, D. Yakhno, D. Dziuba.</i> Influence of helical cutting-edge angle on end-milling stability.....	86
<i>G. Klymenko, Y. Vasylychenko, Y. Reva, D. Korchma, R. Boroday.</i> Determination of the stability period of turning cutters for heavy machine tools.....	95
<i>Y. Garashchenko, O. Harashchenko, R. Kucher.</i> Additive technologies in construction: technical, economic and management analysis.....	103

**A. Mitsyk, V. Fedorovich, N. Kozakova.** The essence of the process of vibrational finishing and cleaning, its technological capabilities and ways to increase efficiency.....116

Наукове видання

**РІЗАННЯ ТА ІНСТРУМЕНТИ**  
**в технологічних системах**

Збірник наукових праць

**Випуск № 101**

Укладач *д.т.н., проф. І.М. Пижов*

Оригінал-макет *А.М. Борзенко*

Відп. за випуск *к.т.н., проф. С.В. Островерх*

В авторській редакції

Матеріали відтворено з авторських оригіналів

Підп. до друку 23.12.2024. Формат 60x84 1/16. Папір СоруРарег.

Друк - ризографія. Гарнітура Таймс. Умов. друк. арк. 10,93. Облік. вид. арк. 11,0. Наклад 30 прим.

1-й завод 1-100. Зам. № 1149. Ціна договірна.

Видавничий центр НТУ «ХП»

Свідоцтво про державну реєстрацію ДК № 116 від 10.07.2000 р.

61002, Харків, вул. Кирпичова, 2

---

Наукове видання

**РІЗАННЯ ТА ІНСТРУМЕНТИ**  
**в технологічних системах**

Збірник наукових праць

**Випуск № 101**

Укладач *д.т.н., проф. І.М. Пижов*

Оригінал-макет *А.М. Борзенко*

Відп. за випуск *к.т.н., проф. С.В. Островерх*

В авторській редакції

Матеріали відтворено з авторських оригіналів

Підп. до друку 27.12.2024. Формат 60x84 1/16. Папір СоруРарег.

Друк - ризографія. Гарнітура Таймс. Умов. друк. арк. 10,93. Облік. вид. арк. 11,0. Наклад 30 прим.

1-й завод 1-100. Зам. № 1149. Ціна договірна.

Видавничий центр НТУ «ХП»

Свідоцтво про державну реєстрацію ДК № 116 від 10.07.2000 р.

61002, Харків, вул. Кирпичова, 2

---